G. ERDTMAN

POLLEN and SPORE MORPHOLOGY/ PLANT TAXONOMY

GYMNOSPERMAE,
PTERIDOPHYTA, BRYOPHYTA
(Gymnospermae)

POLLEN AND SPORE MORPHOLOGY/

PLANT TAXONOMY

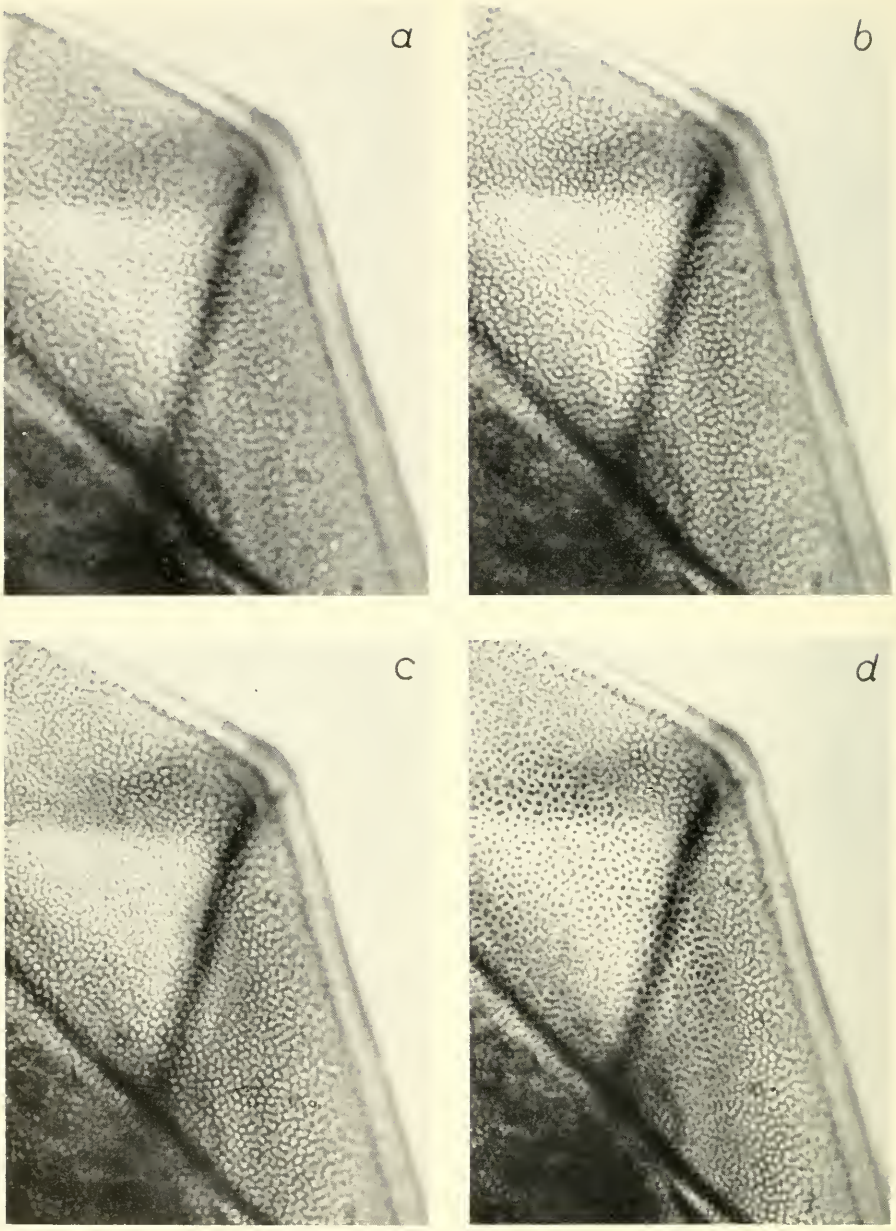

Juniperus communis, part of an acetolyzed megaspore membrane at different adjustments of the microscope from high (a) to low (d). × 1000.

POLLEN AND SPORE MORPHOLOGY/ PLANT TAXONOMY

GYMNOSPERMAE, PTERIDOPHYTA, BRYOPHYTA

(ILLUSTRATIONS)

(An Introduction to Palynology. II)

BY

G. ERDTMAN

With frontispiece, 5 plates and 265 illustrations

ALMQVIST & WIKSELL / STOCKHOLM

THE RONALD PRESS COMPANY / NEW YORK

Almqvist & Wiksell/Gebers Förlag AB

STOCKHOLM 1957

PRINTED IN SWEDEN BY

Almqvist & Wiksells

BOKTRYCKERI AKTIEBOLAG

UPPSALA 1957

PREFACE

The second part of "An Introduction to Palynology" deals, as was originally planned, with pollen and spore morphology in the Gymnospermae, Pteridophyta, and Bryophyta. Although the illustrations and most parts of the text were ready for printing in the autumn of 1956, the completion of the text had to be somewhat postponed on account of my absence abroad for several months. It was accordingly decided to publish the second part in two instalments: thus, the present volume (Vol. II) consists mainly of illustrations, whereas the following volume (Vol. III) will provide the related text.

Most of the illustrations are palynograms drawn after the author's originals by Anna-Lisa Nilsson. They depict, in a standardized manner, a pollen grain or spore in polar and/or lateral view, together with its sporoderm stratification and other details. It should be emphasized, however, that the sporoderm stratification details merely hint at the great array of patterns and layers which exist. Pending thorough morphological investigations, the proper interpretation of these layers etc. is still, in many cases, largely conjectural.

Besides the palynograms, some photomicrographs and electron micrographs of very thin sections through spore walls are included. Stimulated by my eminent friend, Dr. R. W. Kolbe, the microscopist and diatom specialist, I tentatively took up—in the late nineteen-forties—electron microscopy as an aid in sporoderm research. These studies have been continued, with better technique and greater success, by Dr. Barbro Afzelius, to whom I am indebted for the electron micrographs here reproduced (with the exception of those of Pl. IV and V, which were put at my disposal by Dr. D. von Wettstein) and for a chapter (pp. 125–134) on the application of new microscopical techniques in palynological research. Another chapter (pp. 135–147), by J. Radwan Praglowski, deals with the technique of making very thin sections from spore material embedded in plastic. As shown by Fig. 1 (p. 2), this technique can also be applied in the study of very old (Palaeozoic etc.) spores.

In conformity with Vol. I, the present volume has been prepared under the auspices of the Swedish Natural Science Research Council. Help and support of various kinds received from other sources will be duly acknowledged in Vol. III.

Palynological Laboratory,
Stockholm - Bromma, July 1957. *G. E.*

CONTENTS

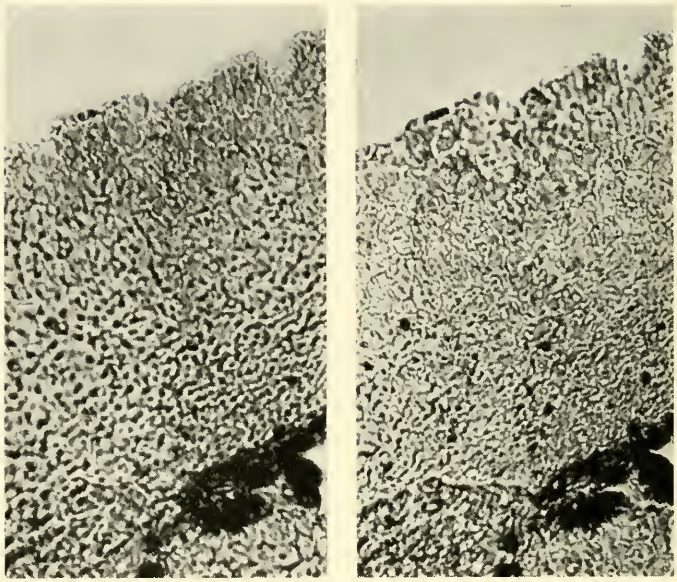

Fig. 1. *Setosisporites* sp. (material supplied by Dr. Gerhard Kremp), section (thickness about 0.5 μ) through part of the sclerine at high (left) and low (right) adjustment of the microscope. × 1000.

INTRODUCTION

ON THE EXINE MORPHOLOGY OF THE SACCATE POLLEN GRAINS IN RECENT GYMNOSPERMS

The saccate pollen grains in recent gymnosperms are heteropolar, bilateral or radiosymmetric (sometimes slightly asymmetric). They consist of a body (corpus) and a varying number of airsacks or bladders (sacci). The aperture is distal, and should often perhaps more appropriately be referred to as a tenuitas (i.e., a thin aperturoid area functioning as an aperture and gradually merging into the surrounding exine). It has earlier, as a rule, been described as a sulcus or a sulcoid groove.

The surface of the corpus of a pollen grain with *n* bladders can be divided into the following areas: *n* saccale areas, forming the floor of the sacci, *n* mesosaccale areas (mesosaccia), i.e. areas between the sacci and in the same latitude as these, and finally two aposaccale areas (aposaccia), one at the distal pole, and the other, usually much larger than the former, in the proximal face of the grain with the proximal pole in its centre.

With respect to the thickness of the exine of the corpus certain pollen types (cf. e.g. Figs. 53 and 57) exhibit two distinct exine areas: a proximal, crassi-exinous (referred to as cap, cappa), and a distal, tenui-exinous (referred to as cappula). The non-saccale exine of the cappa consists of comparatively thick sexine and thin nexine. The outer, ectosexinous part of the sexine is usually thin, tegilloid, and as a rule connected to the nexine—except within the sacci—by baculoid, densely spaced endosexinous elements.

The sacci are separated from the interior, non-exinous parts of the corpus, by saccale nexine. Their outer wall consists of thin ectosexine which is often perforated (shown in electron micrographs—not published—by Erdtman and Thorsson in 1950). The small holes (micropuncta) are usually difficult to observe through an ordinary light microscope. In the majority of the *Tsuga* species the ectosexine of the sacci (as well as that of the corpus, cf. Fig. 73) is studded with spinules or small spines. Attached to the inner surface of the outer wall of the sacci are endo-sexinous elements protruding into the lumen of the bladders (in *Pherosphaera fitzgeraldii* stray endosexinous rods are also found on the saccale nexine). These elements are more widely spaced than those of the body. Branched or unbranched, single or combined in different ways, they tend to produce an array of patterns

which are difficult to draw and hard to describe. Microtome sections (cf particularly Afzelius in Grana palynologica, 1: 2, 1956) make these subtle details of pollen construction easier to observe and safer to interpret.

Near the proximal root of the sacci are often found slight, sexinous ridges or frill-like projections (proximal crests, cristae proximales, also referred to as cristae marginales) varying in appearance in different species. At the distal root of the sacci, where these merge into the distal aposaccium, the characteristic pattern of the bladders comes abruptly to an end.

The height of the corpus coincides with the polar axis (i.e. the perpendicular line connecting the poles); the breadth is identical with its maximum horizontal extension in grains in equatorial longitudinal view (marginal crests extending beyond the general surface of the corpus not included), and the depth (in bilateral grains) is equal to the transverse ("non-sacciferous") diameter of the corpus. It is often preferable and, at the same time, easier to calculate the inner dimensions of the corpus.

The height of a saccus is the shortest distance from the highest point of the saccus (or from a line drawn through this point parallel to the saccale nexine) to the underlying nexine of the corpus. Its breadth is equivalent to the "tangential" diameter of the saccus in pollen grains in polar view. In radiosymmetric grains the breadth can also be measured in pollen grains seen in equatorial view; bilateral grains must be in a transverse equatorial position if the breadth shall be measured. In microscope slides this, however, is seldom the case. Its depth—in bilateral grains—is equal to the maximum diameter of the saccus in grains in equatorial longitudinal view. In radiosymmetric grains the depth is calculated is a similar way. Height, breadth, and depth of corpus and sacci are illustrated in Figs. 2, 3, 13, 23, 27, 43, 53, 57, 58, and 62.

As shown by Afzelius the inner part of the nexine (the endonexine) in *Cedrus* is laminated (Fig. 12, p. 11). In acetolyzed pollen grains of this genus, and of *Abies*, etc., it can often be seen, even by means of an ordinary microscope, that the nexine consists of two distinct layers, which often split apart as a result of the chemical treatment. So striking is this feature that it seems extraordinary that it has not been mentioned until now.

The morphology of bisaccate pollen grains has been dealt with by numerous botanists, among whom was Strasburger, who believed that the floor of the sacci was formed by intine. This opinion has often been echoed right up to recent years, although Strasburger himself soon corrected his mistake.

In conclusion, it ought to be mentioned that, according to Čiguriaeva, the thin ends (with sexine and nexine slightly separate from each other) of the pollen grains in *Ephedra* and *Welwitschia* may be interpreted as the remainder of true sacci.

ILLUSTRATIONS

GYMNOSPERMAE

Frontispiece; Pl. I (facing p. 12), Pl. II (facing p. 20); Figs. 2–73.

MEGASPORES

Cupressaceae: Frontispiece; Figs. 36–41 (pp. 23–25).
Pinaceae: Figs. 44 (p. 28), 52 (p. 32), 63 d (p. 40).
Podocarpaceae: Fig. 19 (p. 14).

POLLEN GRAINS

Araucariaceae: Figs. 5 (p. 8), 7 (p. 9).
Cephalotaxaceae: Pl. I (Fig. 2); Fig. 14 (p. 12).
Cupressaceae: Figs. 4 (p. 8), 11 (p. 10), 29 (p. 18), 42 (p. 26), 49 (p. 30), 54 (p. 34), 71 (p. 43).
Cycadaceae: Figs. 10 (p. 10), 17 (p. 13), 18 (p. 13), 28 (p. 18), 31 B (p. 20), 46 (p. 29), 67 (p. 42).
Ephedraceae: Pl. II; Figs. 30 A, B (p. 19), 31 A (p. 20).
Ginkgoaceae: Fig. 32 (p. 21).
Gnetaceae: Figs. 34, 35 (p. 22).
Pinaceae: Figs. 2 (p. 6), 12, 13 (p. 11), 43 (p. 27), 45 (p. 28), 53 (p. 33), 55–58 (pp. 34–36), 62 (p. 39), 63 a–c (p. 40), 73 (p. 44).
Taxaceae: Figs. 6 (p. 8), 9 (p. 9), 50 (p. 31), 70 (p. 42).
Taxodiaceae: Figs. 8 (p. 9), 15 (p. 12), 16 (p. 12), 33 (p. 21), 47 (p. 29), 65, 66 (p. 41), 68, 69 (p. 42), 72 (p. 43).
Welwitschiaceae: Fig. 30 C (p. 19).

ABIES:—

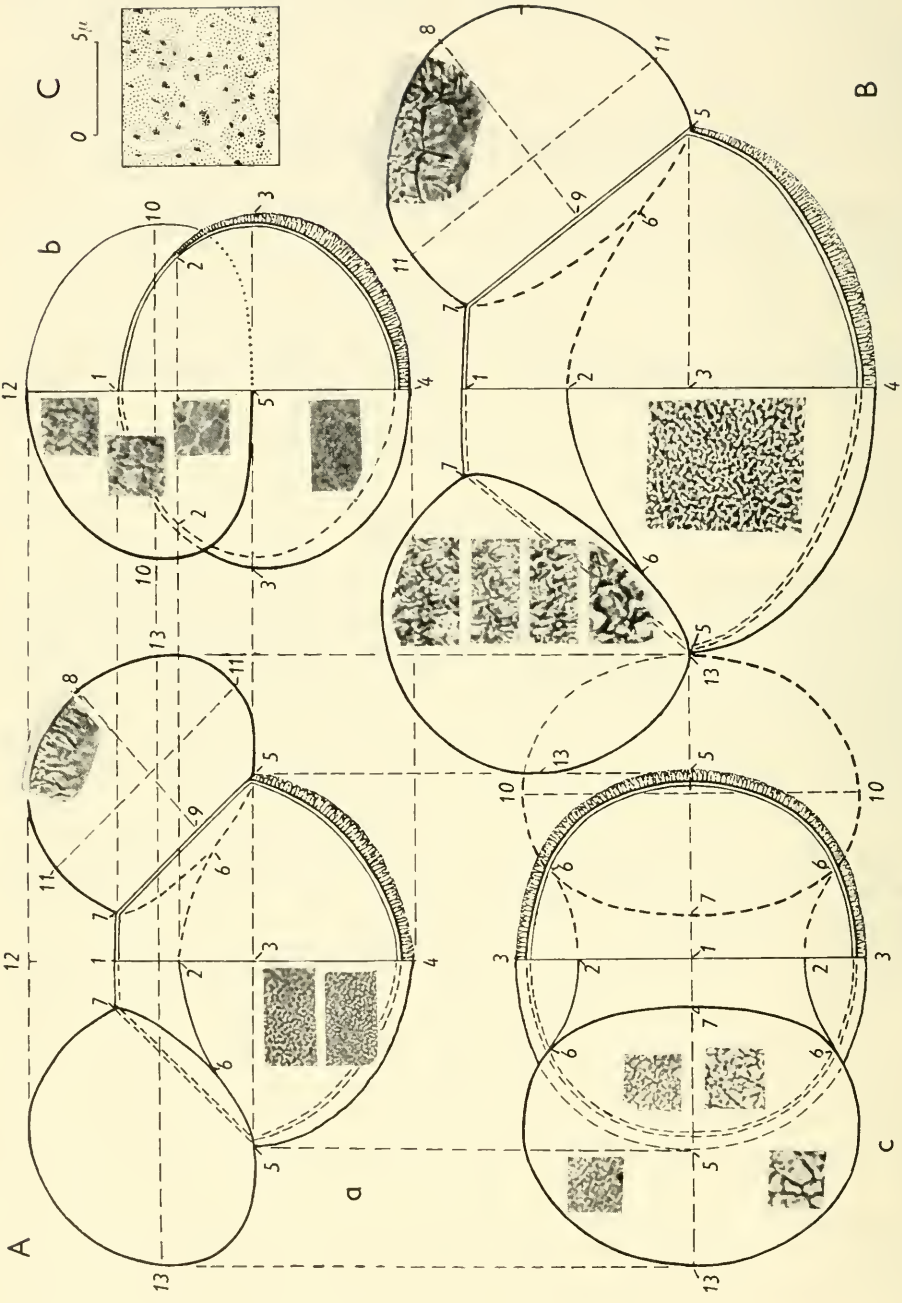

Fig. 2. A, *Abies nephrolepis*; a, lateral longitudinal view; b, lateral transverse view; c, polar view (distal face). × 650. B, *A. magnifica*, lateral longitudinal view. × 650. C, *A. mariesii*, saccus pattern (about × 2500).

1: distal pole, 4: proximal pole. Corpus: height 1–4, breadth 5–5, depth 3–3. Sacci: height 9–8, breadth 10–10, depth 11–11. Total grain: height 4–12 (A: a, b), breadth 13–13, depth 3–5–3 (A: b), 3–2–1–2–3 (A: c). Eleven of the inserted photomicrographs show the pattern of the outer surface of the sacci at different foci (the uppermost photomicrograph in each saccus shows the pattern at high adjustment of the microscope, the lowermost the same at low adjustment). Two of the photomicrographs between numerals 11 and 8 in A: a and B show a part of the saccus in optical cross-section. The remaining four photomicrographs exhibit the pattern of the corpus. Those in A: b are phase contrast pictures. (From Erdtman in Svensk bot. Tidskr. 1954.)

ACMOPYLE:—

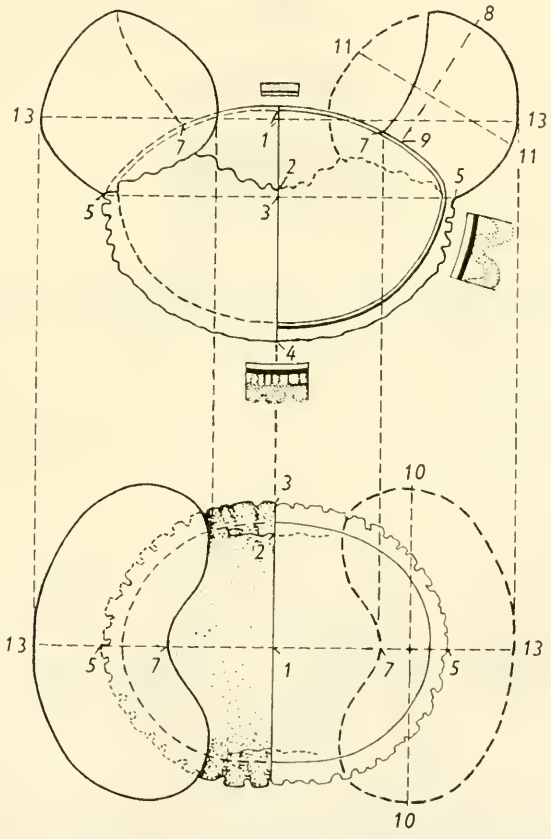

Fig. 3. *Acmopyle pancheri*. For explanation of numerals see Fig. 2.

ACTINOSTROBUS:—

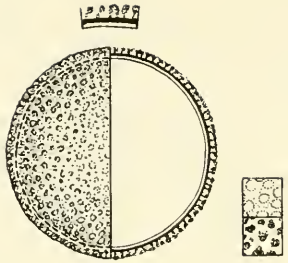

Fig. 4. *Actinostrobus acuminatus,* surface and optical cross-section. ×1000.

AGATHIS:—

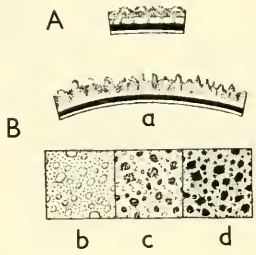

Fig. 5. A, *Agathis microstachya,* exine stratification. × 2000. B, *A. ovata,* exine stratification (a; × 2000) and LO-patterns (b–d).

AMENTOTAXUS:—

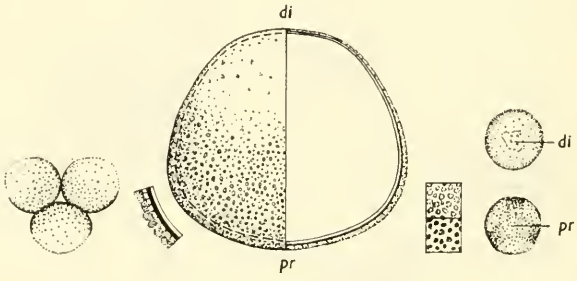

Fig. 6. *Amentotaxus argotaenia*; di, distal pole; pr, proximal pole. From left to right: three still loosely united pollen grains (tenuitas distal; × 250); exine stratification (× 2000); lateral view, surface and optical cross-section (×1000); LO-patterns; pollen grains in polar view (× 250).

ARAUCARIA:—

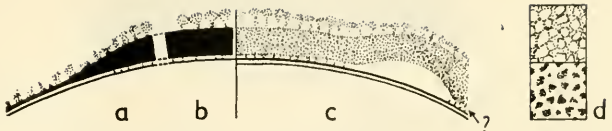

Fig. 7. *Araucaria montana* (exine stratification). a, transition from tenuitas (left) to the thickwalled rest of the grain (right). Layers interpreted in the same way as in b. — b and c, exine stratification outside tenuitas (alternative interpretations); c, shows a thin "nexine" (possibly consisting of two layers) overlain with a thick "sexine" exhibiting three layers: an "endosexinous" faintly-marked layer (consisting of baculoid rods?) merging into a thick, ± granular "ectosexine" ("tegillum"), beset with piloid "suprategillar" processes. According to the interpretation given in b, thin "sexine" ("pila") covers a thick "nexine" (the rest of the exine). — d, LO-patterns ("pila"). × 2000.

ARCEUTHOS: see Fig. 42 B, p. 26.

ATHROTAXIS:—

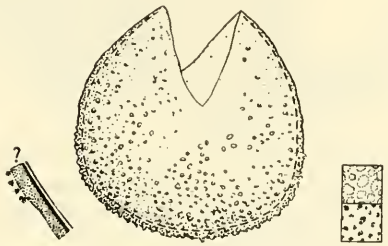

Fig. 8. *Athrotaxis cupressoides*. From left to right: exine stratification (×2000); lateral view of opened grain (× 1000); LO-patterns.

AUSTROTAXUS:—

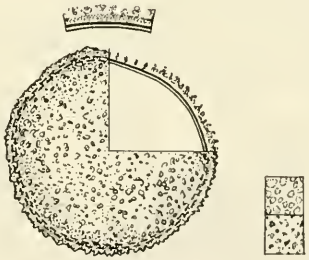

Fig. 9. *Austrotaxus spicata*. Main figure: surface and optical cross-section (× 1000). Details: exine stratification (× 2000) and LO-patterns.

BOWENIA:—

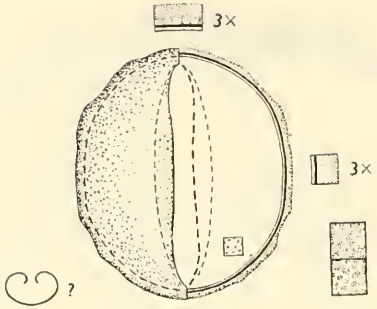

Fig. 10. *Bowenia spectabilis*. Details marked 3 × enlarged 3000 times. The main figure shows the distal face (surface and optical cross-section). × 1000.

CALLITRIS:—

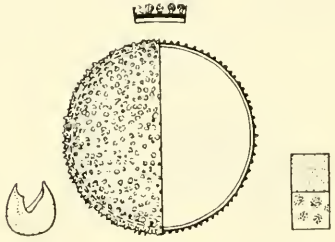

Fig. 11. *Callitris balansae* var. *alpina*. Main figure: surface and optical cross-section (× 1000). Details (from left to right): lateral view of opened grain (× 250); exine stratification (× 2000); LO-patterns.

CEDRUS:—

C. atlantica [Pl. I (facing p. 12); Fig. 12 a, b], *C. deodara* (Fig. 13).

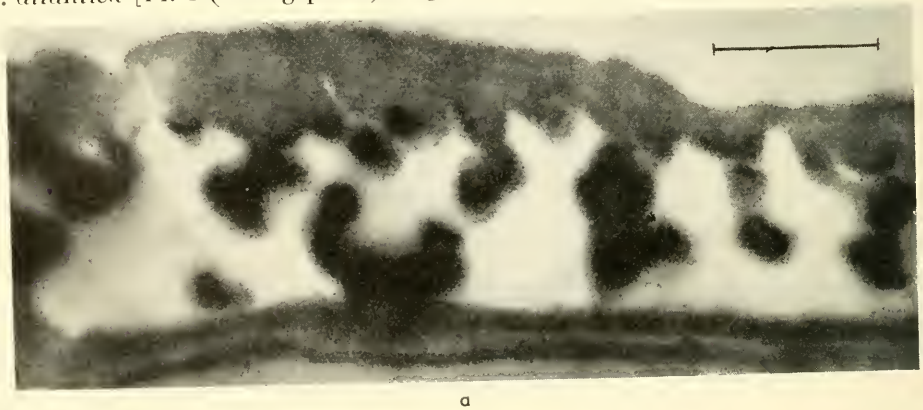

a

b

Fig. 12. *Cedrus atlantica*. a, section through part of an acetolyzed pollen wall; from top to bottom: ectosexine, endosexinous rods, ectonexine (homogeneous), endonexine (laminated; the black horizontal line indicates 1 μ; × 22.000); b, endonexine (from another section; magnification greater than in a). EMG B. M. Afzelius.

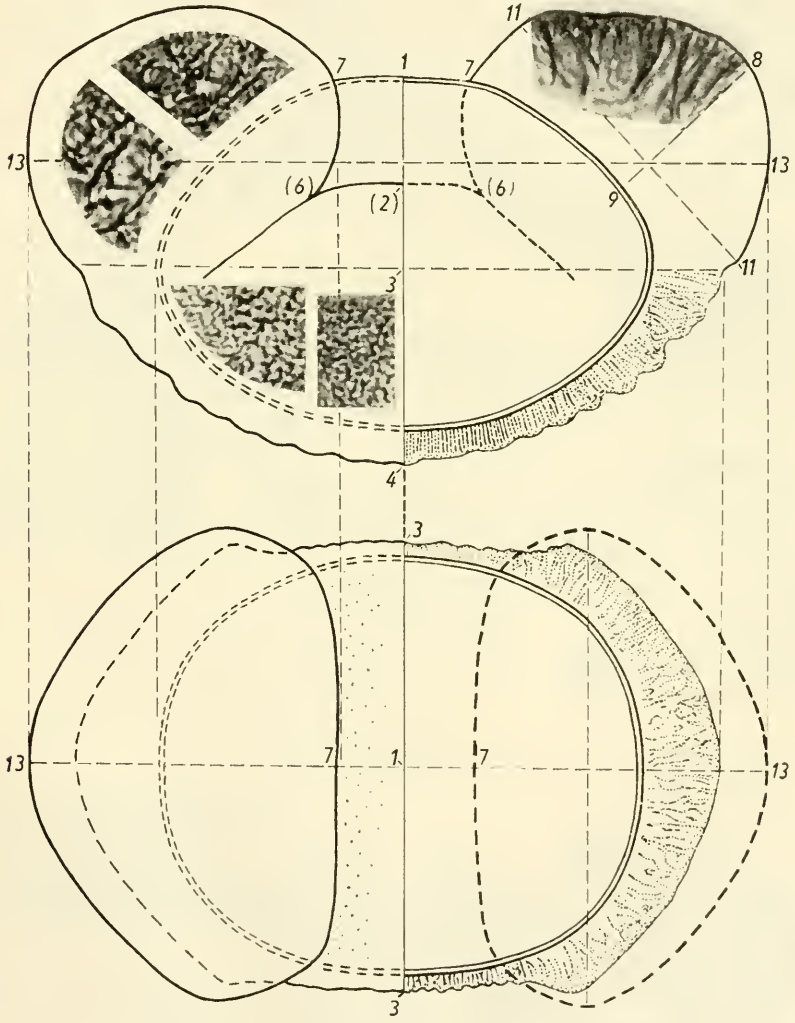

Fig. 13. *Cedrus deodara*. For explanation of numerals see Fig. 2, p. 7.

CEPHALOTAXUS:—

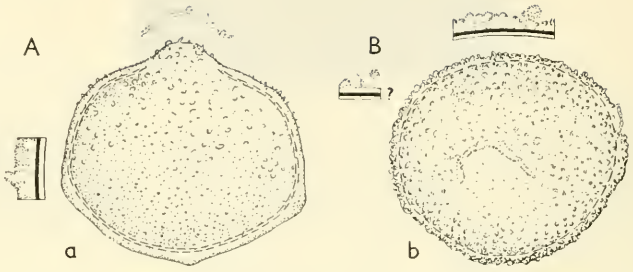

Fig. 14. A, *Cephalotaxus drupacea*; a, pollen grain with evaginated tenuitas (lateral view, × 1000); b, pollen grain with invaginated tenuitas (distal face, × 1000). B, *C. nana*, exine stratification (× 2000). — The drawings for this figure were ready before the electron micrograph, Pl. 1, Fig. 2, was taken. The white counterpart ("endonexine") to the lamellar layer in the EMG is clearly seen. Superimposed on the "endonexine" is a black layer ("ectonexine") corresponding, it would seem, to the granular part of the "nexine" shown in the EMG. Also with regard to sexine details there is an obvious similarity between Fig. 14 and the EMG, Pl. 1, Fig. 2.

CHAMAECYPARIS:—

Megaspore membrane: *Chamaecyparis lawsoniana*, see Fig. 36, p. 23.
Pollen grains: *Chamaecyparis pisifera*, see Fig. 42 A, p. 26.

CRYPTOMERIA:—

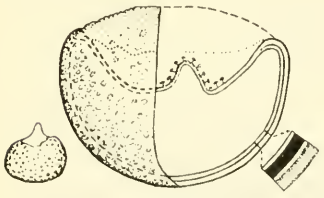

Fig. 15. *Cryptomeria japonica*. From left to right: pollen grain in lateral view, surface (× 250); pollen grain (distal face invaginated) in lateral view, surface and optical section (× 1000); exine stratification (× 2000).

CUNNINGHAMIA:—

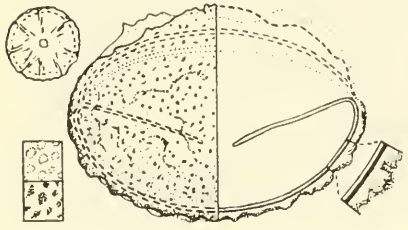

Fig. 16. *Cunninghamia lanceolata*. From left to right: distal face (upper detail-figure; × 250), LO-patterns (lower detail-figure); lateral view, surface and optical section (distal face invaginated; × 1000); exine stratification (× 2000).

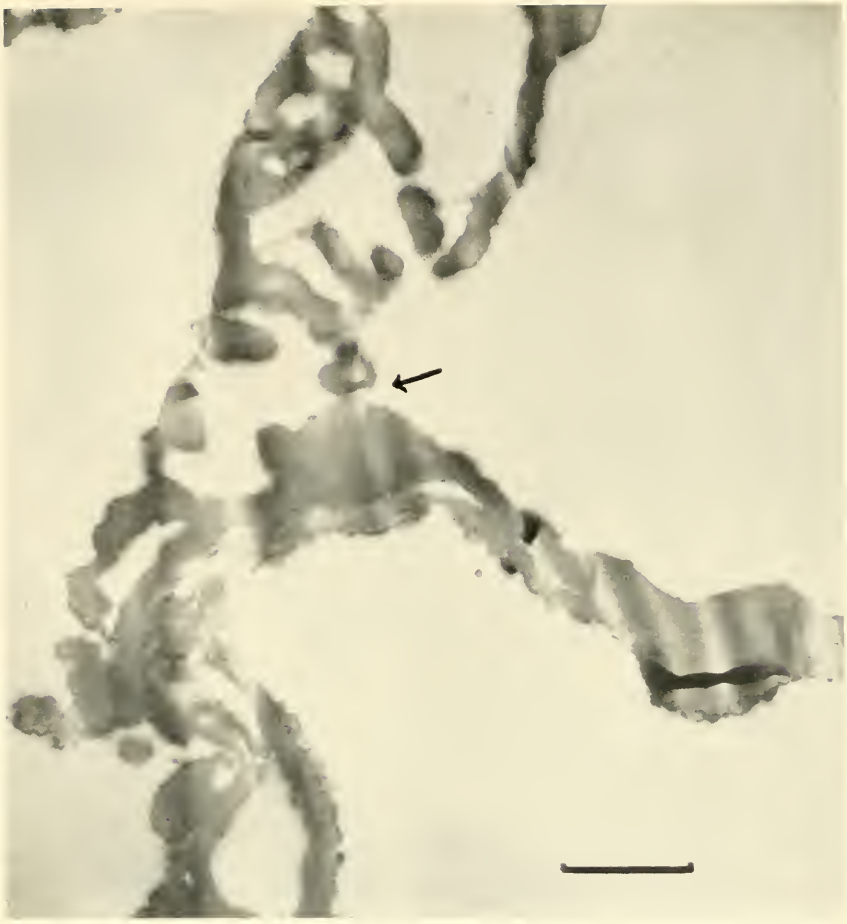

Fig. 1. *Cedrus atlantica*, section through part of an acetolyzed pollen wall. The nexine has been split off from the sexine at the point indicated by the arrow. The endonexine is laminated. × 18,000. The black horizontal line indicates 1 μ. (EMG; from Afzelius, in Grana palynologica, 1: 2, 1956.)

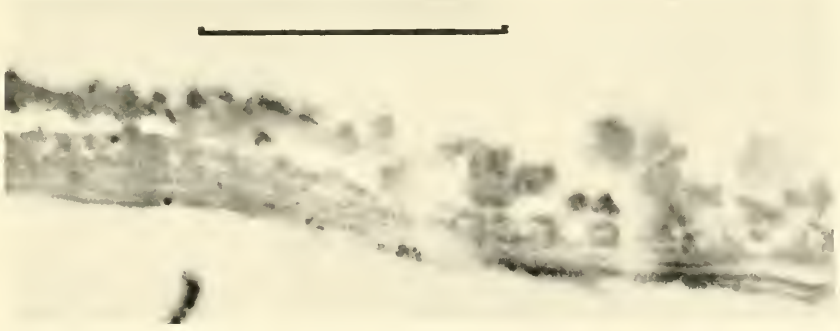

Fig. 2. *Cephalotaxus nana*, exine stratification. × 42,000. The black horizontal line indicates 1 μ. (EMG; from Afzelius, in Grana palynologica, 1: 2, 1956.)

CUPRESSUS: —

Megaspore membrane: *Cupressus arizonica*, see Fig. 37, p. 23; *C. whitleyana*, see Fig. 38, p. 24.

CYCAS (see also Fig. 31 B, p. 20):—

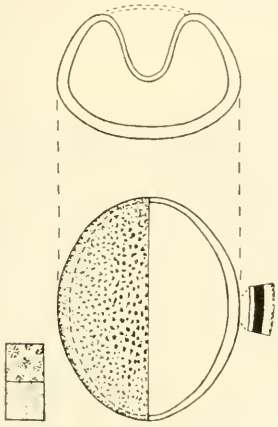

Fig. 17. *Cycas revoluta*; outline of transverse median section (upper detail-figure); proximal face (lower detail-figure).

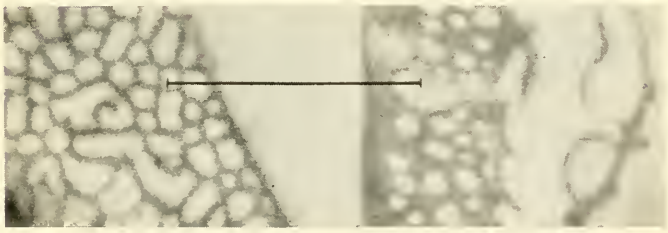

Fig. 18. *Cycas revoluta*, sections through part of acetolyzed pollen walls: cf. tangential, ± oblique section (left); ± radial section (right; × 34,000). The black horizontal line indicates 1 μ. EMG B. M. Afzelius.

DACRYDIUM:—

Megaspore membrane: *D. cupressinum* (Fig. 19).

Pollen grains: *D. araucarioides* (Fig. 20 B), *D. bidwillii* (Fig. 21), *D. elatum* (Fig. 20 A), *D. falciforme* (Fig. 22), *D. fonkii* (Fig. 23), *D. franklinii* (Fig. 24), *D. guillauminii* (Figs. 25 and 26), *D. taxoides* (Fig. 27).

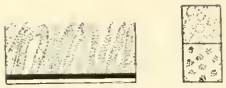

Fig. 19. *Dacrydium cupressinum*; megaspore membrane (× 2000) and LO-patterns of same.

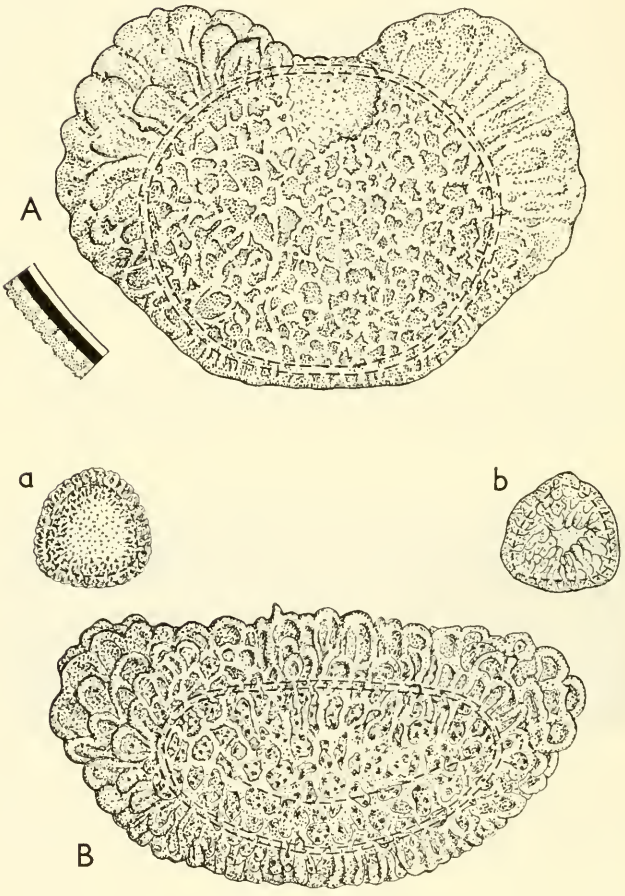

Fig. 20. A, *Dacrydium elatum*; exine stratification in proximal aposaccium (× 2000) and pollen grain in lateral, longitudinal view (surface; nexine contours indicated by broken lines; × 1000). B, *D. araucarioides*; pollen grain in lateral, longitudinal view (surface; distal face invaginated as indicated by the broken line just below the centre of the figure; × 1000); a, proximal face (× 250); b, distal face (× 250).

Fig. 21. *Dacrydium bidwillii*; distal face (left) and pollen grain in lateral, longitudinal view (surface, optical section, and LO-patterns). × 1000.

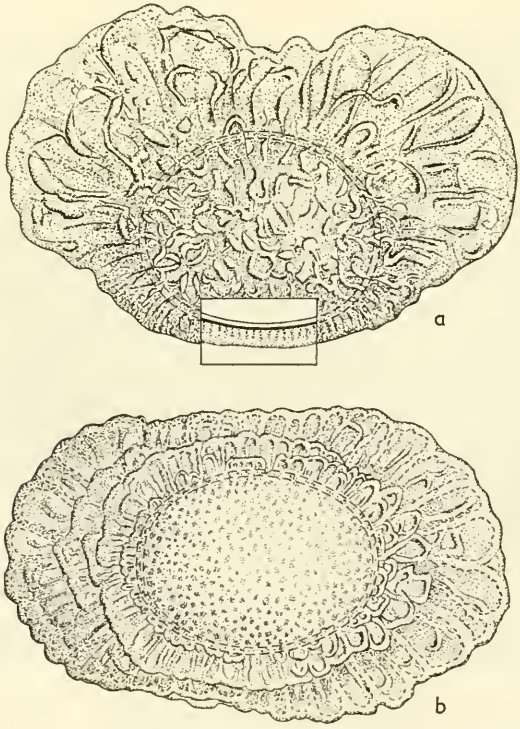

Fig. 22. *Dacrydium falciforme*; a, lateral view; b, proximal face. × 1000.

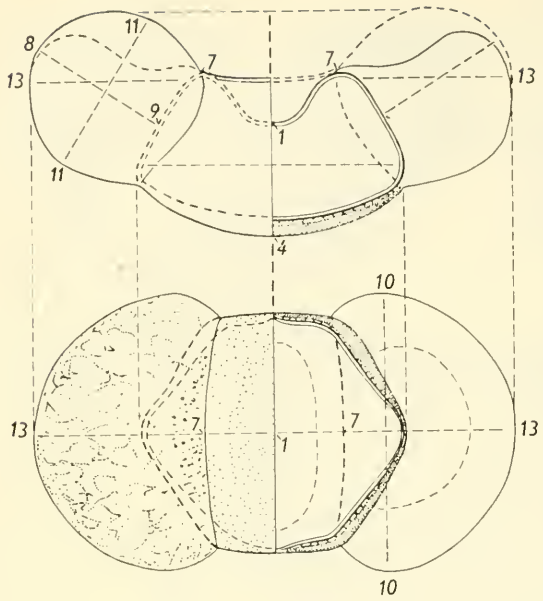

Fig. 23. *Dacrydium fonkii*; upper figure: outline of pollen grain in lateral, longitudinal view (× 1000). Lower figure: distal face, surface and optical section (× 1000). For explanation of numerals see Fig. 2, p. 7. The curved broken line in the extreme right part of the lower figure indicates the approximate delimitation of a concavity in the distal face of the saccus.

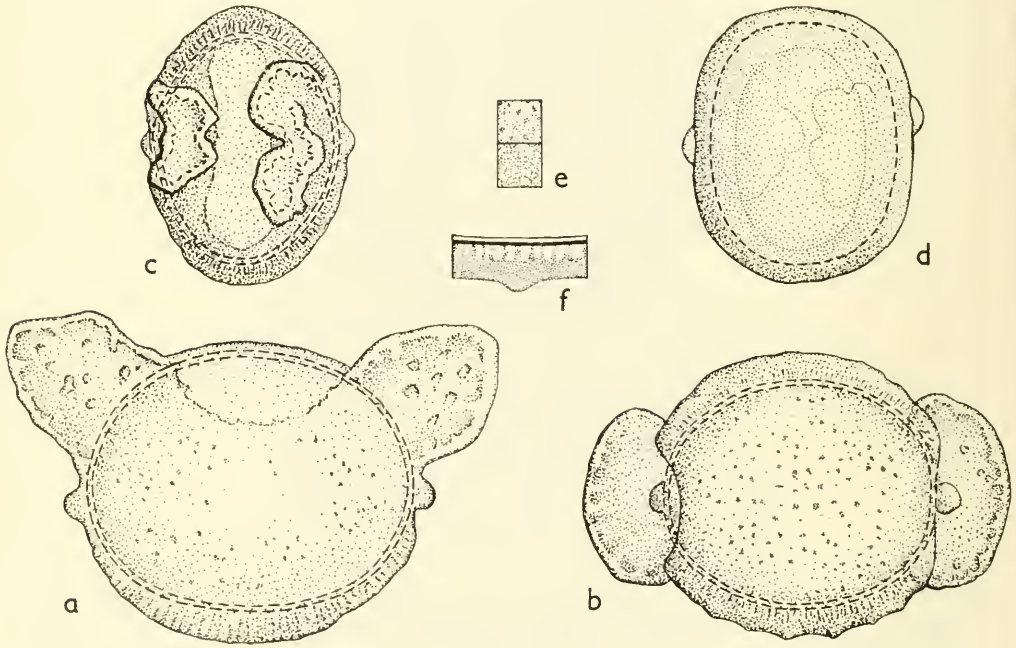

Fig. 24. *Dacrydium franklinii*; a, lateral, longitudinal view; b, proximal face; c–d, ± deviating grains (c distal, d proximal face); e, LO-patterns; f, exine stratification, proximal face (× 2000; a–d × 1000).

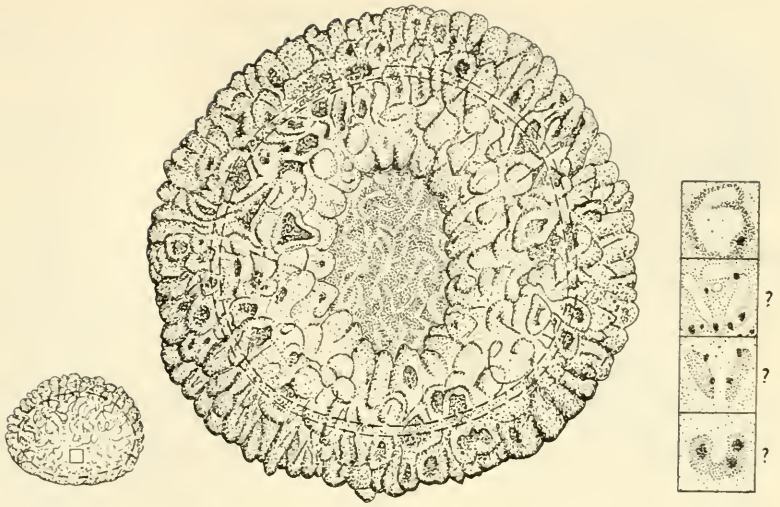

Fig. 25. *Dacrydium guillauminii*. From left to right: lateral view (× 250); distal face (× 1000); LO-patterns at high and successively lower focus.

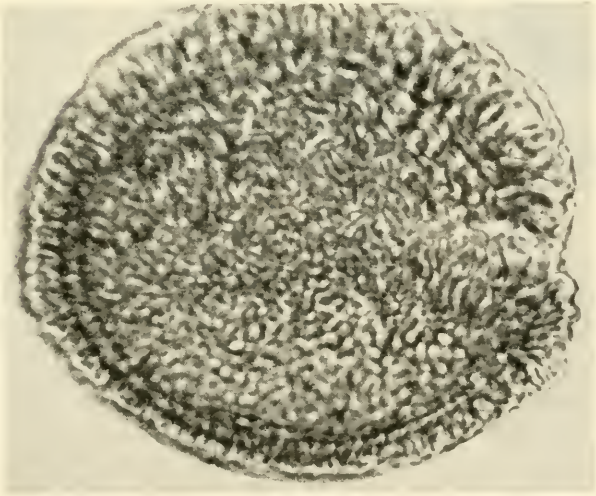

Fig. 26. *Dacrydium guillauminii*; oblique view (slightly > × 1000).

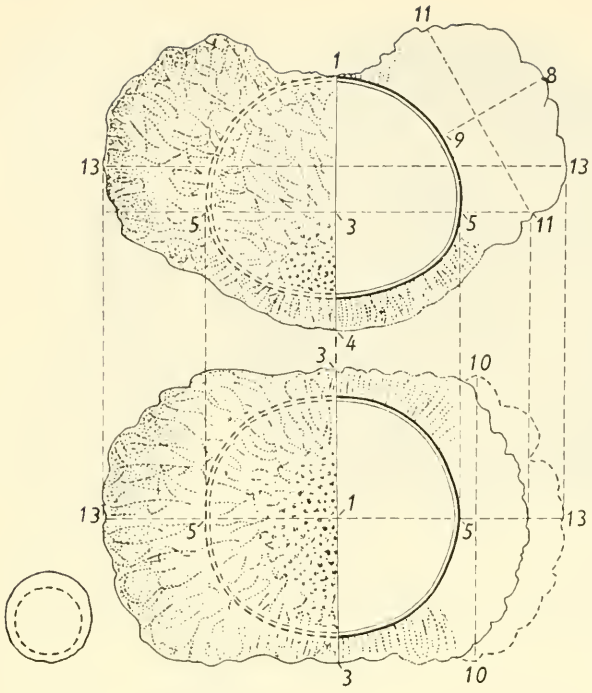

Fig. 27. *Dacrydium taxoides.* Upper figure: pollen grain in lateral, longitudinal view, surface and section. Lower figure: proximal face, surface (left) and optical section (right; × 1000). Lower left-hand detail-figure: outline of pollen grain in lateral, transverse view (×250; outer contour of the corpus marked by the broken line). For explanation of numerals see Fig. 2, p. 7.

DIOON:—

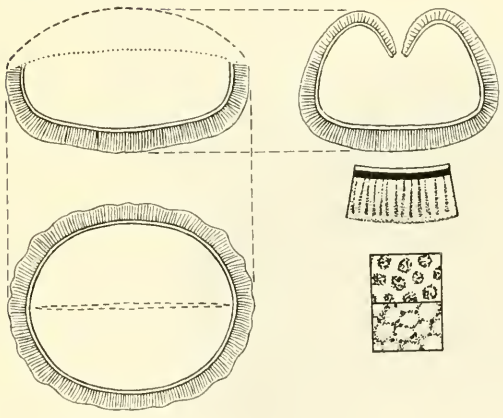

Fig. 28. *Dioon edule*; upper left-hand detail figure: median sagittal section; lower left-hand detail-figure: frontal section; upper right-hand detail-figure: transverse section (all × 1000); lower right-hand detail-figures: exine stratification (× 1000) and LO-patterns.

DISELMA:—

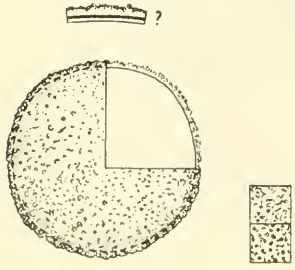

Fig. 29. *Diselma archeri*; surface and optical section (× 1000); exine stratification (× 2000); LO-patterns.

EPHEDRA [Fig. 30 A, B, Fig. 31 A, Pl. II (facing p. 20)], WELWITSCHIA (Fig. 30 C): —

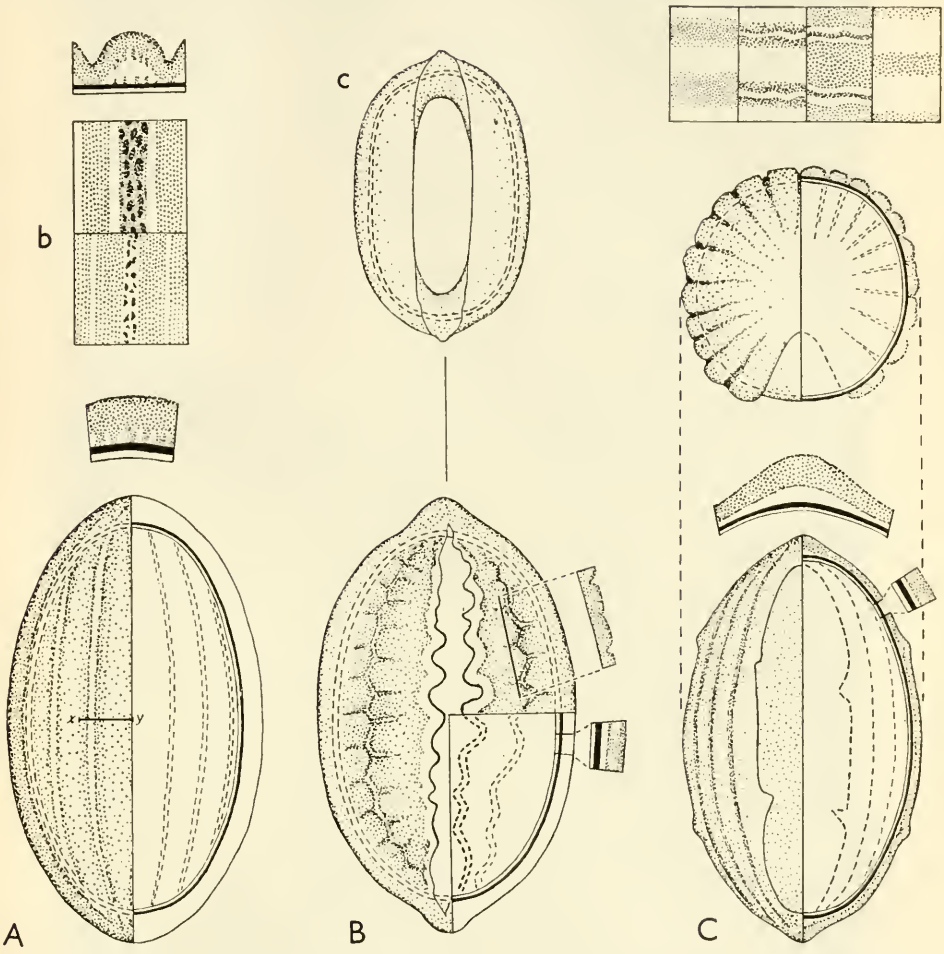

Fig. 30. A, *Ephedra antisyphilitica*; uppermost detail-figure: section through the exine along line x–y in the main figure (× 2000); b, LO-patterns; the detail-figure (× 2000) between this figure and the main figure (× 1000) shows a section through the exine at one of the short ends. B, *E. equisetina*; cf. distal face (× 1000), surface and optical section; c, young grain with sulcoid aperture. C, *Welwitschia mirabilis*; cf. lateral, transverse view (× 1000), exine stratification (× 2000), and cf. distal face (× 1000); uppermost detail-figure: LO-analysis of part of the exine surface (to be read from left to right); as the two central details show there is a very low and narrow ridge (bright in the second, dark in the third detail from the left) at the bottom of the valleys (stippled in the extreme left, white in the extreme right detail) separating the hollow sexine ridges (white in the extreme left, stippled in the extreme right detail).

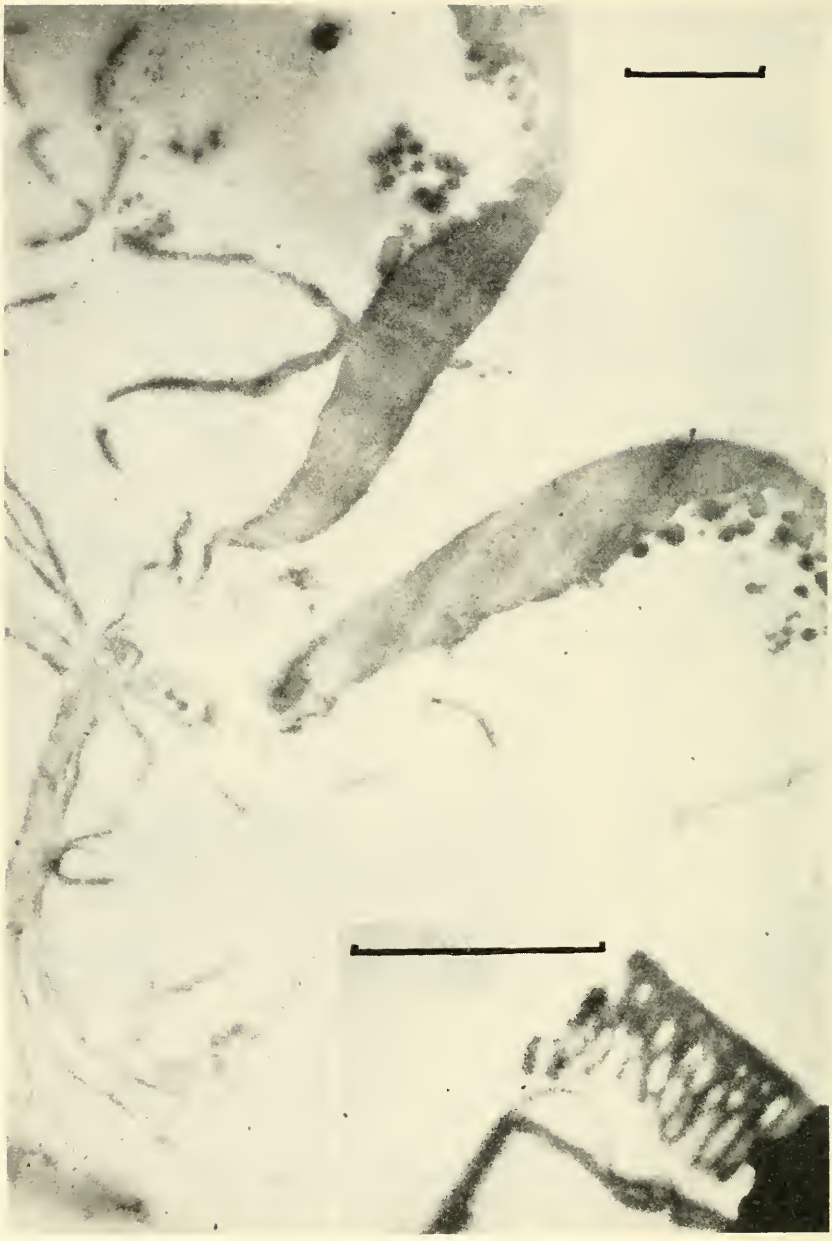

Fig. 31. A (main figure): *Ephedra monosperma*; section through an acetolyzed pollen wall. × 19,000. B (lower right-hand corner): *Cycas revoluta*; section through part of an acetolyzed pollen wall. × 35,000. The black horizontal lines indicate 1 μ. (EMG; from Afzelius in Grana palynologica, 1: 2, 1956.)

Ephedra monosperma; section through part of the inner laminated layer of an acetolyzed pollen wall (the inner part of the pollen grain is to the left; the black horizontal line indicates 1 μ). × 93,000. (EMG; from Afzelius in Grana palynologica, 1: 2, 1956.)

FITZROYA: see Fig. 42 G, H, p. 26.

GINKGO:—

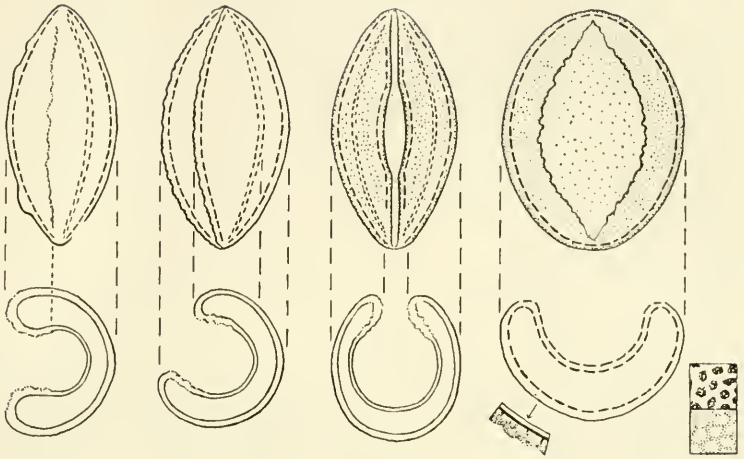

Fig. 32. *Ginkgo biloba*; extreme left detail-figure: pollen grain in lateral, longitudinal view with an outline of the accompanying median transverse section. Second detail-figure from the left: pollen grain slightly tilted with the entrance to the concavity which lodges the tenuitas shown to the left. The remaining figures exhibit the distal face of an unexpanded and an expanded grain. The lower detail figure of the latter gives the outline of a pollen grain in lateral transverse view (owing to an omission a full line uniting the upper extremities of the figure is not shown). × 1000.

GLYPTOSTROBUS:—

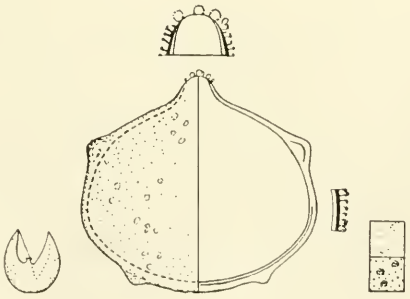

Fig. 33. *Glyptostrobus pensilis*. From left to right: opened grain (× 250); lateral view, surface and optical section (× 1000); exine stratification (× 2000); LO-patterns. Uppermost detail-figure: tenuitas (optical section; × 2000).

GNETUM:—

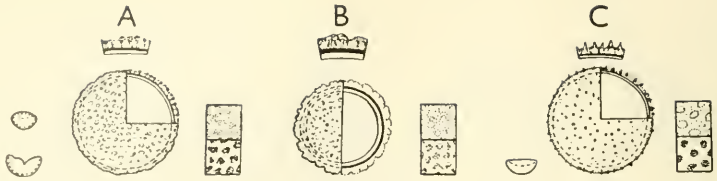

Fig. 34. A, *Gnetum venosum.* — B, *G. africanum.* — C, *G. montanum.* (From Erdtman in Bot. Notiser 1954.)

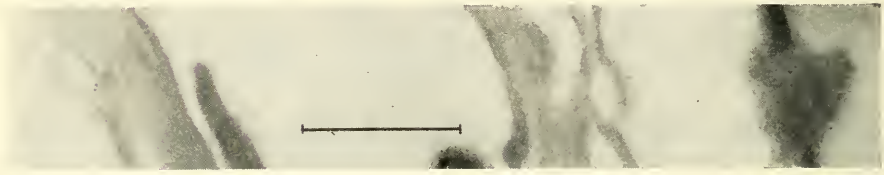

Fig. 35. *Gnetum montanum,* section through part of an acetylyzed, very compressed pollen grain. To the extreme right is a spinule. The black horizontal line (indicating 1 μ) is drawn within the lumen of the grain. × 21.000. EMG B. M. Afzelius.

JUNIPERUS, ARCEUTHOS, CHAMAECYPARIS, CUPRESSUS, FITZROYA, LIBOCEDRUS, WIDDRINGTONIA:—

Megaspore membranes: *Chamaecyparis lawsoniana* (Fig. 36, p. 23), *Cupressus arizonica* (Fig. 37, p. 23), *C. whitleyana* (Fig. 38, p. 24), *Juniperus communis* (Frontispiece and Fig. 39, p. 24), *J. sabina* (Fig. 41, p. 25).

Pollen grains: *Arceuthos drupacea* (Fig. 42 B, p. 26), *Chamaecyparis pisifera* (Fig. 42 A), *Fitzroya cupressoides* (Fig. 42 G, H), *Juniperus californica* (Fig. 42 D), *J. prostrata* (Fig. 42 E), *Libocedrus decurrens* (Fig. 42 F), *Widdringtonia cupressoides* (Fig. 42 C).

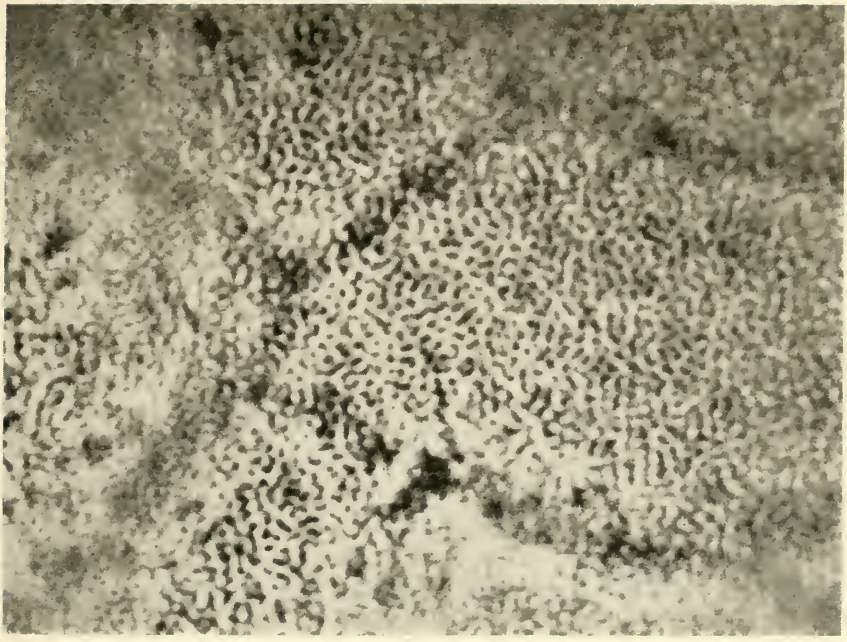

Fig. 36. *Chamaecyparis lawsoniana*; megaspore membrane (surface), phase contrast. × 4000. (From von Lürzer in Grana palynologica, 1: 2, 1956.)

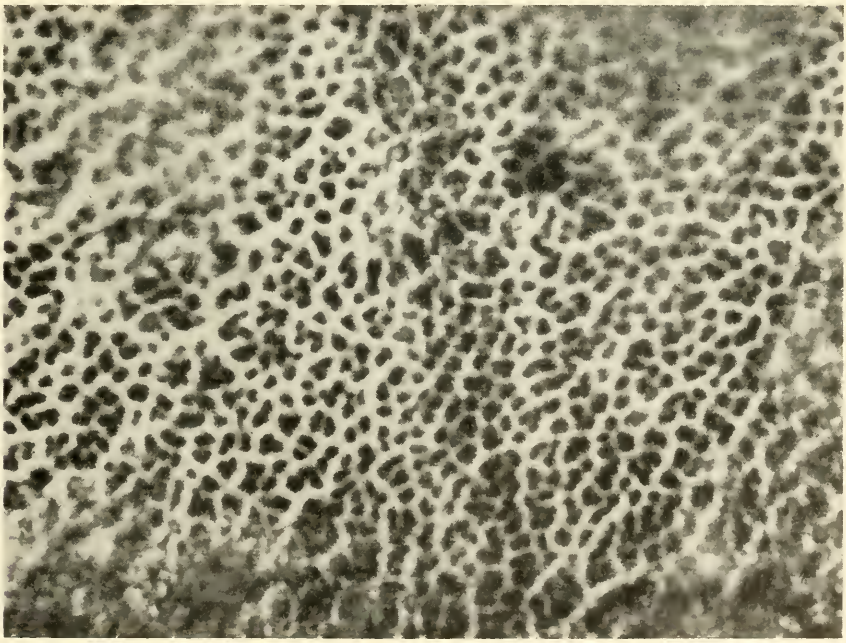

Fig. 37. *Cupressus arizonica*; megaspore membrane (surface), phase contrast. × 4000. (From von Lürzer in Grana palynologica, 1: 2, 1956.)

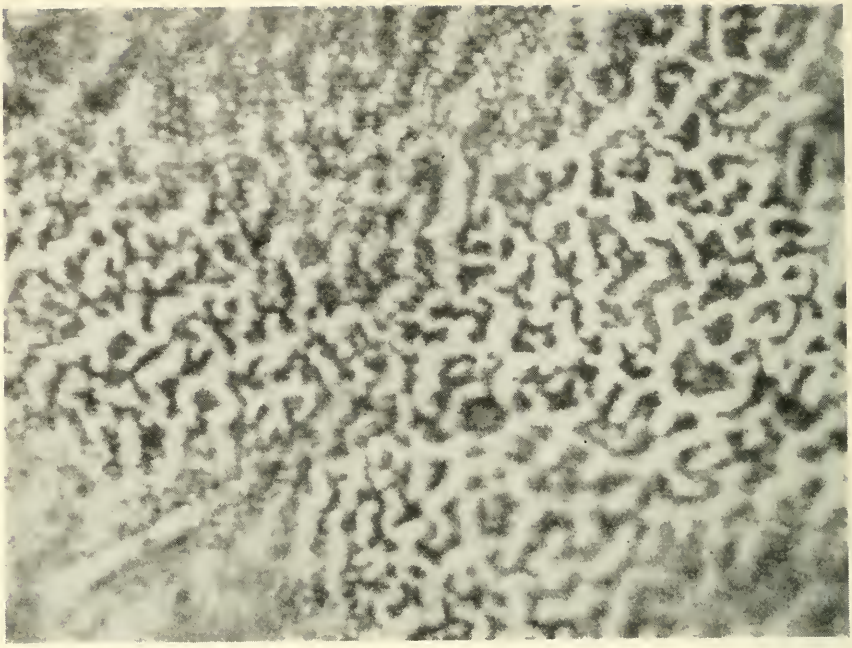

Fig. 38. *Cupressus whitleyana*; megaspore membrane (surface), phase contrast. × 4000. (From von Lürzer in Grana palynologica, 1: 2, 1956.)

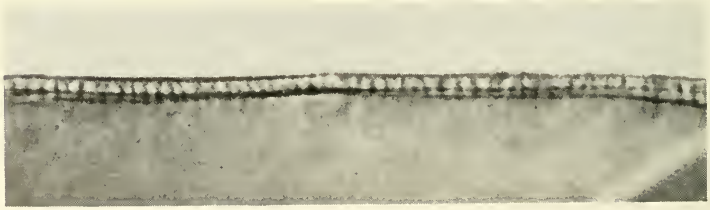

Fig. 39. *Juniperus communis*; megaspore membrane (optical section). × 1000. (For LO-patterns of the membrane surface, see Frontispiece.)

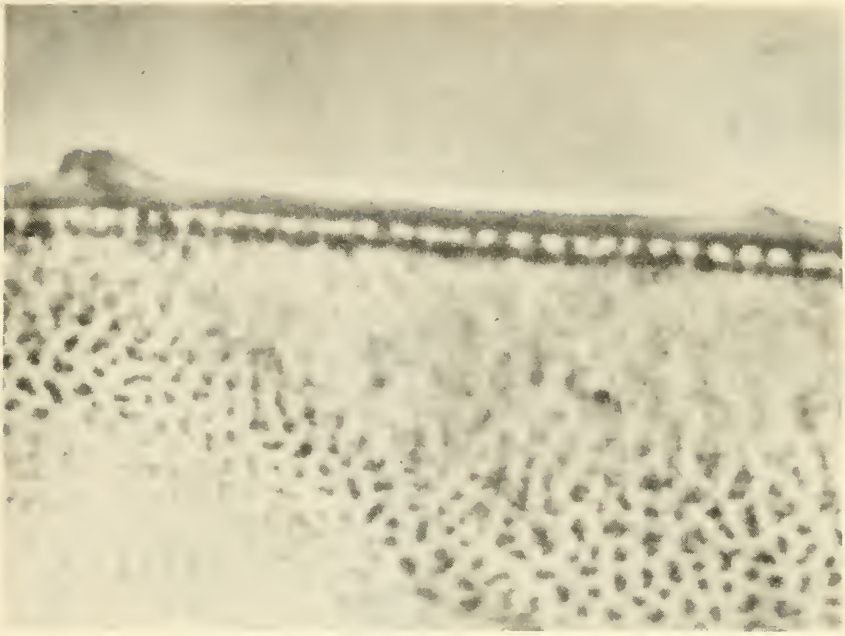

Fig. 40. *Juniperus sabina*; megaspore membrane (optical section), phase contrast. × 4000. (From von Lürzer in Grana palynologica, 1: 2, 1956.)

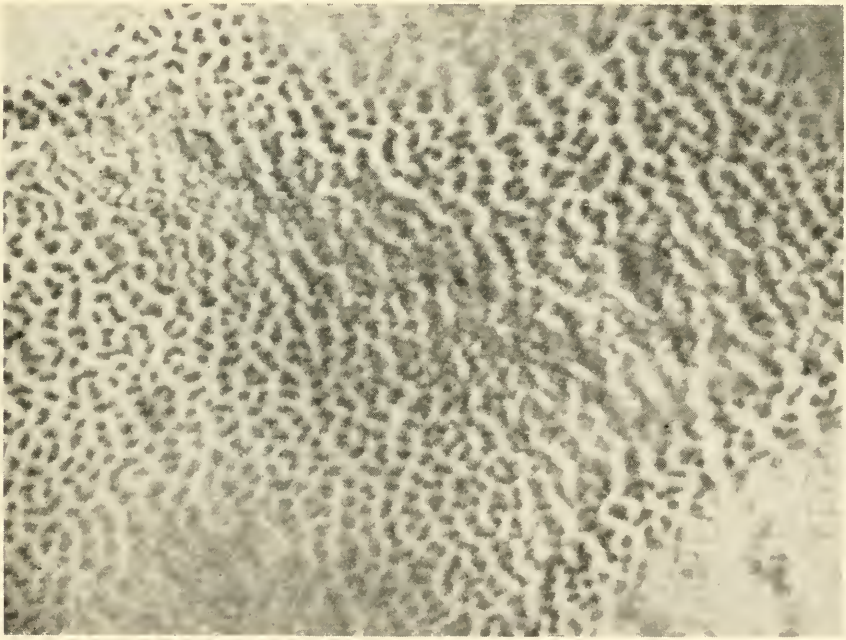

Fig. 41. *Juniperus sabina*; megaspore membrane (surface), phase contrast. × 4000. (From von Lürzer in Grana palynologica, 1: 2, 1956.)

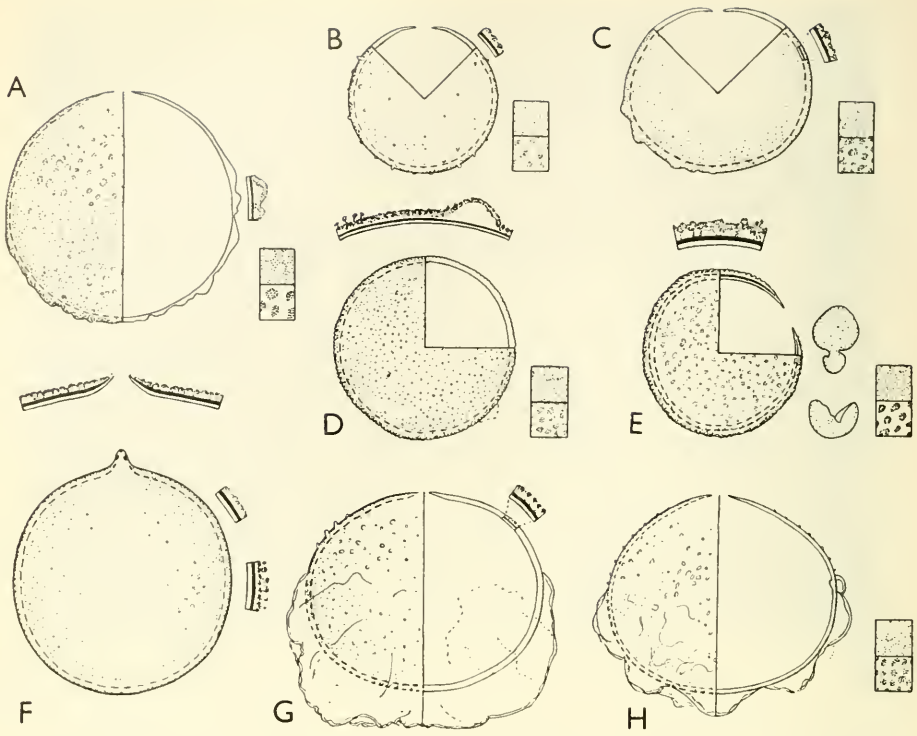

Fig. 42. Cupressaceae. A, *Chamaecyparis pisifera*. B, *Arceuthos drupacea*. C, *Widdringtonia cupressoides*. D, *Juniperus californica*. E, *J. prostrata*. F, *Libocedrus decurrens*. G, H, *Fitzroya cupressoides*. — The main figures (× 1000) exhibit grains in lateral view with (in A–C, and F–H) the distal pole at the top. An aperturoid spot is faintly marked in the upper left-hand quadrant in D. The detail figures show the exine stratification enlarged 2000 times. The detail-figures between the main figure and the LO-patterns in E show an irregular grain (upper detail-figure) and an opened grain (both × 250). H is a *Fitzroya* pollen grain of ± normal type whereas in G a deviating, ± "subsaccate" grain is shown. — Pollen grains of other cupressaceous plants are shown in Figs. 4 (*Actinostrobus*), 11 (*Callitris*), 29 (*Diselma*), 49 (*Neocallitropsis*), 54 (*Pilgerodendron*), and 71 (*Thujopsis*).

KETELEERIA:—

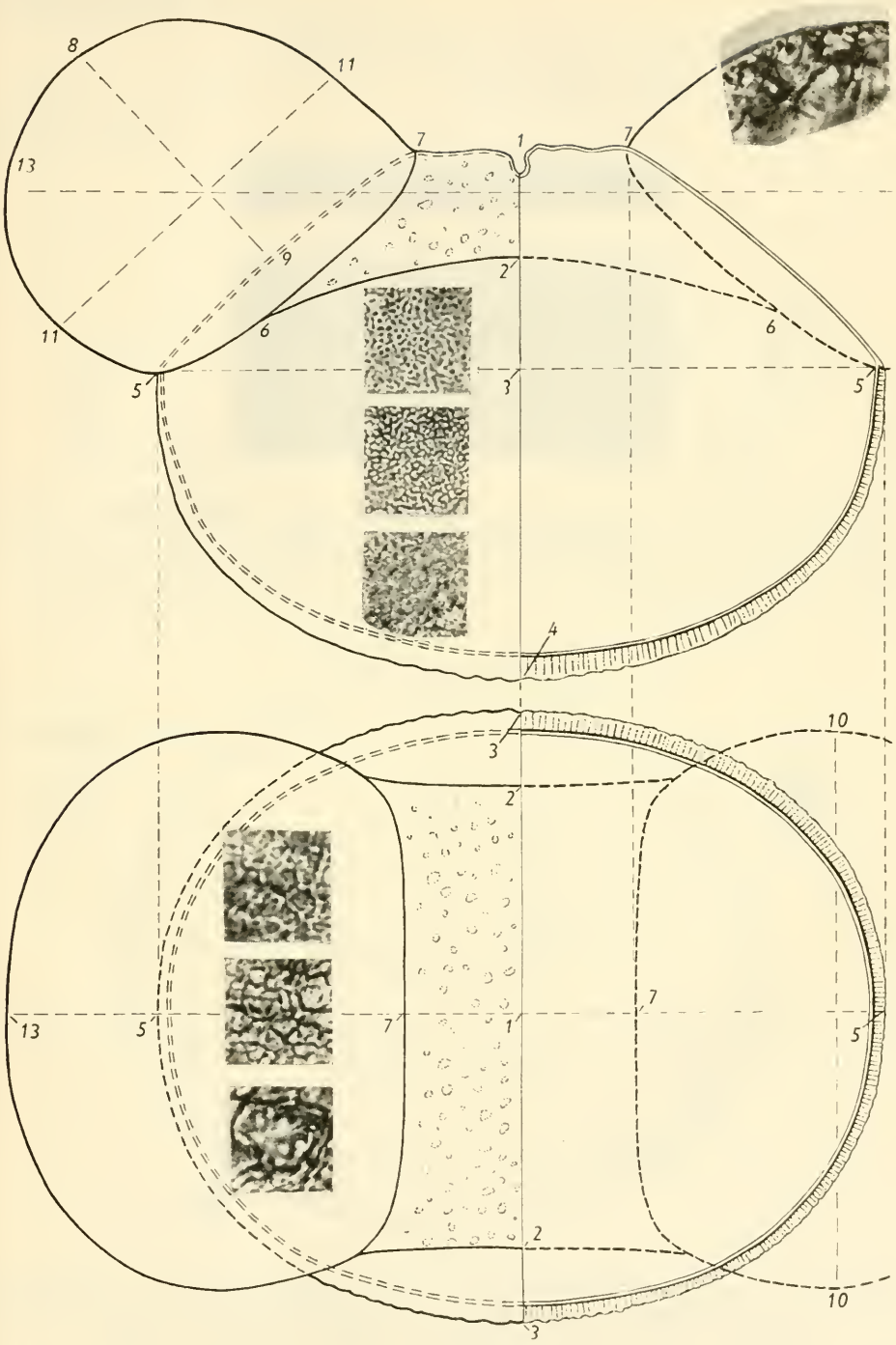

Fig. 43. *Keteleeria davidiana*; lateral, longitudinal view and distal face (× 1000). For explanation of numerals see Fig. 2, p. 7. (From Erdtman in Svensk bot. Tidskr. 1954.)

LARIX:—

Megaspore membrane: *Larix occidentalis* (Fig. 44).
Pollen grains: *Larix decidua* f. *polonica* (Fig. 45 B), *L. gmelini* var. *japonica* (Fig. 45 A), *L. occidentalis* (Fig. 45 C).

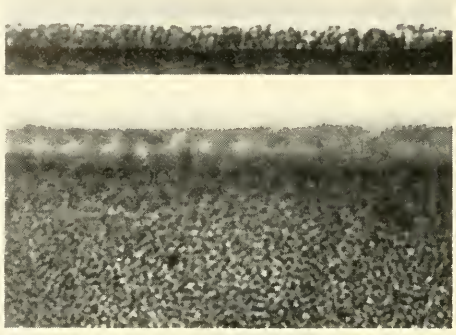

Fig. 44. *Larix occidentalis*; acetolyzed megaspore wall, optical section (above) and surface (below). × 1000.

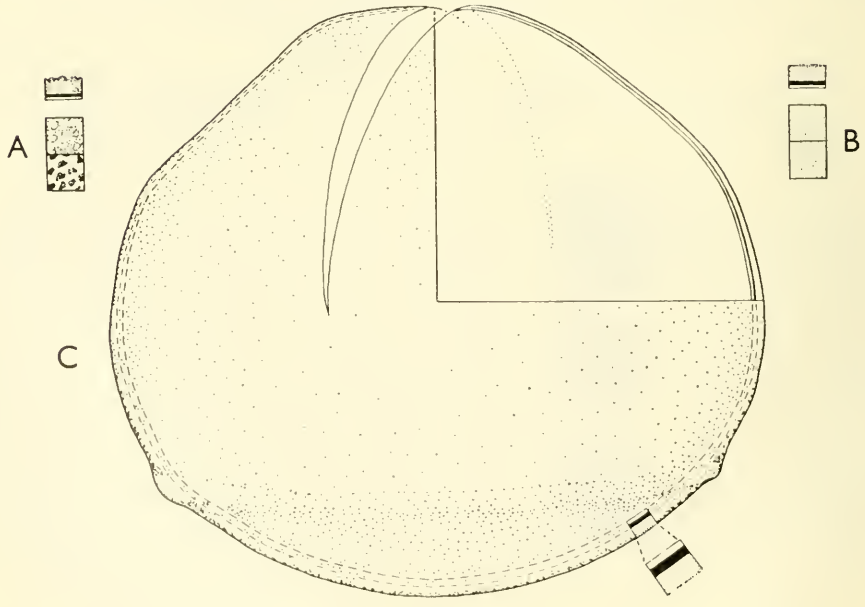

Fig. 45. A, *Larix gmelini* var. *japonica*; exine stratification and LO-patterns. B, *L. decidua* f. *polonica;* exine stratification and "LO-patterns". C, *L. occidentalis;* lateral view, surface and optical section (× 1000).

LIBOCEDRUS: see Fig. 42 F, p. 26.

MACROZAMIA:—

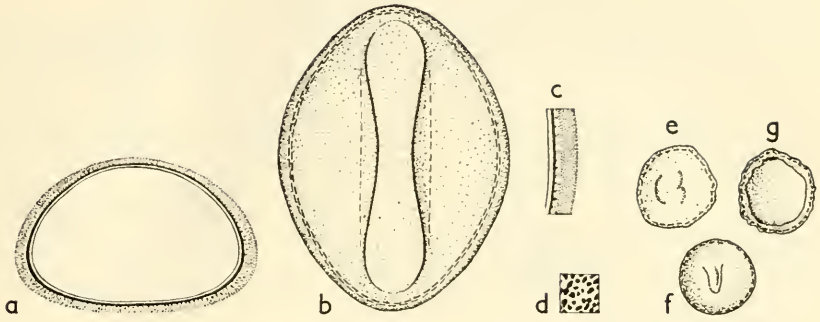

Fig. 46. *Macrozamia spiralis*; a, transverse, equatorial view (optical cross-section); b, distal face; c, exine stratification at amb at right angles to central part of the sulcoid tenuitas; d, pattern caused by endosexinous rods (phase contrast); e–g, morphological variants. a, b × 1000, c × 2000, e–g × 250.

METASEQUOIA:—

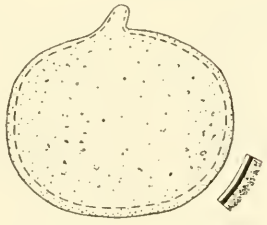

Fig. 47. *Metasequoia glyptostroboides*; lateral view (× 1000) and exine stratification (× 2000).

MICROCACHRYS (Fig. 48 A), MICROSTROBUS (Fig. 48 B):—

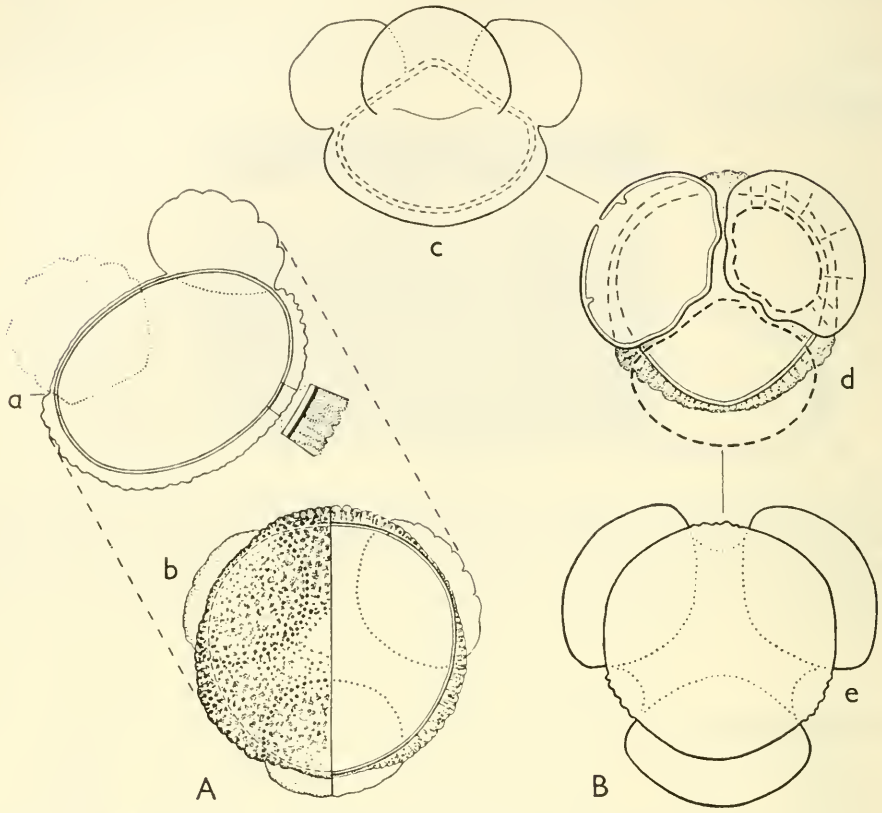

Fig. 48. A, *Microcachrys tetragona*; a, oblique lateral view (outline; the sexine of the proximal face in the upper right half part of the figure should be thinner); b, proximal face (× 1000). B, *Microstrobus* (*Pherosphaera*) *fitzgeraldii*; c, lateral view (outline); d, distal face; e, proximal face (outline; × 1000).

MICROSTROBUS: see Fig. 48 B.

NEOCALLITROPSIS:—

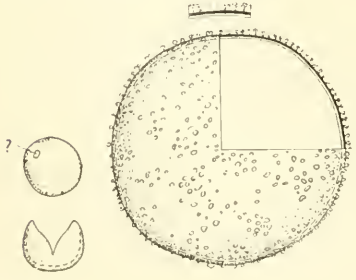

Fig. 49. *Neocallitropsis araucarioides*. Main figure: surface and optical cross-section (× 1000). Details: opened and unopened grains (× 250); exine stratification (× 2000).

NOTHOTAXUS:—

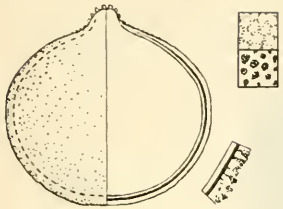

Fig. 50. *Nothotaxus chienii*. From left to right: lateral view, surface and optical section (× 1000); exine stratification (× 2000); LO-patterns.

PHEROSPHAERA: see Fig. 48 B, p. 30.

PHYLLOCLADUS:—

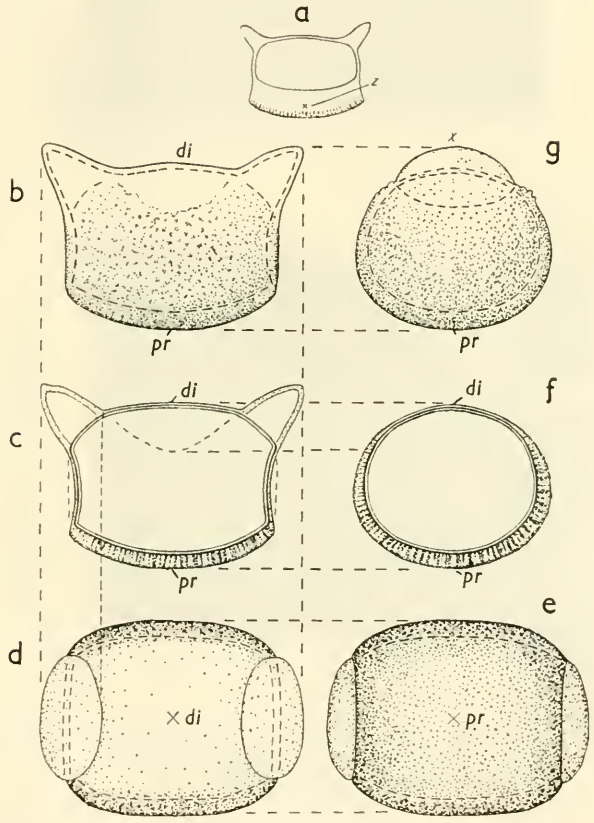

Fig. 51. *Phyllocladus protractus*; a, lateral, longitudinal view of a pollen grain (× 500) with the proximal face covered by a "saccus" (z), possibly an artificial feature resulting from the loosening of the sexine from the nexine; b, g, lateral (longitudinal and transverse) view (surface); c, f, same as b and g, in optical section; d, distal face (× di = distal pole); e, proximal face (× pr = proximal pole). — b–g × 1000.

PICEA:—

Megaspore membrane: *Picea abies* (Fig. 52).
Pollen grains: *Picea jezoensis* (Fig. 53).

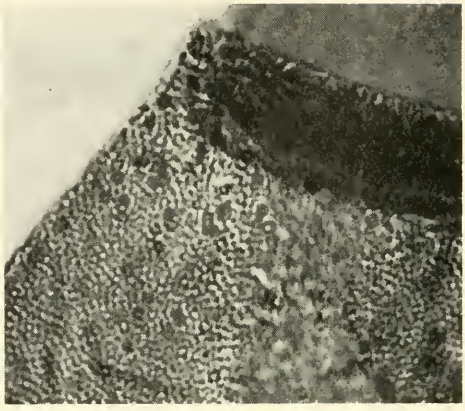

a

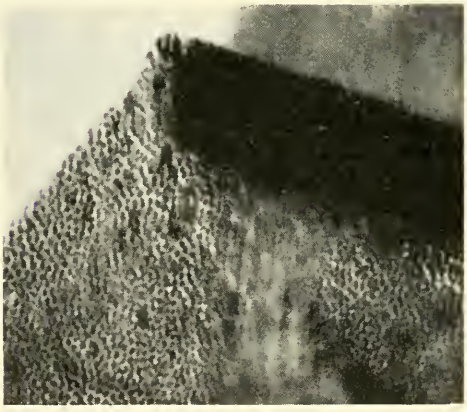

b

Fig. 52. *Picea abies*; part of an acetolyzed megaspore membrane at high (a) and low (b) focus.

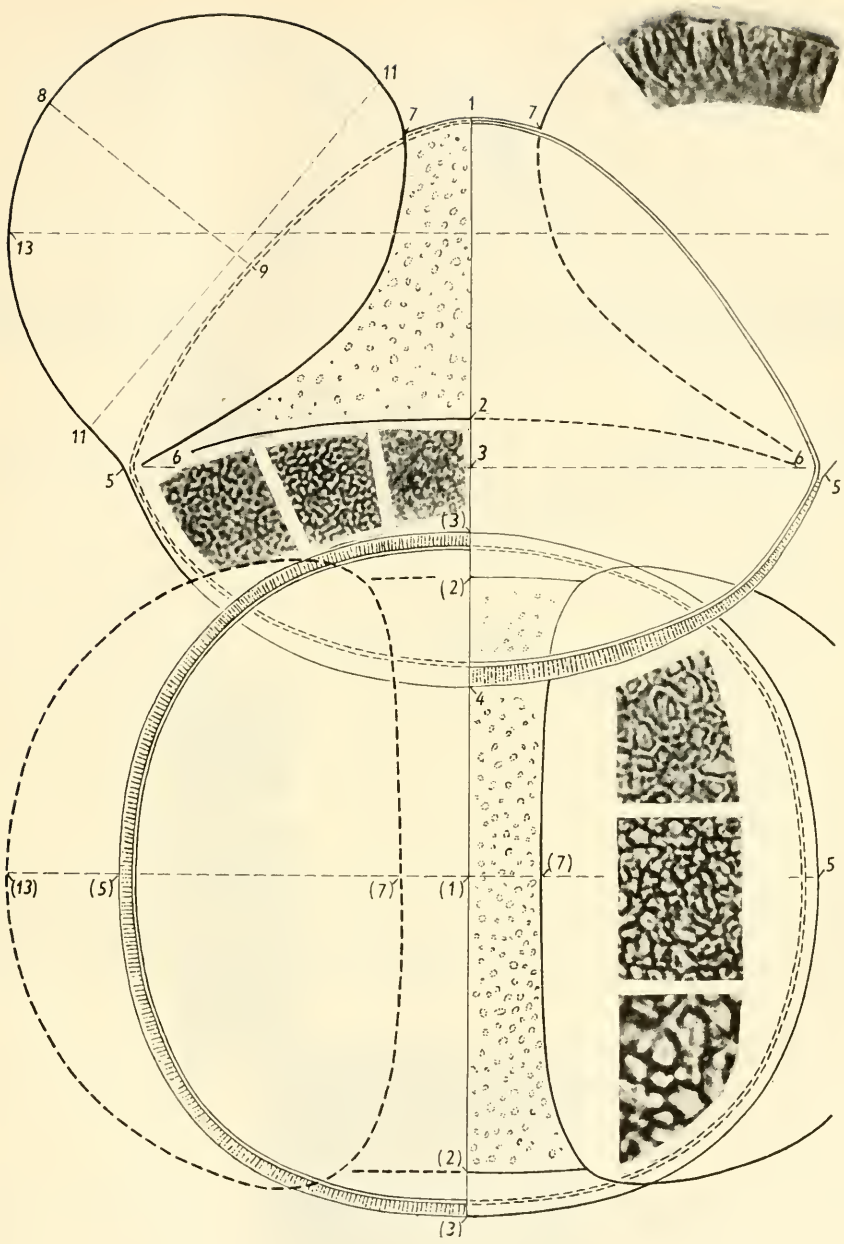

Fig. 53. *Picea jezoensis*; lateral, longitudinal view and distal face (surface and optical section; × 1000); for explanation of numerals see Fig. 2, p. 7. (From Erdtman in Svensk bot. Tidskr. 1954.)

PILGERODENDRON:—

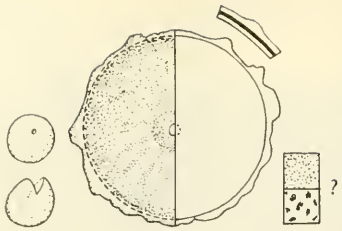

Fig. 54. *Pilgerodendron uviferum*. From left to right: two pollen grains (× 250); distal face (surface and optical section; × 1000); exine stratification (× 2000); LO-patterns.

PINUS:—

P. canariensis (Fig. 55), *P. excelsa* (Fig. 57), *P. mugo* (Fig. 56), *P. peuce* (Fig. 55), *P. pinea* (Fig. 55), *P. thunbergii* (Fig. 58).

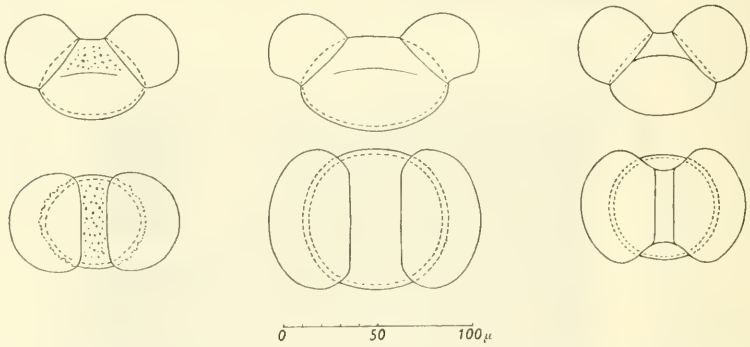

Fig. 55. Left, *Pinus peuce* (subg. Haploxylon). Centre, *P. canariensis* (subg. Diploxylon, sect. Sula). Right, *P. pinea* (subg. Diploxylon, sect. Pinea). × 250.

Fig. 56. *Pinus mugo*; section through saccus and, in the lower right-hand corner, part of the exine in the proximal face. About × 1000.

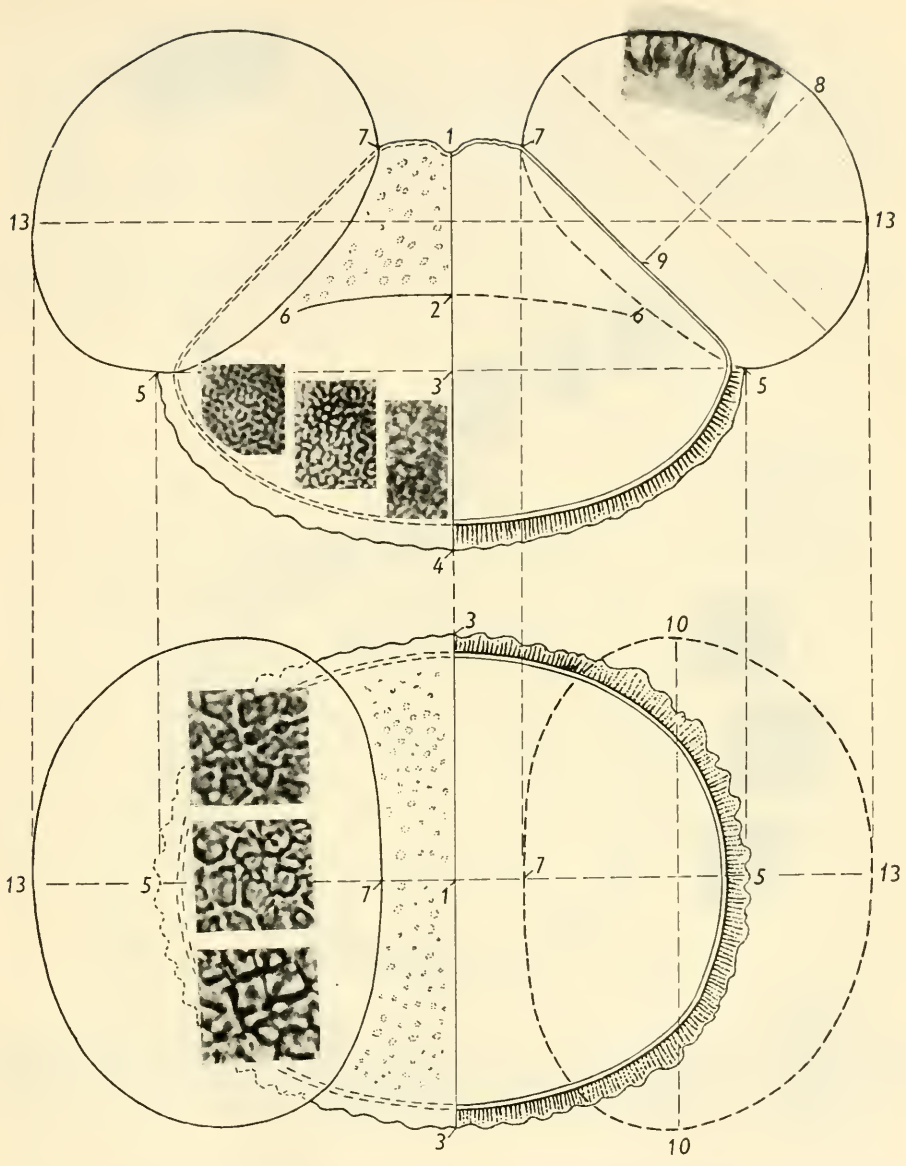

Fig. 57. *Pinus excelsa*; lateral, longitudinal view and distal face (surface and section; × 1000). For explanation of numerals see Fig. 2, p. 7. (From Erdtman in Svensk bot. Tidskr. 1954.)

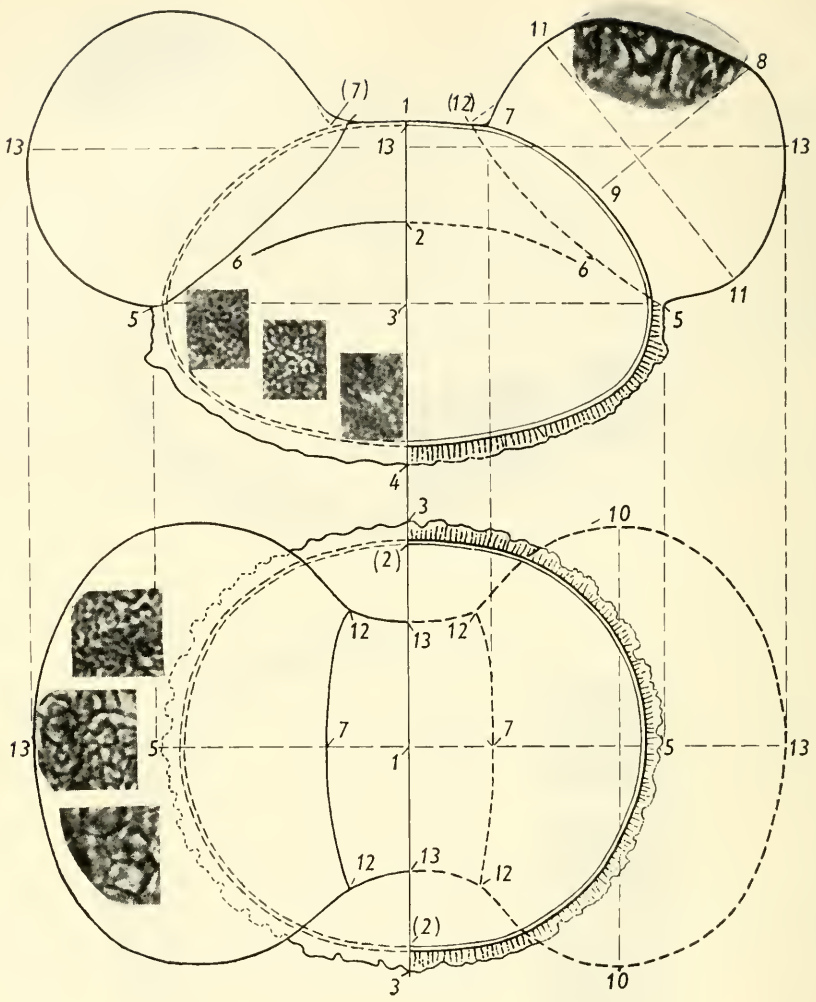

Fig. 58. *Pinus thunbergii*; lateral, longitudinal view and distal face (surface and section; × 1000). For explanation of numerals see Fig. 2, p. 7. (From Erdtman in Svensk bot. Tidskr. 1954.)

PODOCARPUS:—

P. alpinus var. *caespitosus* (Fig. 59 C), *P. angustifolius* var. *wrightii* (Fig. 59 A), *P. blumei* (Fig. 60 B), *P. coriaceus* (Fig. 59 B), *P. dacrydioides* (Fig. 60 A), *P. minor* (Fig. 61 C), *P. nagi* (Fig. 61 D), *P. nubigenus* (Fig. 61 B), *P. wallichianus* (Fig. 61 A).

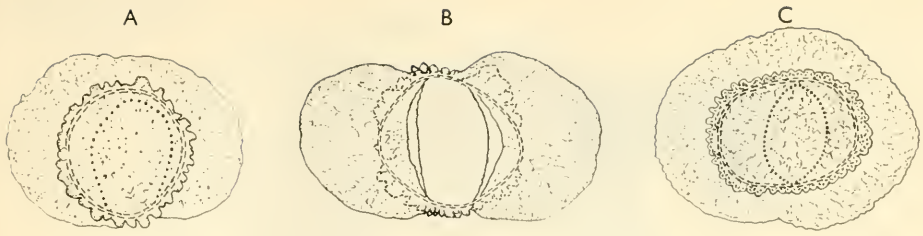

Fig. 59. A, *Podocarpus angustifolius* var. *wrightii*; proximal face. B, *P. coriaceus*; distal face. C, *P. alpinus* var. *caespitosus*; proximal face. × 250.

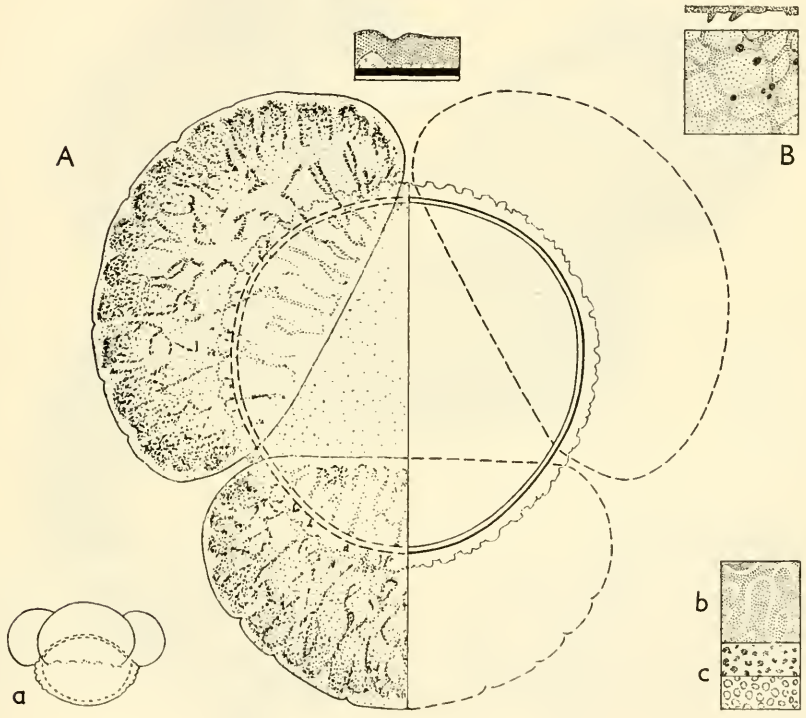

Fig. 60. A, *Podocarpus dacrydioides*; a, equatorial view (× 250); b, saccus pattern at high focus; c, pattern of distal face at high (upper detail figure) and low focus; above the main figure (× 1000) is an optical section through the exine at the amb (× 2000). — B, *P. blumei*; saccus pattern and optical section through the outer wall of the saccus.

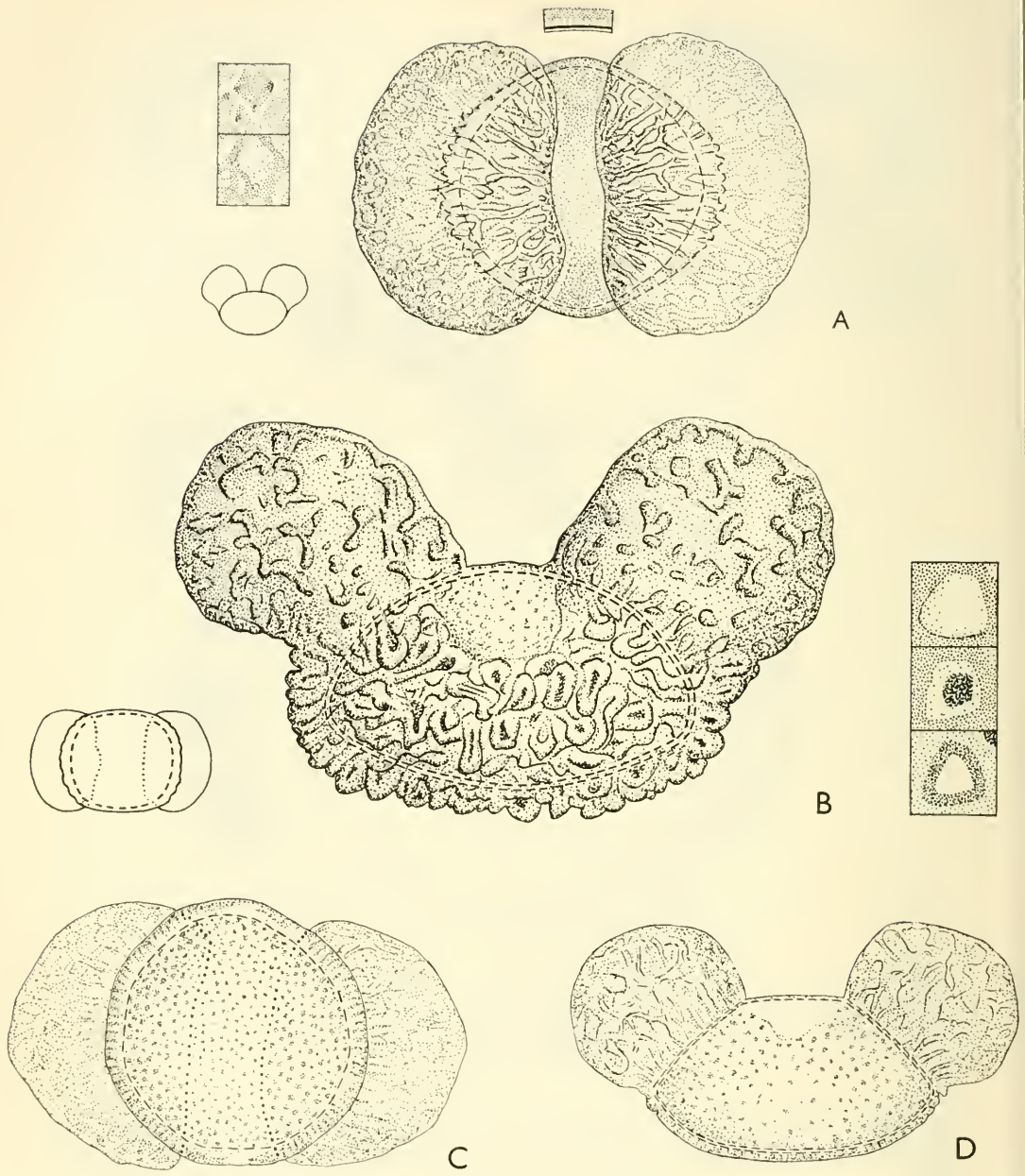

Fig. 61. A, *Podocarpus wallichianus*; lateral, longitudinal view (contour only; × 250), distal face (× 1000). B, *P. nubigenus*. From left to right: proximal face (× 250); lateral, longitudinal view (× 1000); LO-patterns (proximal face). C, *P. minor*; proximal face (× 1000). D, *P. nagi*; lateral, longitudinal view (× 1000).

PSEUDOLARIX:—

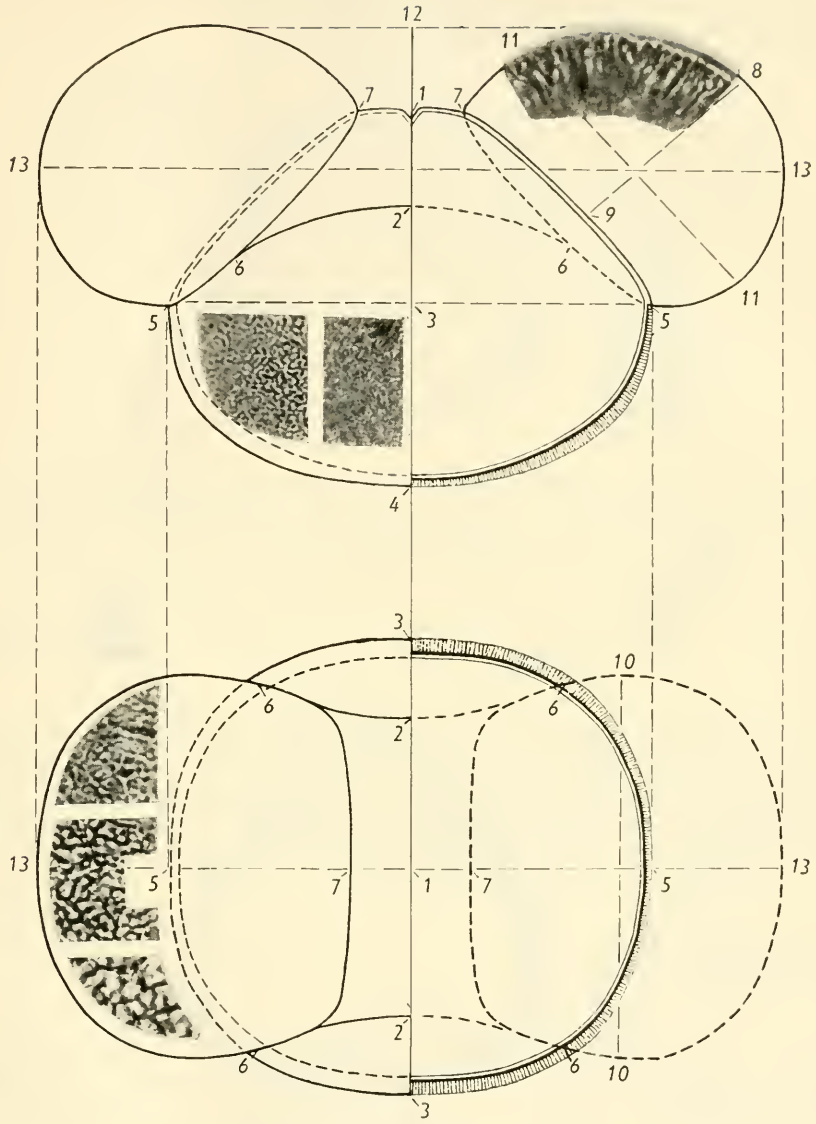

Fig. 62. *Pseudolarix amabilis*; lateral, longitudinal view and distal face (surface and optical section; × 1000). For explanation of numerals see Fig. 2, p. 7. (From Erdtman in Svensk bot. Tidskr. 1954.)

PSEUDOTSUGA:—

Megaspore membrane: *Pseudotsuga taxifolia* (Fig. 63 d).
Pollen grains: *Pseudotsuga taxifolia* (Fig. 63 a–c).

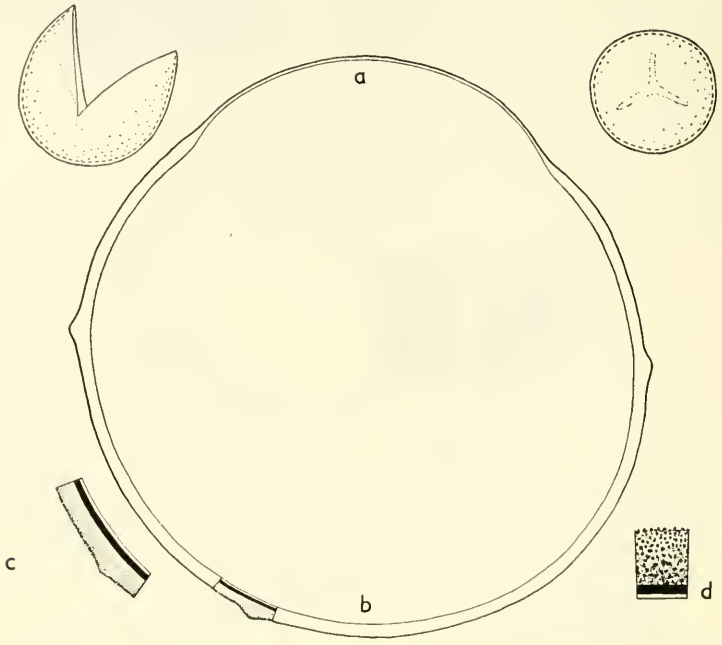

Fig. 63. *Pseudotsuga taxifolia*; a, distal pole (with tenuitas); b, proximal pole; c, part of the microspore exine (optical cross-section, × 2000); d, part of megaspore exine (optical cross-section, × 1000). The upper left-hand detail-figure shows the exine of an opened pollen grain (× 250), the upper right-hand detail-figure a young pollen grain with markings similar to a "tetrad scar".

SAXEGOTHAEA:—

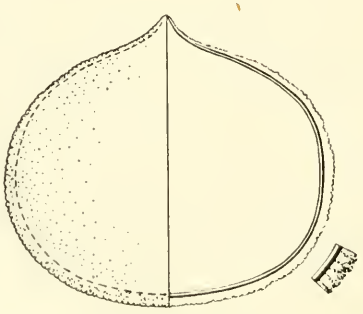

Fig. 64. *Saxegothaea conspicua;* lateral view, surface and optical cross-section (× 1000).

SCIADOPITYS:—

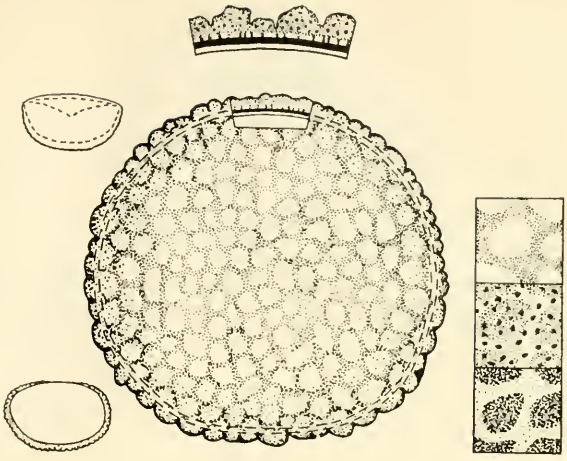

Fig. 65. *Sciadopitys verticillata*; proximal face (× 1000), exine stratification (× 2000), and LO-patterns. Upper left-hand detail: lateral view (distal pole upwards; × 250). Lower left-hand detail: optical section (distal pole upwards; × 250).

SEQUOIA:—

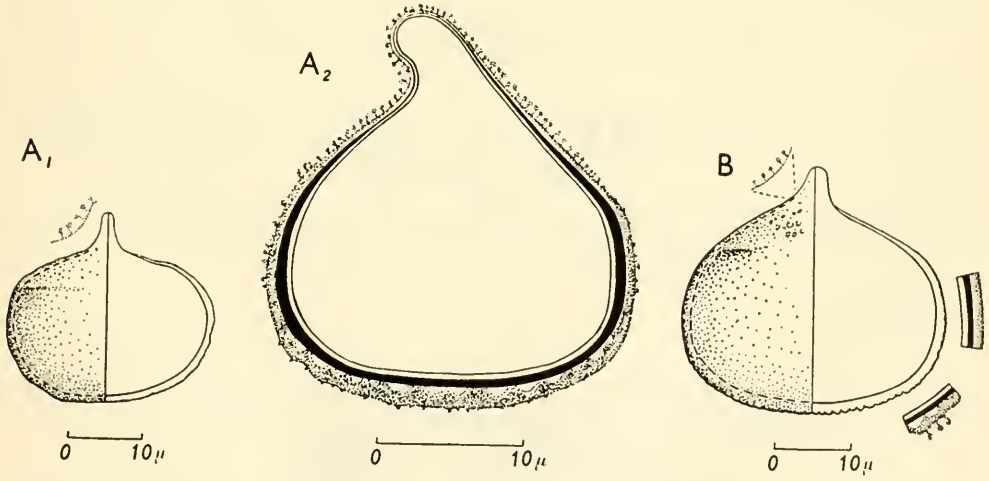

Fig. 66. A, *Sequoia* (*Sequoiadendron*) *gigantea*; lateral view, surface and optical cross-sections (A_1 × 1000, A_2 × 2000). B, *S. sempervirens*; lateral view (surface and section; × 1000).

SEQUOIADENDRON: see Fig. 66 A.

STANGERIA:—

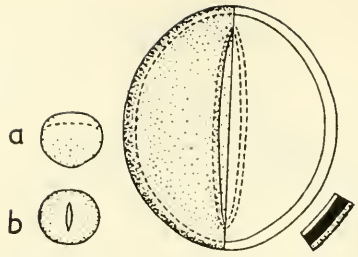

Fig. 67. *Stangeria paradoxa*; distal face (surface and optical section; × 1000); a, lateral view (×250); b, distal face of a grain more broad than long (×250).

TAIWANIA:—

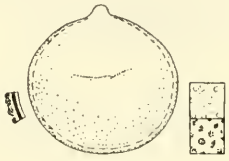

Fig. 68. *Taiwania cryptomerioides.* From left to right: exine stratification (× 2000); lateral view (× 1000); LO-patterns.

TAXODIUM:—

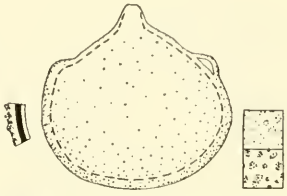

Fig. 69. *Taxodium mucronatum.* From left to right: exine stratification (×2000); lateral view (× 1000); LO-patterns.

TAXUS:—

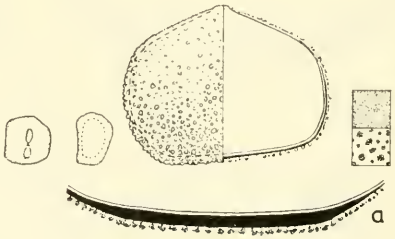

Fig. 70. *Taxus baccata.* From left to right: distal face (× 250); proximal face (× 250); lateral view (surface and optical section; × 1000); LO-patterns. a, exine stratification (× 2000).

THUJOPSIS:—

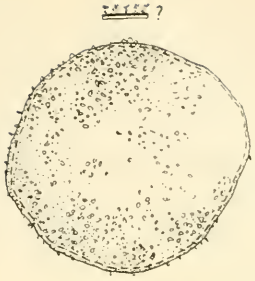

Fig. 71. *Thujopsis dolabrata*; surface (× 1000) and exine stratification (× 2000).

TORREYA:—

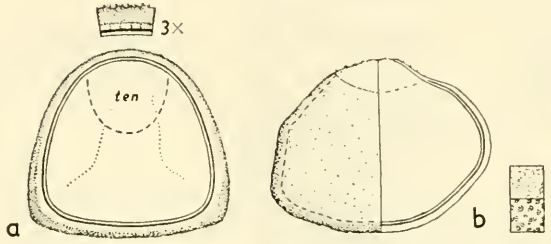

Fig. 72. a, *Torreya californica*; optical section (× 1000) and exine stratification (× 3000). b, *T. nucifera*; lateral view (surface and optical section; × 1000) and LO-patterns.

TSUGA:—

T. chinensis (Fig. 73 m, o), *T. diversifolia* (Fig 73 g, h), *T. dumosa* (Fig. 73 k), *T. forrestii* (Fig. 73 a–f), *T. pattoniana* (Fig. 73 n), *T. sieboldii* (Fig. 73 i, j), *T. yunnanensis* (Fig. 73 l).

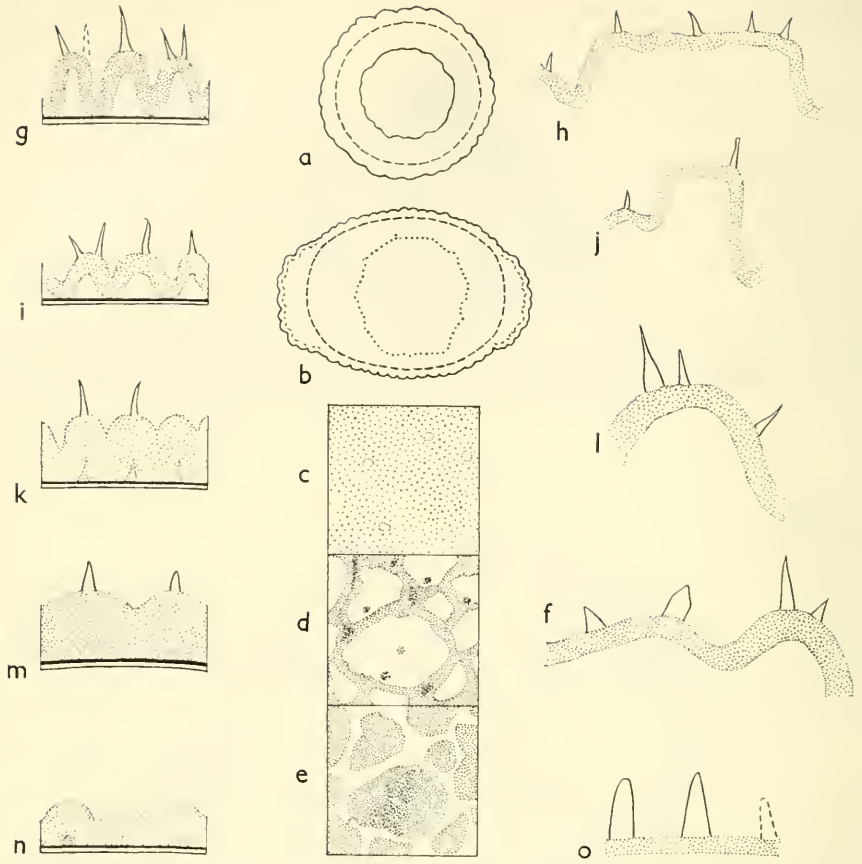

Fig. 73. a–f, *Tsuga forrestii*; a, distal face (outline; × 250); b, proximal face (outline of an aberrant grain; × 250); c–e, LO-patterns [c: four spinules (L); d: the same spinules (O) and upper parts of the undulating tegillum (L); e: the fleck near the centre (L) is a small infrategillar hollow, also vaguely shown in d (O)]; f, tegillum. — Left column (g, i, k, m, n): outline of exine stratification, proximal face (× 2000); g, *T. diversifolia*; i, *T. sieboldii*; k, *T. dumosa*; m, *T. chinensis*; n, *T. pattoniana*. — Right column (h, j, l, f, o): tegillum of the puffy frill (× 2000); h, *T. diversifolia*; j, *T. sieboldii*; l, *T. yunnanensis*; f, *T. forrestii*; o, *T. chinensis*.

WELWITSCHIA: see Fig. 30 C, p. 19.

WIDDRINGTONIA: see Fig. 42 C, p. 26.

PTERIDOPHYTA

Pl. III (facing p. 94); Figs. 74–191.

MEGASPORES

Isoetaceae: Figs. 123–125 (pp. 67, 68).
Pilulariaceae: Fig. 162 d, p. 87.
Selaginellaceae: Pl. III; Figs. 171–173 (pp. 90, 91).

ISOSPORES AND MICROSPORES

Families (in accordance with Engler's Syllabus, 12. Ed., Vol. 1, 1954):

Angiopteridaceae: Fig. 144 A–C (p. 79).
Azollaceae: Fig. 85 (p. 50).
Christenseniaceae: Fig. 144 D (p. 79).
Cyatheaceae: Figs. 78 (p. 47), 96 (p. 56), 112 (p. 62).
Danaeaceae: Fig. 144 F (p. 79).
Dicksoniaceae: Figs. 101 (p. 58), 169 B (p. 90), 186 (p. 95).
Dipteridaceae: Fig. 103 (p. 58).
Equisetaceae: Fig. 106 (p. 60).
Gleicheniaceae: Fig. 114 (p. 63).
Hymenophyllaceae: Fig. 188 (p. 96).
Hymenophyllopsidaceae: Figs. 119, 120 (pp. 65, 66).
Isoetaceae: Figs. 126, 127 (p. 68).
Loxsomaceae: Fig. 136 (p. 73).
Lycopodiaceae: Pl. III; Figs. 138–142 (pp. 75–77), 161 (p. 87).
Marattiaceae: Fig. 144 E (p. 79).
Marsileaceae: Fig. 145 (p. 80).
Matoniaceae: Fig. 159 (p. 86).
Ophioglossaceae: Figs. 89, 90 (pp. 52, 53).
Osmundaceae: Fig. 155 (p. 84).
Parkeriaceae: Figs. 89, 90 (pp. 52, 53).
Pilulariaceae: Fig. 162 a–c (p. 87).
Plagiogyriaceae: Fig. 163 (p. 88).
Polypodiaceae: Figs. 74–77, 81–84, 86–88, 91–95, 97–101, 103–107, 109–111, 115–117, 122, 128–132, 135, 146, 147, 149, 151, 152, 154, 156, 158, 164, 165, 167–169, 183–186, 189–191.
Protocyatheaceae: Figs. 79 (p. 47), 113 (p. 71), 134 (p. 72).
Psilotaceae: Fig. 166 (p. 89).
Salviniaceae: Fig. 170 (p. 90).
Schizaeaceae: Fig. 143 (p. 78).
Selaginellaceae: Figs. 174–182 (pp. 91–94).
Tmesipteridaceae: Fig. 187 (p. 96).

ACROSTICHUM:—

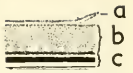

Fig. 74. *Acrostichum aureum* f. *hastaefolium*. Sclerine stratification (× 2000). a, perine; b, cf. sexine; c, cf. nexine.

ACTINIOPTERIS:—

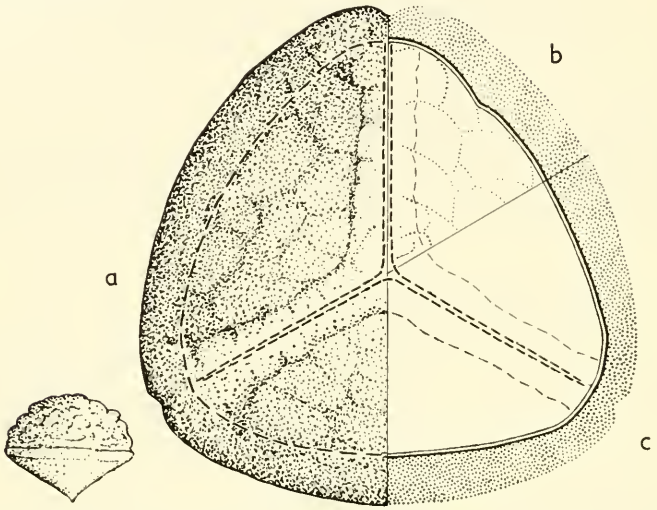

Fig. 75. *Actiniopteris australis*. Spore in lateral view (left; × 250); proximal face, surface (a) and optical section (b + c; in b the contours of the verrucae in the distal face are marked; the faint nick in the nexine is quite accidental; × 1000).

ADIANTOPSIS:—

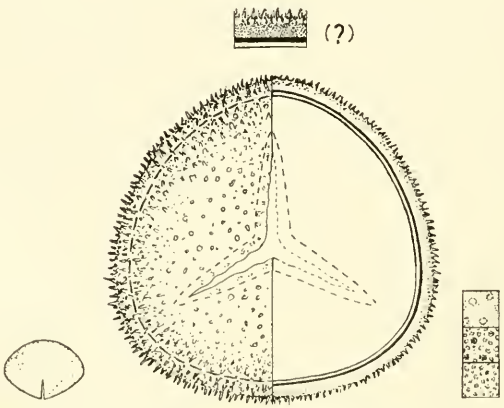

Fig. 76. *Adiantopsis chlorophylla*. From left to right: spore in lateral view (× 250); proximal face (× 1000; surface and optical section); LO-patterns.

ADIANTUM:—

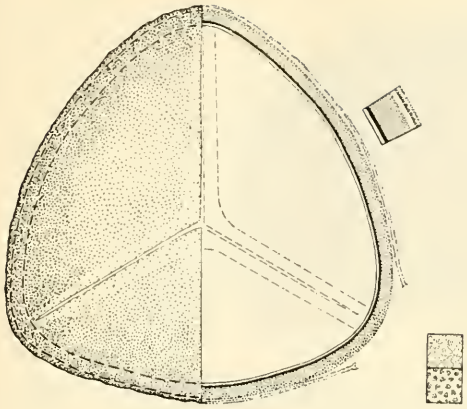

Fig. 77. *Adiantum reniforme*. Proximal face, surface (left) and optical section (right; × 1000).

ALSOPHILA:—

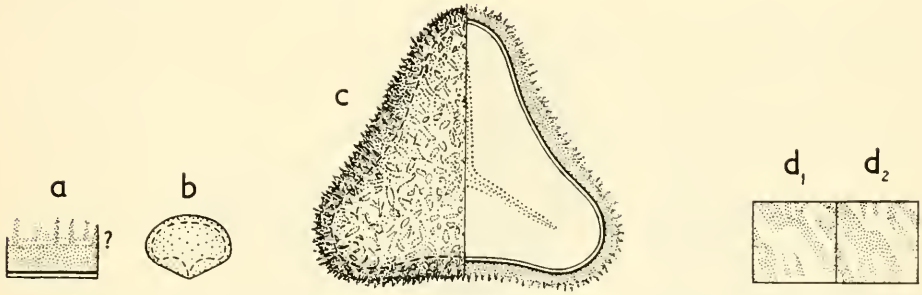

Fig. 78. *Alsophila glabra*; a, sclerine stratification (× 2000); b, spore, lateral view (× 250); c, distal face (× 1000), surface (left) and optical section (right); d_1 and d_2, LO-patterns.

AMPHIDESMIUM:—

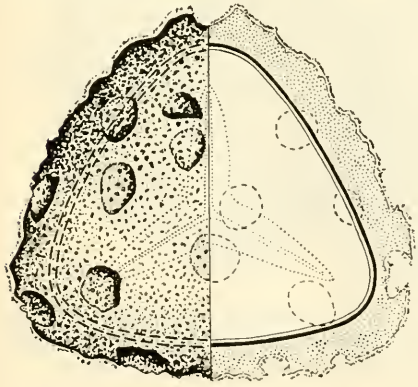

Fig. 79. *Amphidesmium blechnoides*. Distal face (× 1000), surface (left) and optical section (right).

ANARTHROPTERIS:—

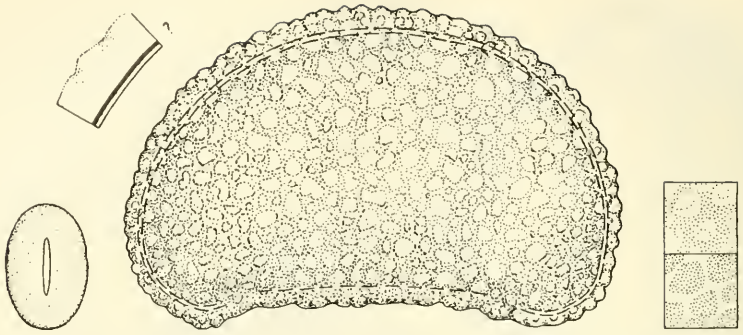

Fig. 80. *Anarthropteris dictyopteris.* From left to right: proximal face (× 250); exine stratification (with a query; × 2000); spore in lateral view (× 1000); LO-patterns.

ANEMIA: see Fig. 143 G–I, p. 78.

ANGIOPTERIS: see Fig. 144 A, p. 79.

ARCHANGIOPTERIS: see Fig. 144 C, p. 79.

ASPLENIOPSIS:—

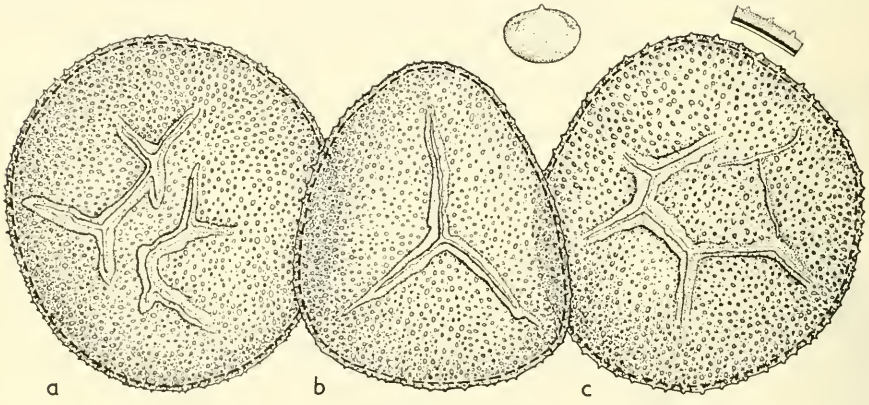

Fig. 81. *Aspleniopsis decipiens*; a and c, deviating spores; b, normal spore (proximal face; × 1000). Upper right-hand details: lateral view (proximal face up; × 250); exine stratification (× 2000).

ASPLENIUM:—

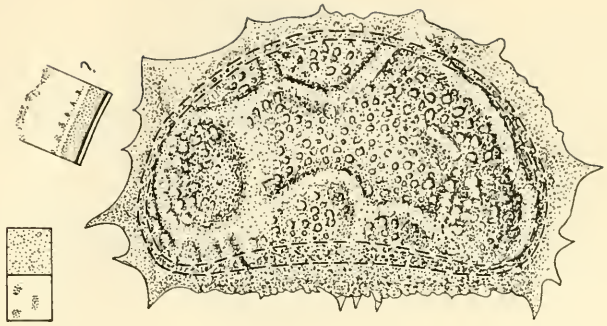

Fig. 82. *Asplenium monanthes.* From left to right: LO-patterns; sclerine stratification (× 2000); spore in lateral view (× 1000).

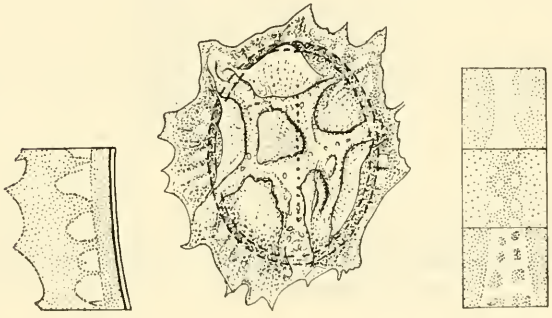

Fig. 83. *Asplenium hemionitis.* From left to right: sclerine stratification (× 2000); distal face (× 1000); LO-patterns.

ATHYRIUM:—

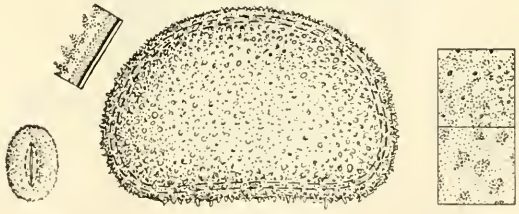

Fig. 84. *Athyrium filix-femina.* From left to right: proximal face (× 250); sclerine stratification (× 2000); spore in lateral view; LO-patterns.

AZOLLA:—

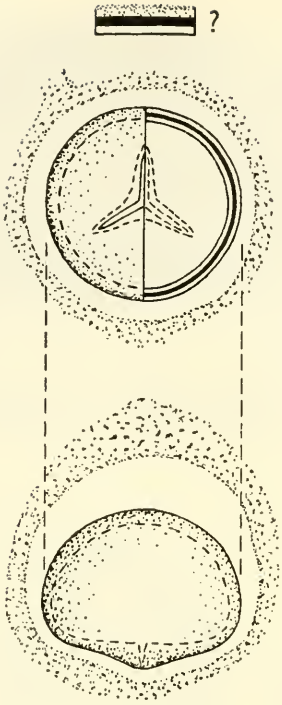

Fig. 85. *Azolla filiculoides*, microspores. From above to below: exine stratification (× 2000); proximal face (× 1000; spore surrounded by perine); spore in lateral view (× 1000).

BLECHNUM:—

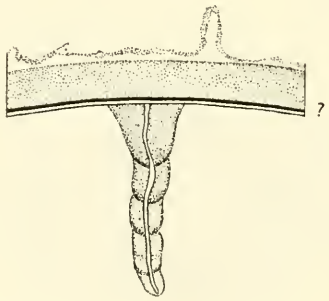

Fig. 86. *Blechnum palmiforme*, part of the sclerine (optical section, × 2000). Attached to the inner surface of the exine is a peculiar (abnormal) process leading into the interior of the spore.

BOLBITIS:—

Fig. 87. *Bolbitis turrialbae*. From left to right: proximal face (× 250); sclerine stratification (× 2000); lateral, longitudinal view (× 1000).

BOTRYCHIUM: a note on the spores in *B. simplex* is found in the caption of Fig. 153, p. 83.

BRAINEA:—

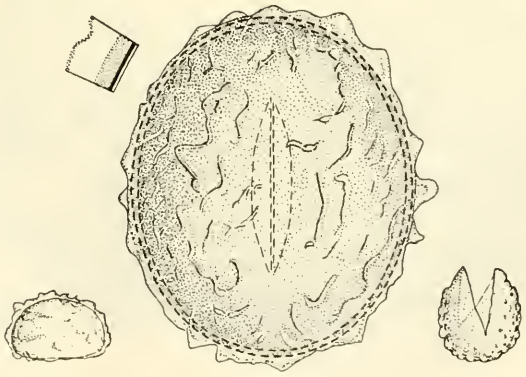

Fig. 88. *Brainea insignis*. From left to right: lateral, longitudinal view (×250); sclerine stratification (× 2000); proximal face (× 1000); deviating spore (× 250).

CERATOPTERIS:—

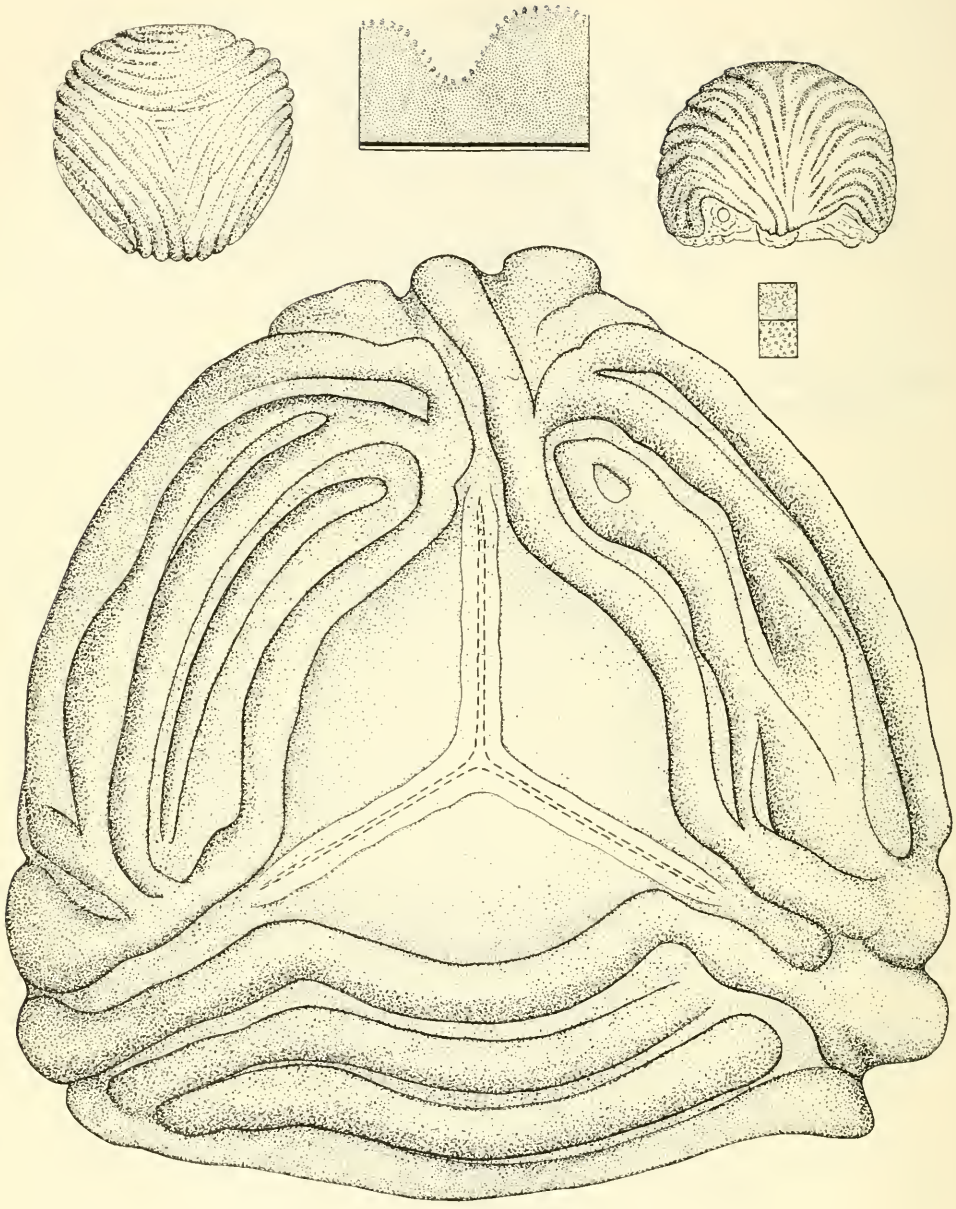

Fig. 89. *Ceratopteris siliquosa*, proximal face (× 1000); upper detail figures (from left to right): distal face (× 250); sclerine stratification (× 2000); lateral view (× 250) and LO-patterns.

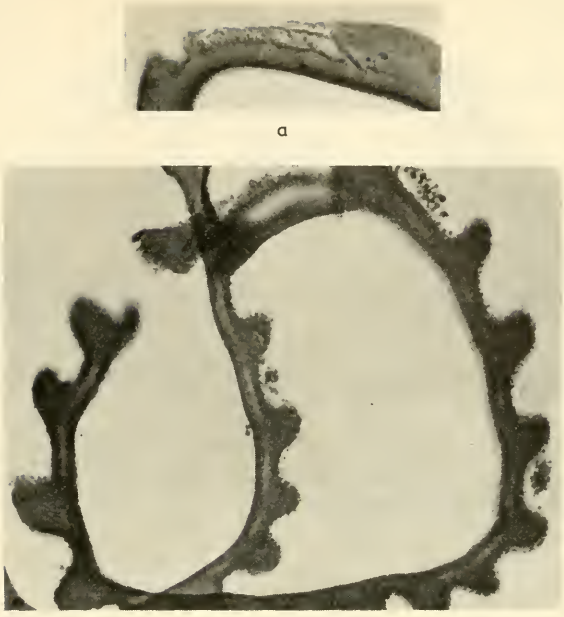

Fig. 90. *Ceratopteris siliquosa*. Sections through acetolyzed sclerine. The sclerine, as shown in b, consists of a thin perine (the outermost granular layer) and a thick exine faintly subdivided into cf. sexine (showing ± parallel ridges separated by U-shaped valleys) and cf. nexine (of equal thickness throughout). The upper figure (a) intimates that the sexine has a fine (granular) structure. × 700.

CETERACH:—

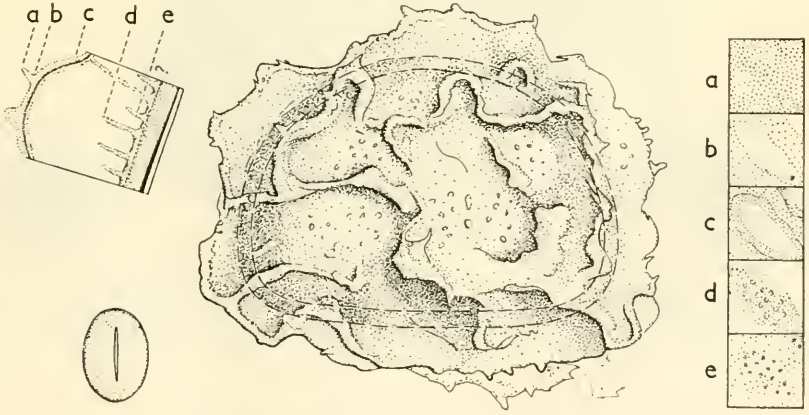

Fig. 91. *Ceterach officinarum*. From left to right: proximal face (× 250); sclerine stratification (× 2000); lateral, longitudinal view (× 1000); LO-patterns.

CHEIROPLEURIA:—

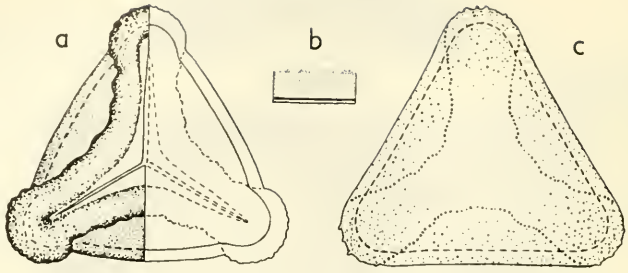

Fig. 92. *Cheiropleuria bicuspis*; a, proximal face (× 1000); b, sclerine stratification (× 2000); c, distal face (× 1000).

CHRISTENSENIA: see Fig. 144 D, p. 79.

CIBOTIUM:—

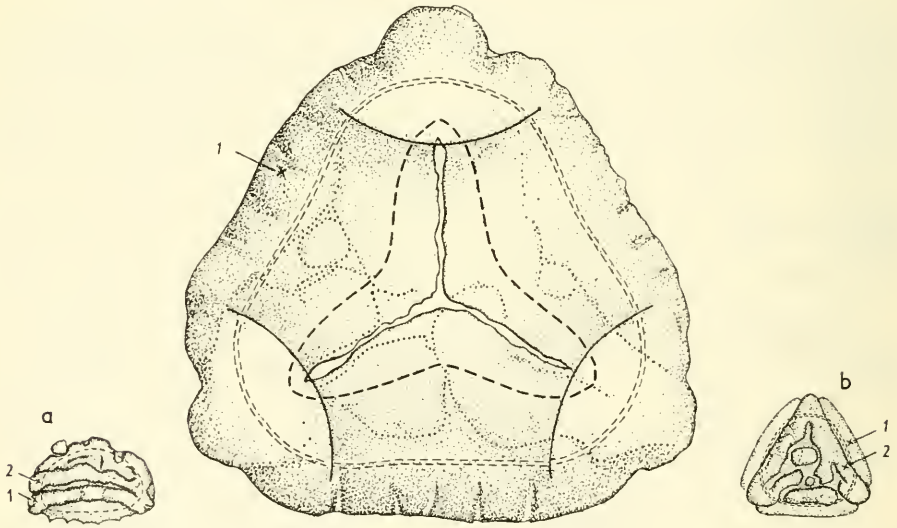

Fig. 93. *Cibotium barometz*, proximal face (× 1000). a, lateral view (× 250); b, distal face (× 250). 1 and 2, respectively, are identical.

CNEMIDARIA:—

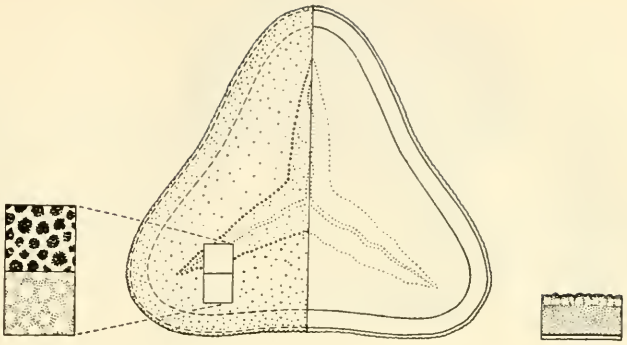

Fig. 94. *Cnemidaria speciosa*. From left to right: LO-patterns, distal face (× 1000) and sclerine stratification (× 2000).

CRYPTOGRAMMA:—

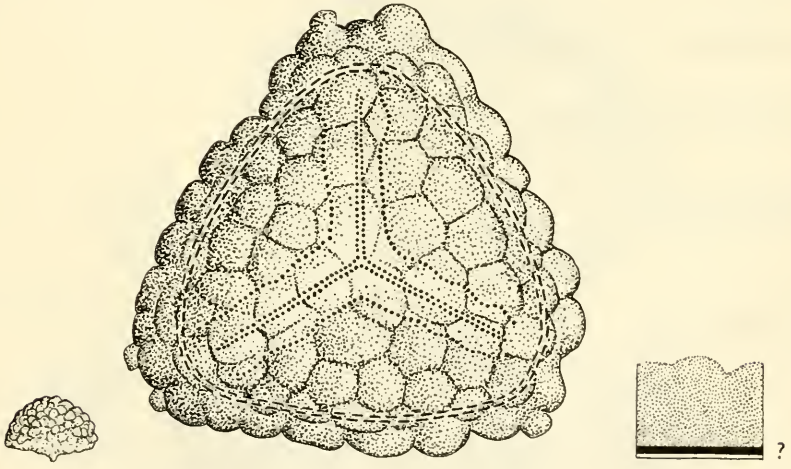

Fig. 95. *Cryptogramma brunoniana*. From left to right: lateral view (× 250), distal face (× 1000), exine stratification (× 2000).

CYATHEA (see also HEMITELIA):—

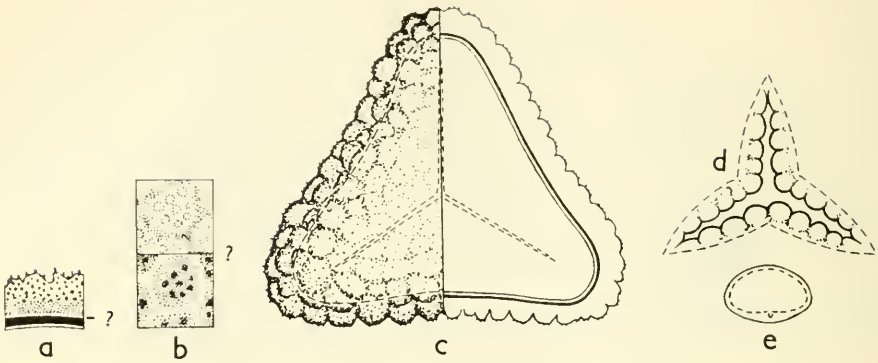

Fig. 96. *Cyathea vestita*. a, sclerine stratification (× 2000); b, LO-patterns; c, distal face (aperture wrongly marked by broken instead of dotted lines); d, laesura (open); e, lateral view (× 250).

CYCLOPHORUS: see PYRROSIA, p. 89.

CYRTOMIUM: see PHANEROPHLEBIA, p. 85.

CYSTODIUM: see Fig. 169 B, p. 90.

CYSTOPTERIS:—

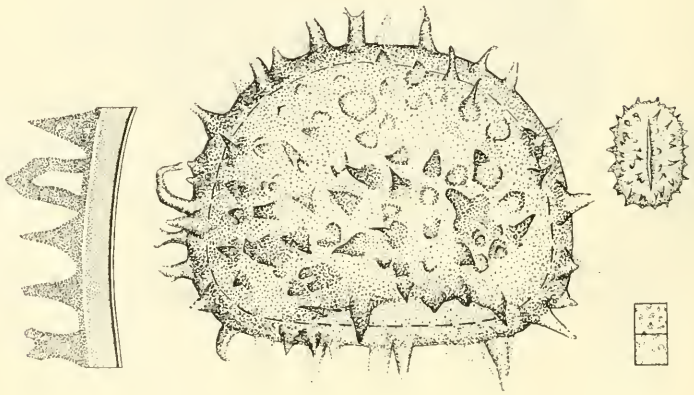

Fig. 97. *Cystopteris fragilis*. From left to right: sclerine stratification (× 2000); lateral, longitudinal view (× 1000); proximal face (× 250) and LO-patterns.

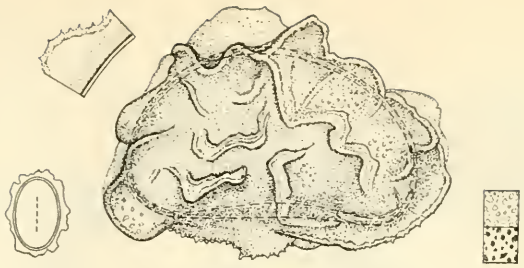

Fig. 98. *Cystopteris fragilis* f. *dickieana*. From left to right: proximal face (optical section, × 250); sclerine stratification (× 2000); lateral, longitudinal view (× 1000); LO-patterns.

DANAEA: see Fig. 144 F, p. 79.

DAVALLIA:—

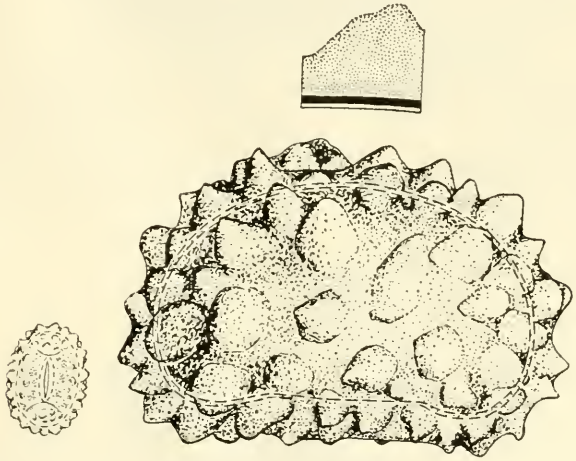

Fig. 99. *Davallia canariensis*. Proximal face (× 250); lateral, longitudinal view (× 1000), and exine stratification (× 2000).

DENNSTAEDTIA:—

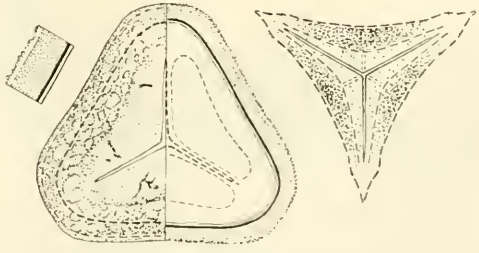

Fig. 100. *Dennstaedtia punctilobula*. From left to right: sclerine stratification (× 2000); proximal face, surface and section (× 1000); analysis of laesura.

DICKSONIA:—

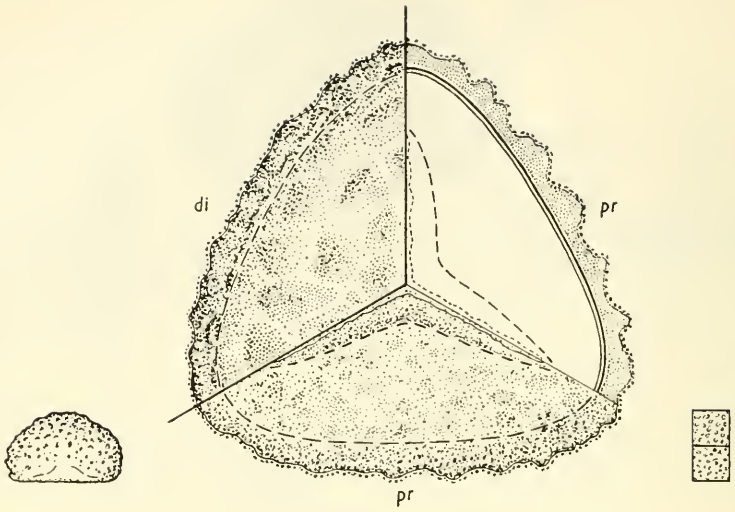

Fig. 101. *Dicksonia youngiae*. From left to right: lateral view (× 250); distal (di) and proximal (pr; surface and optical section) face; LO-patterns.

DIPLAZIUM:—

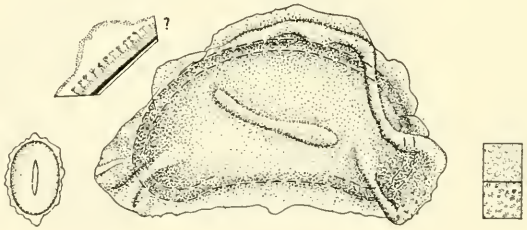

Fig. 102. *Diplazium proliferum*. From left to right: proximal face (× 250); sclerine stratification (× 2000); lateral, longitudinal view (× 1000); LO-patterns.

DIPTERIS:—

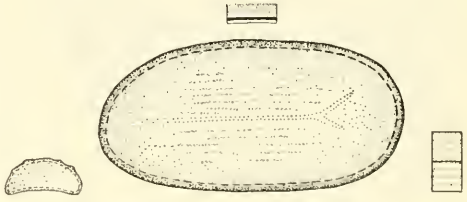

Fig. 103. *Dipteris chinensis*. From left to right: lateral, longitudinal view (× 250); distal face (× 1000) and exine stratification (× 2000); LO-patterns.

DRYMOGLOSSUM:—

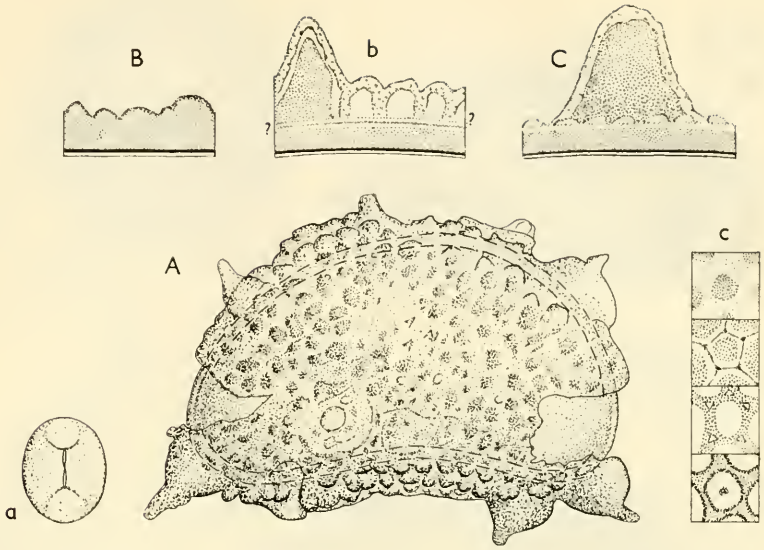

Fig. 104. A, *Drymoglossum heterophyllum*, lateral, longitudinal view (× 1000); a, proximal face (× 250); b and C, sclerine stratification (× 2000); c, LO-patterns. B, *D. carnosum*, sclerine stratification (× 2000).

DRYNARIA:—

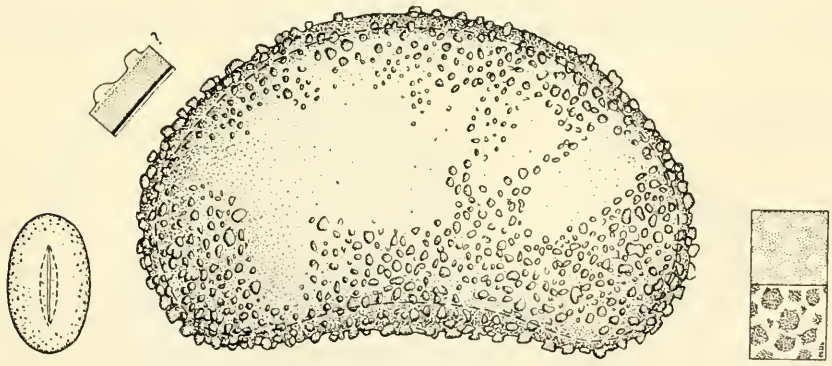

Fig. 105. *Drynaria fortunei*. From left to right: proximal face (× 250); sclerine stratification (× 2000); lateral, longitudinal view (× 1000); LO-patterns.

DRYOPTERIS:—

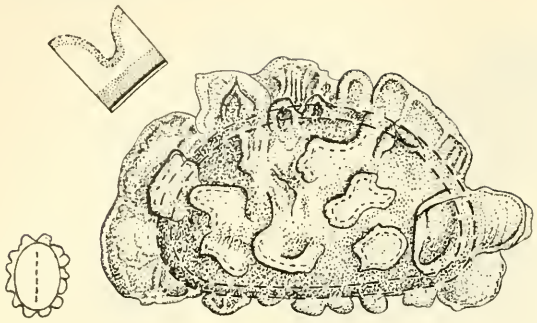

Fig. 106. *Dryopteris filix-mas.* From left to right: proximal face (optical section, × 250); sclerine stratification (× 2000); equatorial, longitudinal view (× 1000).

ELAPHOGLOSSUM:—

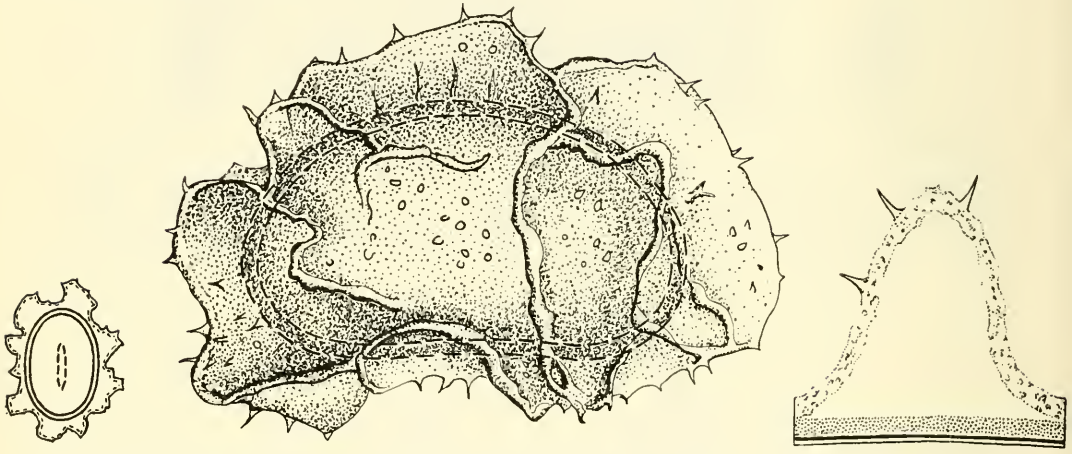

Fig. 107. *Elaphoglossum vieillardii.* From left to right: proximal face (optical section, × 250); lateral, longitudinal view (× 1000); sclerine stratification (× 2000).

EQUISETUM:—

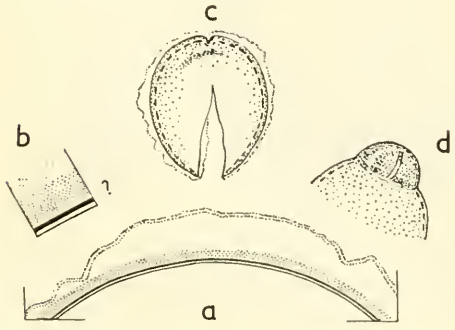

Fig. 108. *Equisetum giganteum.* a, part of sclerine of an acetolyzed spore, optical cross-section (× 1000); amplectators ("elaters", "hapters") dissolved; b, sclerine stratification (× 2000); c, opened spore (× 250); d, part of an abnormal spore tetrad (one large, three small spores; × 250).

GRAMMITIS:—

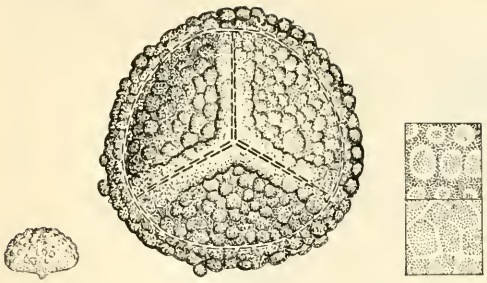

Fig. 109. *Grammitis deplanchei.* From left to right: lateral view (× 250); proximal face (× 1000); LO-patterns.

GYMNOGRAMME:—

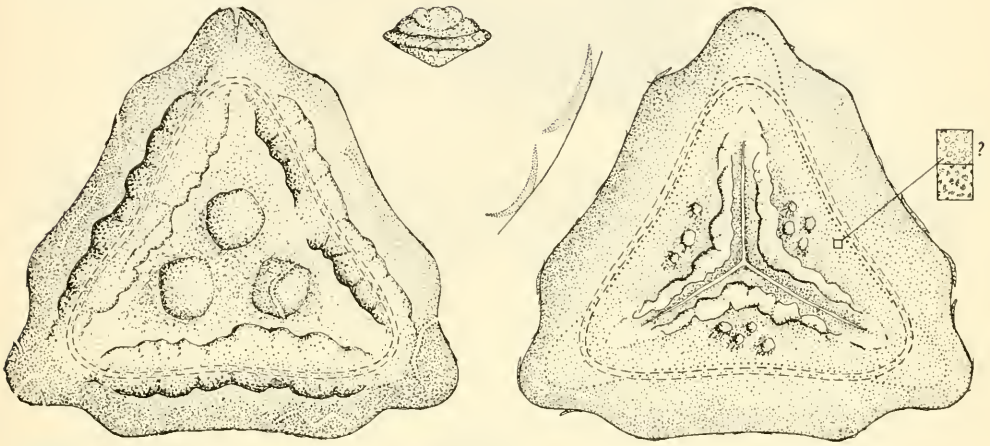

Fig. 110. *Gymnogramme* (*Eriosorus*) *congesta.* From left to right: distal face (× 1000); lateral view (× 250); cf. perine fragments (optical section, × 2000); proximal face (× 1000) and LO-patterns.

HEMIONITIS:—

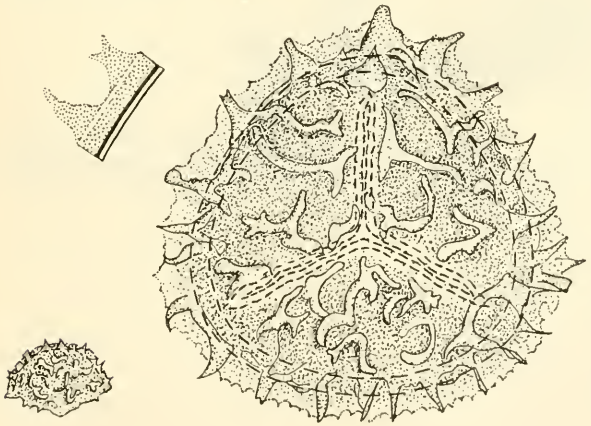

Fig. 111. *Hemionitis arifolia.* From left to right: lateral view (× 250); sclerine stratification (× 2000); proximal face (× 1000).

HEMITELIA:—

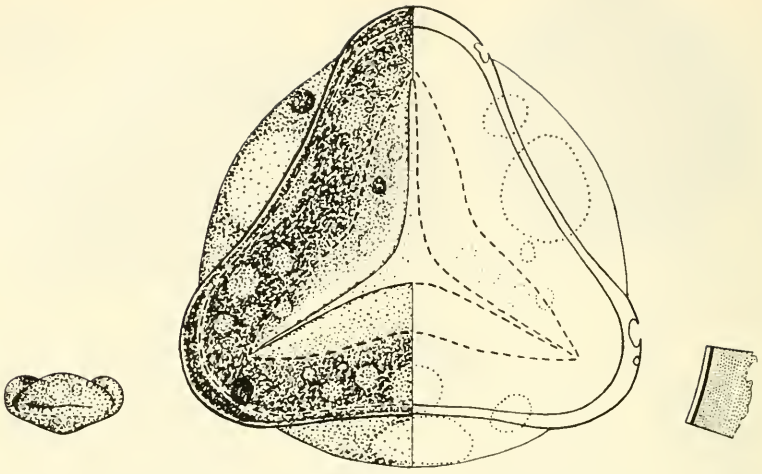

Fig. 112. *Hemitelia maxonii*. From left to right: lateral view (× 250); proximal face (surface and optical cross-section, × 1000); sclerine stratification (× 2000). From Erdtman in Potonié, Svensk bot. Tidskr. 1954.

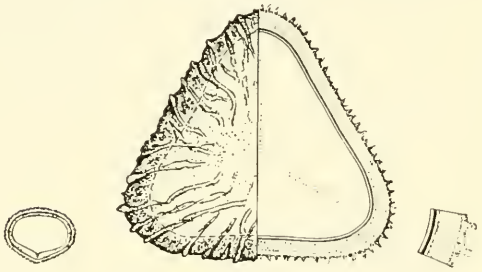

Fig. 113. *Hemitelia setosa*. From left to right: lateral view (× 250); distal face, surface and optical cross-section (× 1000); sclerine stratification (× 2000).

HICRIOPTERIS (Fig. 114 C), PLATYZOMA (Fig. 114 D), STICHERUS (Fig. 114 B), STROMATOPTERIS (Fig. 114 A):—

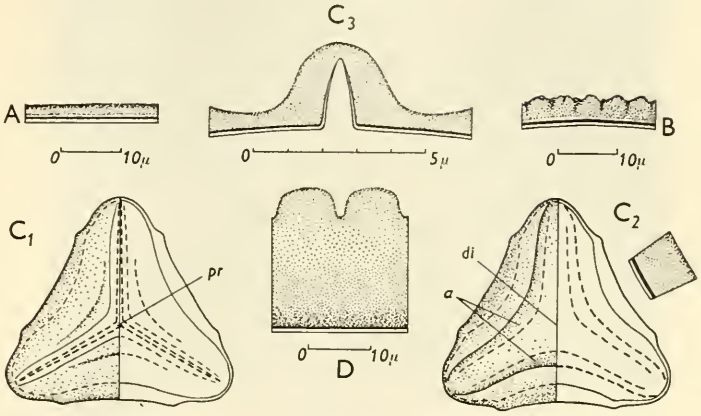

Fig. 114. Gleicheniaceae. A, *Stromatopteris moniliformis,* sclerine stratification. B, *Sticherus penniger,* sclerine stratification. C, *Hicriopteris laevissima*; C_1, proximal face; C_2, distal face; C_3, part of laesura (optical cross-section), C_4, LO-patterns of same. D, *Platyzoma microphyllum,* sclerine stratification. — A, B, D × 800, C_1 and C_2 × 1000, C_3 × 4600.

HISTIOPTERIS:—

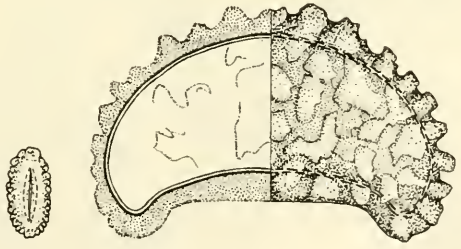

Fig. 115. *Histiopteris incisa*; proximal face (× 250) and lateral, longitudinal view (optical cross-section and surface; × 1000).

HOLTTUMIELLA:—

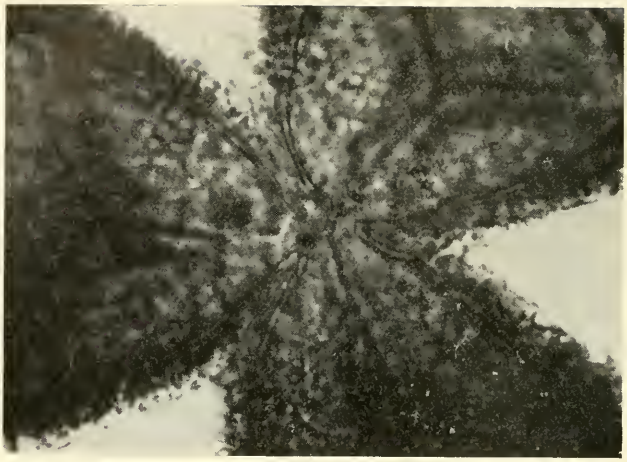

Fig. 116. *Holttumiella flabellivenium*. Three spores of a tetrad still slightly adhering. × 700.

HUMATA:—

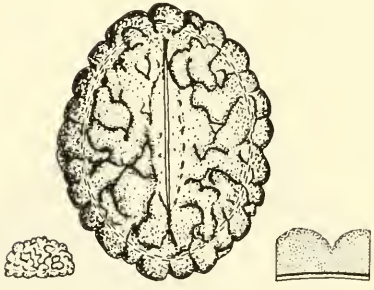

Fig. 117. *Humata gaimardiana*. From left to right: lateral, longitudinal view (× 250); proximal face (× 1000); sclerine stratification (× 2000).

HYMENOGLOSSUM: see Fig. 188 C, p. 96.

HYMENOLEPIS:—

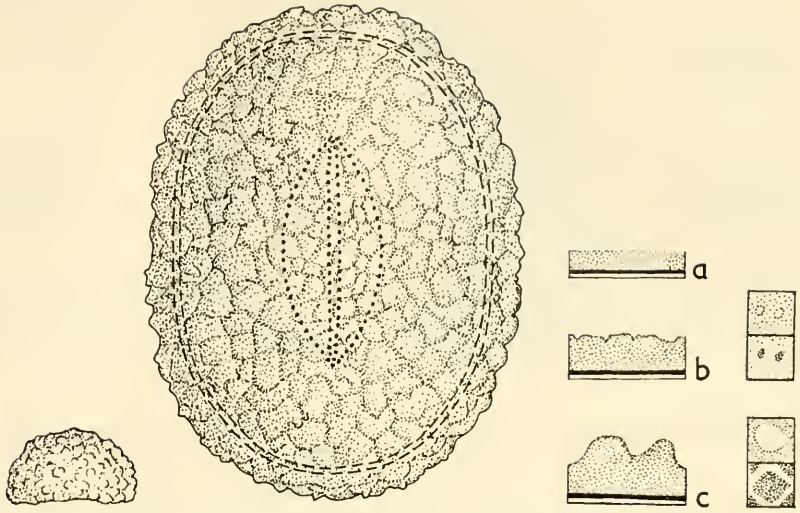

Fig. 118. *Hymenolepis spicata.* From left to right: lateral, longitudinal view (× 250); distal face (× 1000); a–c, exine stratification showing the successive increase in thickness (× 2000); LO-patterns.

HYMENOPHYLLOPSIS (Figs. 119, 120):—

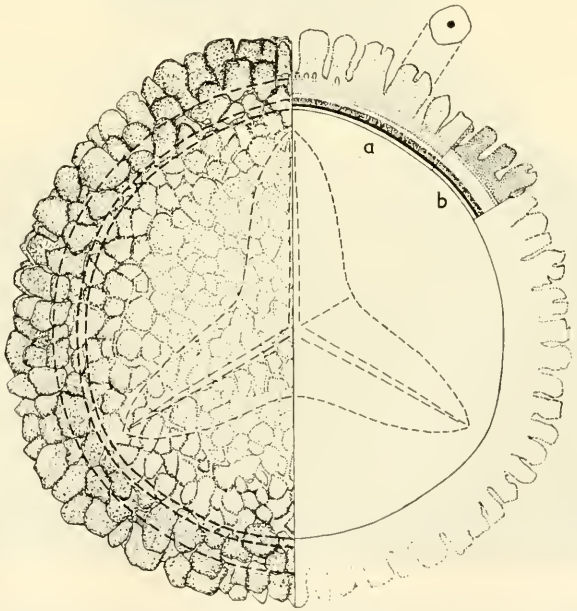

Fig. 119. *Hymenophyllopsis asplenioides,* proximal face, surface and optical cross-section (× 1000). In some spores the sclerine stratification appears as indicated at a, and in other spores as indicated at b.

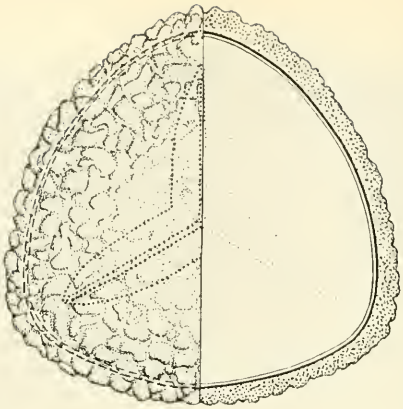

Fig. 120. *Hymenophyllopsis dejecta*; distal face (surface and optical cross-section). × 1000.

HYMENOPHYLLUM (see also Fig. 188 C, p. 96):—

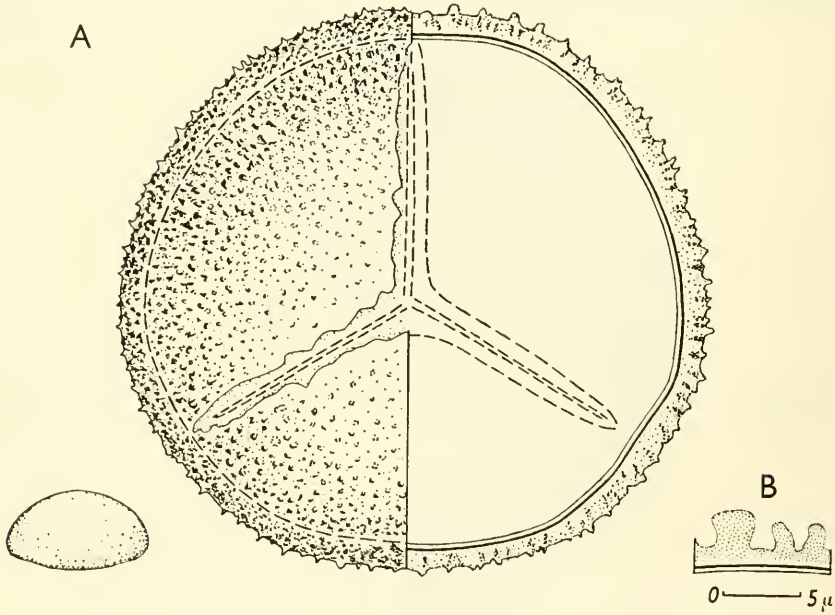

Fig. 121. A, *Hymenophyllum recurvum*; lateral view (× 250) and proximal face, surface and optical cross-section (× 1000). B, *H. peltatum*, exine stratification (× 2000).

HYPOLEPIS:—

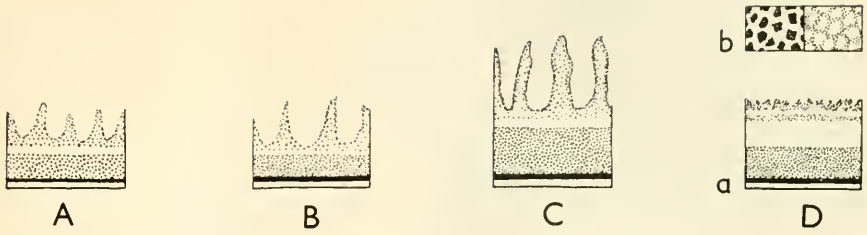

Fig. 122. Sclerine stratification in *Hypolepis*. A, *H. repens*. B, *H. tenuifolia*. C, *H. rugosula*. D:a, *H. distans*. (× 2000). — LO-patterns at high (left) and low (right) focus in *H. distans* are shown in D:b.

ISOËTES:—

Megaspores: *Isoëtes durieui* (Fig. 123), *I. echinosporum* (Figs. 124, 125).
Microspores: *Isoëtes adspersa* (Fig. 126), *I. baetica* (Fig. 127).

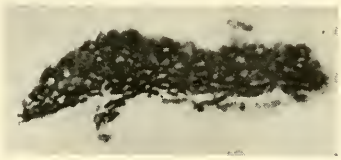

Fig. 123. *Isoëtes durieui*, part of megaspore wall (section). × 1000.

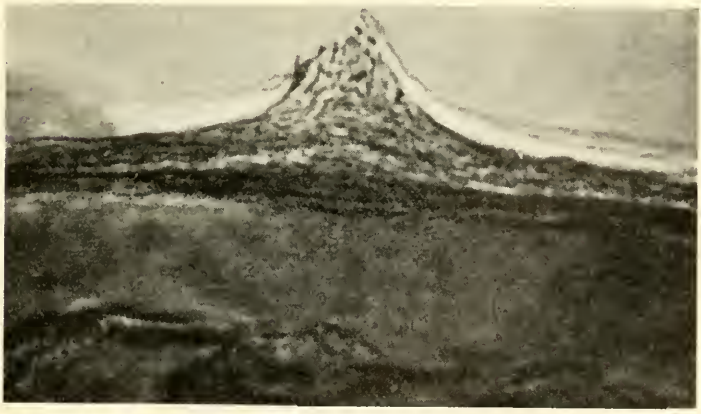

Fig. 124. *Isoëtes echinosporum*; part of megaspore wall (optical section). The inner contour of the silicified perine is faintly seen left and right of the cf. sexinous outgrowth in the centre of the figure. The "sexine" is underlain by thinner "nexine". × 2000.

Fig. 125. *Isoëtes echinosporum*, acetolyzed megaspore embedded in glycerine jelly (× 125). In some places the spiny perine is faintly shown.

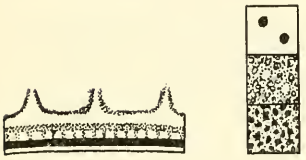

Fig. 126. *Isoëtes adspersa*; sclerine stratification and LO-patterns. A thin cf. perine with hollow, tapering processes, open at top (OL), is underlain by an exine consisting of a tegillate and baculate sexine (LO = bacula) and nexine.

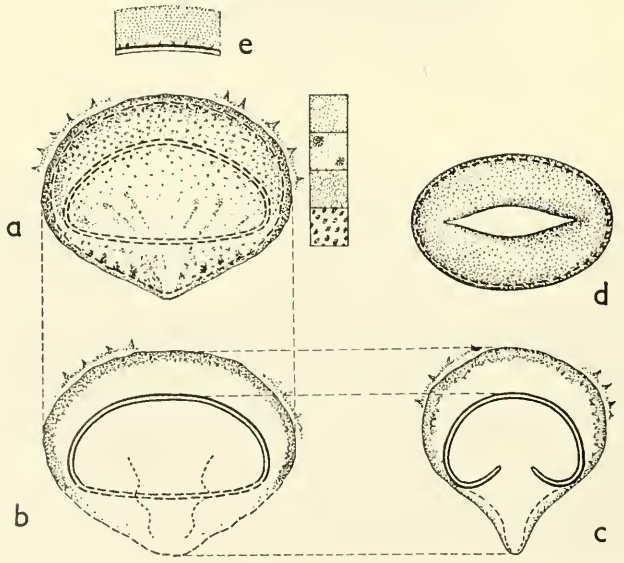

Fig. 127. *Isoëtes baetica*. a, lateral, longitudinal view (surface); b, lateral, longitudinal view (optical section); c, lateral transverse view (optical section); c, lateral transverse view (optical section); d, polar view (proximal face; sculptine not included); e, exine from a young spore with sexine still adhering to the nexine; × 4000 (a–d × 1000).

ISOLOMA:—

Fig. 128. *Isoloma divergens.* From left to right: proximal face (×250); lateral, longitudinal view (× 1000); exine stratification.

JAMESONIA:—

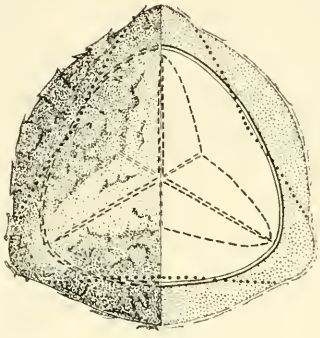

Fig. 129. *Jamesonia imbricata*; proximal face, surface and optical section (× 1000).

LASTREA:—

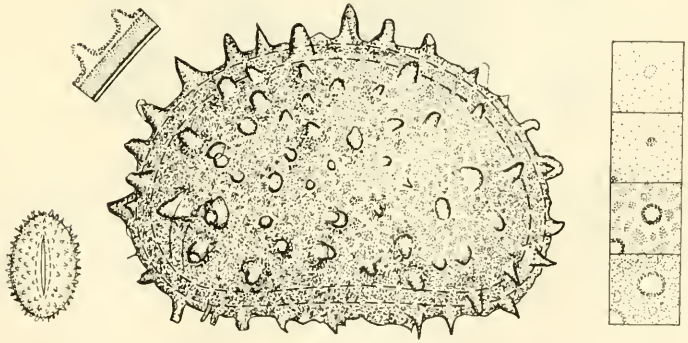

Fig. 130. *Lastrea thelypteris.* From left to right: proximal face (× 250); sclerine stratification (× 2000); lateral, longitudinal view (× 1000); LO-patterns.

LEPTOLEPIA:—

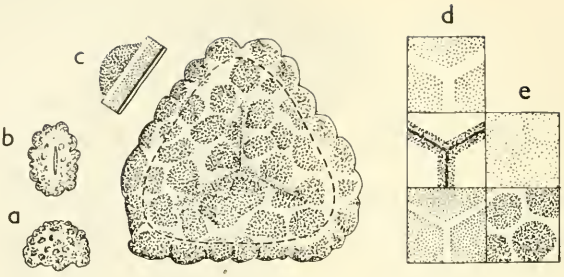

Fig. 131. *Leptolepia novae-zelandiae*; proximal face (× 1000). — a, equatorial view (× 250); b, proximal face of monolete spore (× 250); c, sclerine stratification showing perine (densely dotted) on the outside of the exine; d, proximal pole at various focuses from high (above) to low; e, general surface of spore at different focuses. — N.B. Exceptionally, the "verrucae" in the main figure are shown at low focus (i.e. dark), and not, as otherwise in this book, at high focus (bright).

LEPTOPTERIS: see Fig. 155 G, p. 84.

LINDSAEA:—

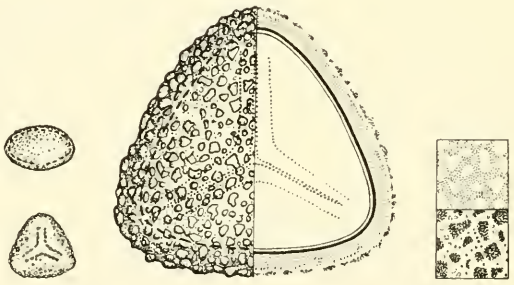

Fig. 132. *Lindsaea orbiculata*. From left to right: lateral view and proximal face (both × 250); distal face (× 1000); LO-patterns.

LOPHOSORIA (Figs. 133, 134):—

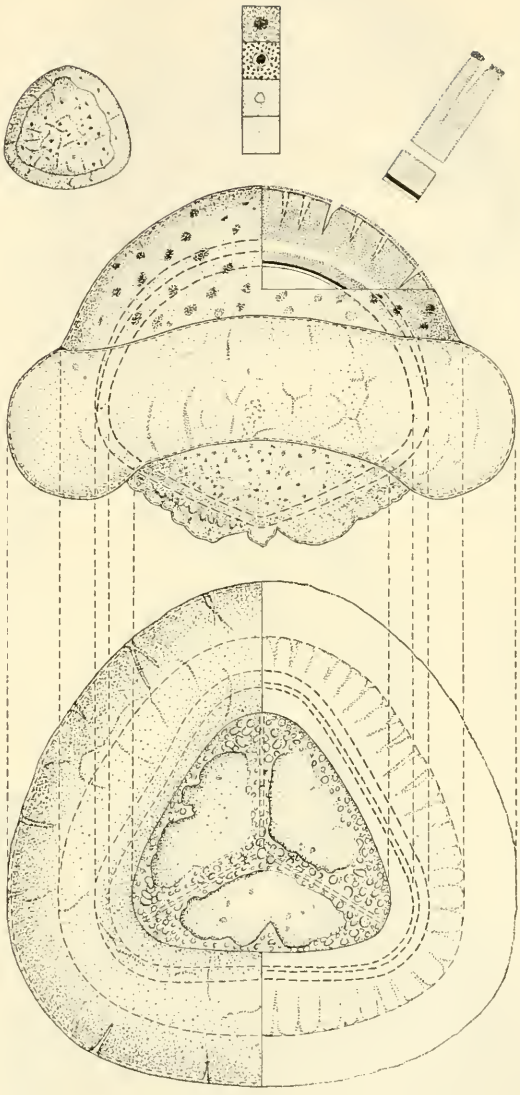

Fig. 133. *Lophosoria quadripinnata* (Puerto Rico; Sintenis 1333, ex herb. Paris); lateral view (surface and section) and proximal face (× 1000). At top, from left to right: distal face (× 250), LO-patterns, sclerine stratification (× 2000).

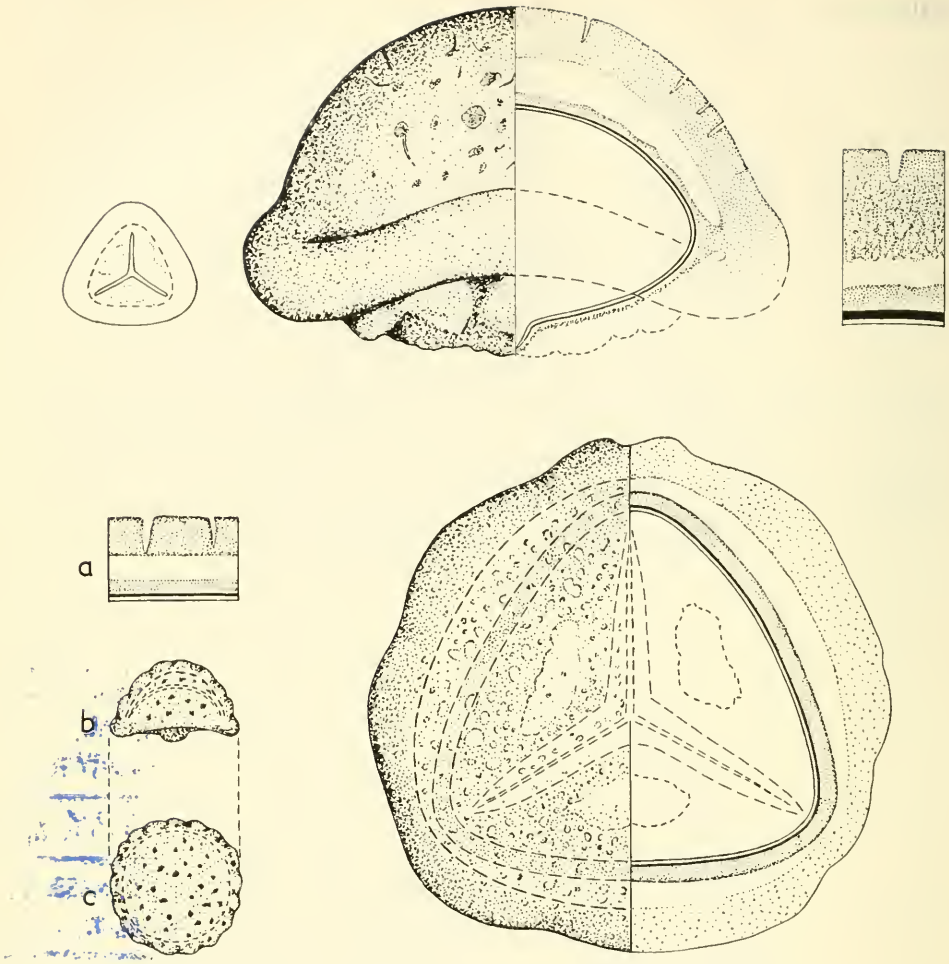

Fig. 134. *Lophosoria quadripinnata*. Upper figures (Weberbauer 1333; ex herb. Berlin), from left to right: proximal face (× 250); lateral view (× 1000); sclerine stratification (× 2000). Lower figures: proximal face of a *Lophosoria* spore found in a slide made from *Serpyllopsis caespitosa* var. *densifolia* (collected by C. Skottsberg in the Juan Fernandez Islands August 27th, 1908); a, sclerine stratification (× 1000); b, lateral view (× 250); c, distal face (× 250).

LORINSERIA:—

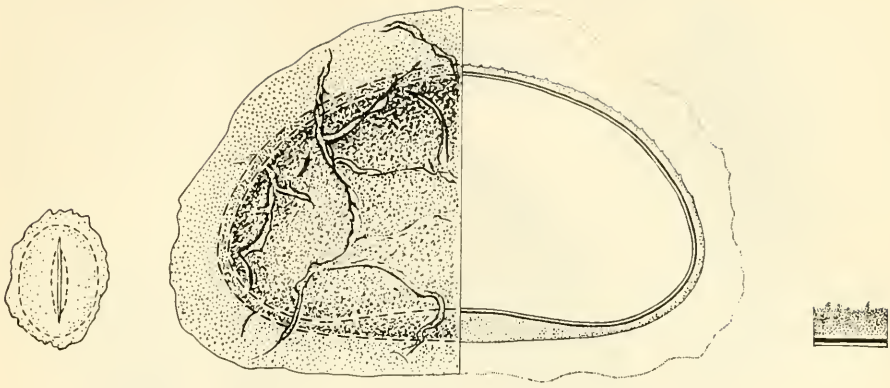

Fig. 135. *Lorinseria areolata*. From left to right: proximal face (× 250); lateral, longitudinal view (× 1000); exine stratification (perine not considered; × 2000).

LOXSOMA:—

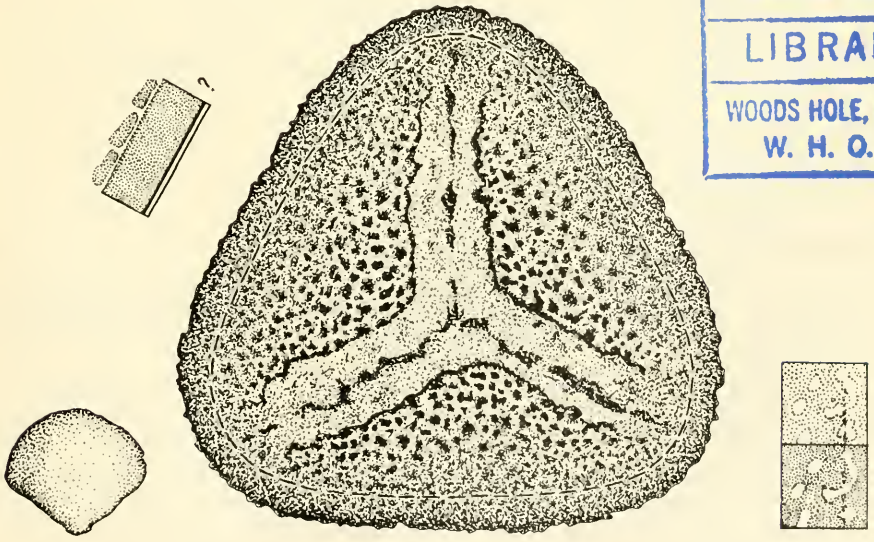

Fig. 136. *Loxsoma cunninghamii*. From left to right: lateral view (× 250); sclerine stratification (× 2000); proximal face (× 1000); LO-patterns.

LOXSOMOPSIS:—

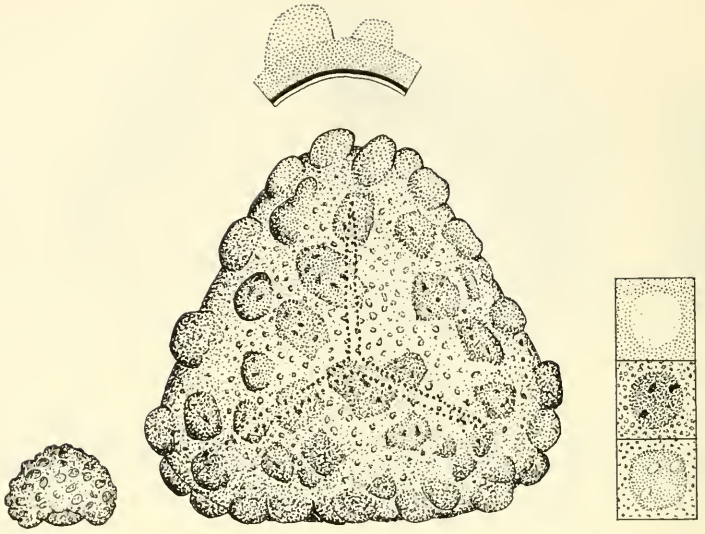

Fig. 137. *Loxsomopsis lehmannii*. Lateral view (× 250), distal face (× 1000), and LO-patterns. At top sclerine stratification (× 2000).

LYCOPODIUM:—

L. clavatum [Pl. III (facing p. 94); Figs. 138 B, 142], *L. densum* (Fig. 139), *L. diaphanum* (Fig. 138 A), *L. drummondii* (Fig. 140), *L. insulare* Fig. 141).

Fig. 138. A, *Lycopodium diaphanum*; a + b, distal face (a, at high, b, at low adjustment of the microscope; the different foci correspond to levels a_1 and b_1 in Fig. A: d; c, proximal face (main part of figure: surface view at high adjustment; upper right-hand part: section through the exine; d and e: outline of exine stratification at distal pole, e at the equator). — B, *L. clavatum*: detail corresponding to that in *L. diaphanum* shown in Fig. A: e. — × 2000 (A: a–c), × 4000 (A: d and e; B), × 500 (lower left-hand detail figure=spore of *L. diaphanum* in lateral view, distal face up). — From Erdtman in Afzelius, Erdtman and Sjöstrand, Svensk bot. Tidskr. 1954.

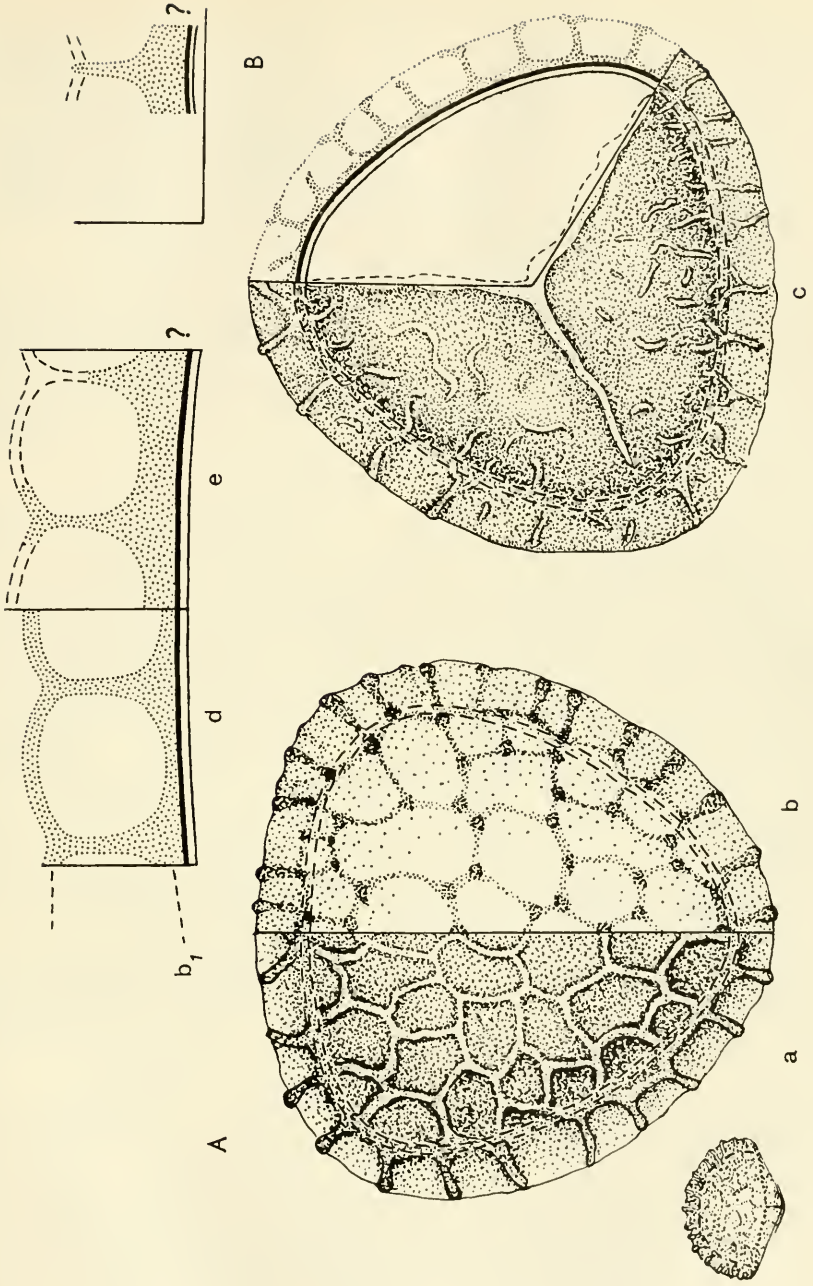

Fig. 138.

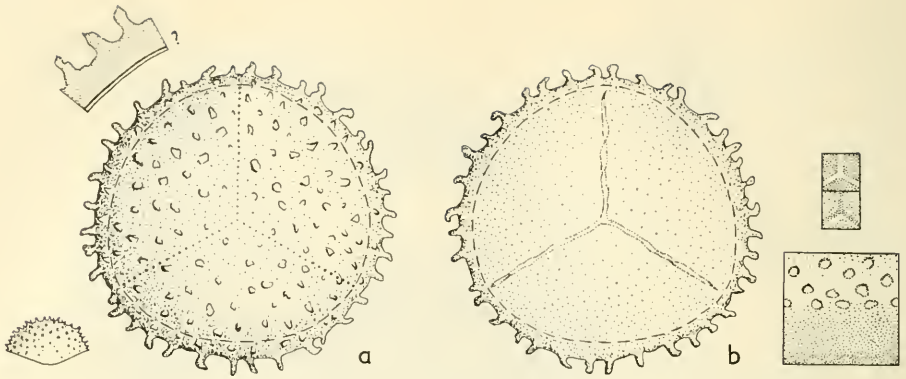

Fig. 139. *Lycopodium densum*; a, distal, b, proximal face (both × 1000); lower right detail-figure: part of exine surface at the transition between the distal and the proximal face.

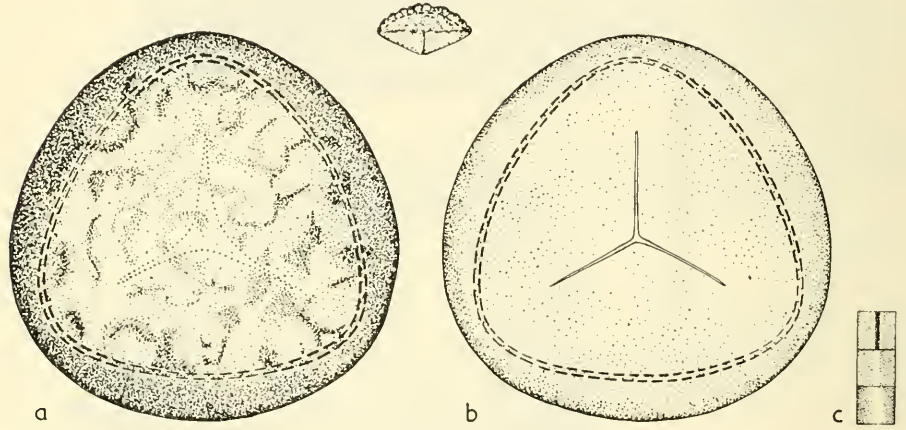

Fig. 140. *Lycopodium drummondii*; a, distal, b, proximal face (× 1000); c, part of laesura at different adjustments of the microscope from high to low.

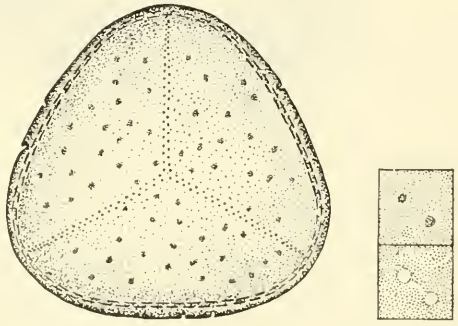

Fig. 141. *Lycopodium insulare*; distal face (× 1000) and LO-patterns.

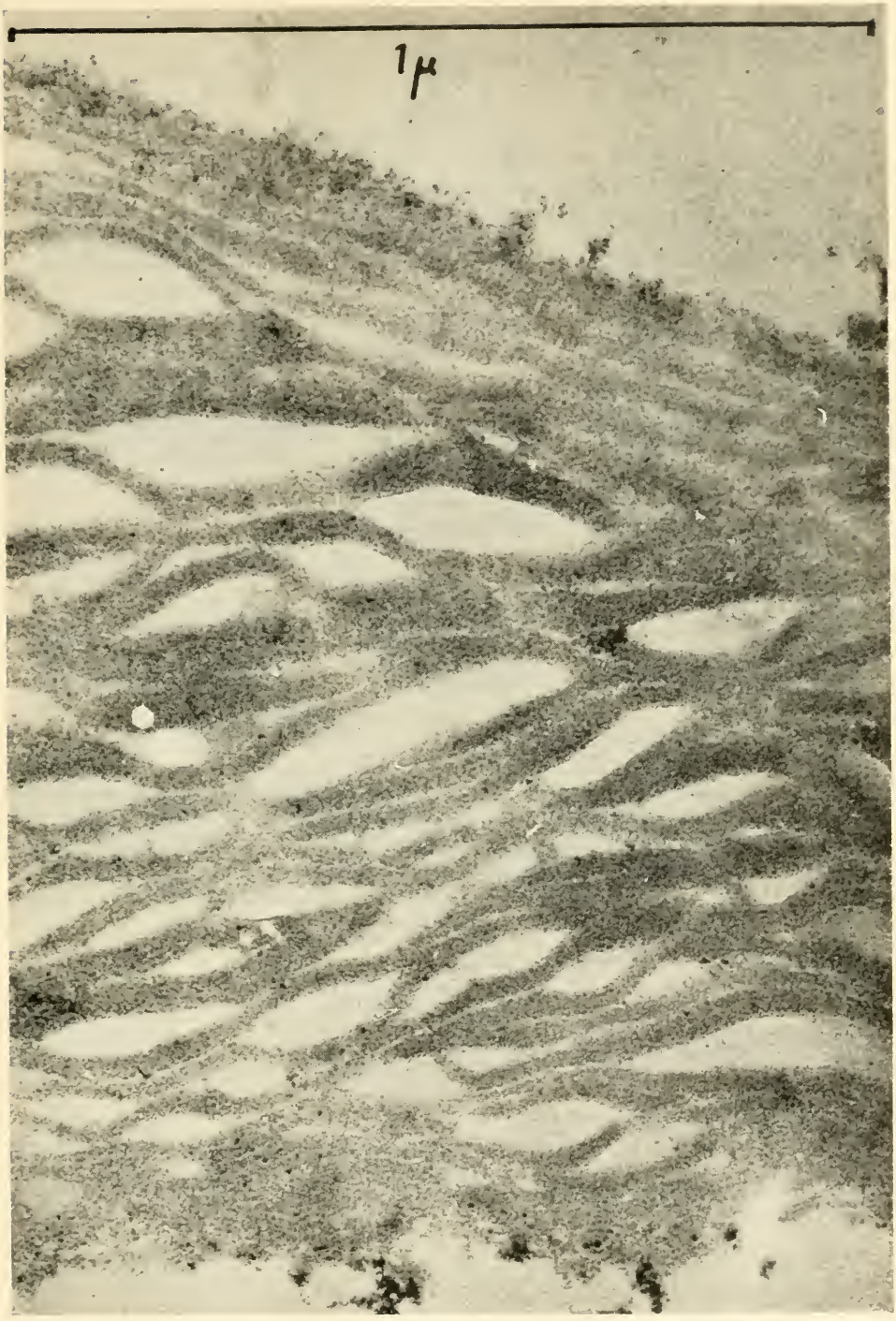

Fig. 142. *Lycopodium clavatum*; section through an acetolyzed spore wall (× 125,000) exhibiting the fine, granular-lamellar, structure of the outer part of the exine. The distinct lamellae shown in this figure are multiples of fine lamellae (thickness 50–60 Å). Each of these consists of a single layer of granules. EMG B. M. Afzelius. (From Grana palynologica, 1: 2, 1956.)

LYGODIUM (Fig. 143 A–D), ANEMIA (Fig. 143 G–I), MOHRIA (Fig. 143 J), SCHIZAEA (Fig. 143 E, F):—

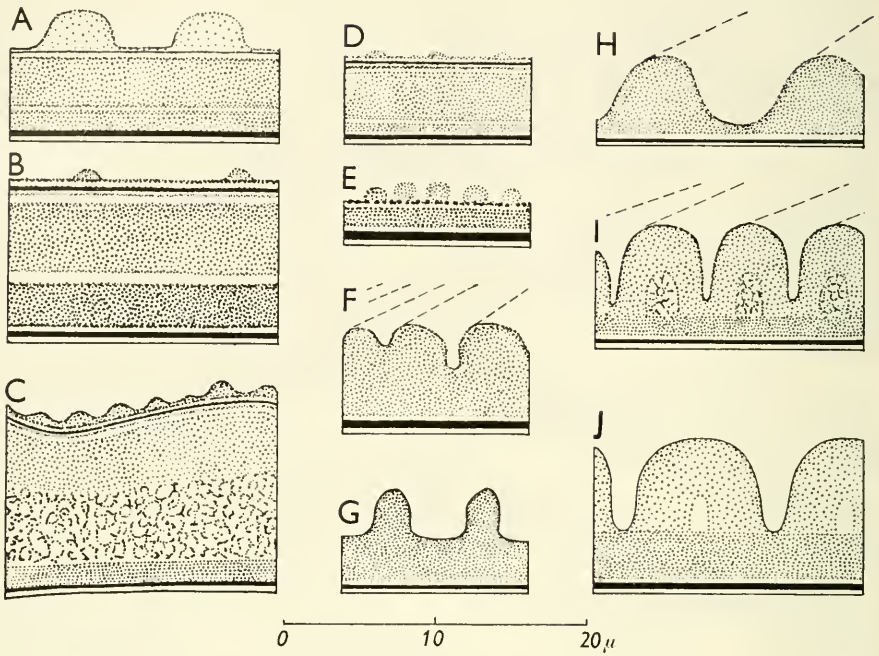

Fig. 143. Schizaeaceae, sclerine stratification (× 2000). A, *Lygodium circinnatum*. B, *L. volubile*. C, *L. micans*. D, *L. japonicum*. E, *Schizaea fluminensis*. F, *S. melanesica*. G, *Anemia phyllitidis*. H, *A. adiantifolia*. I, *A. anthriscifolia*. J, *Mohria caffrorum*. (From Erdtman in Svensk bot. Tidskr. 1954.)

MACROGLENA: see Fig. 188 B, p. 96.

MACROGLOSSUM: see Fig. 144 B, p. 79.

MARATTIA (Fig. 144 E), ANGIOPTERIS (Fig. 144 A), ARCHANGIOPTERIS (Fig. 144 C), CHRISTENSENIA (Fig. 144 D), DANAEA (Fig. 144 F), MACROGLOSSUM (Fig. 144 B):—

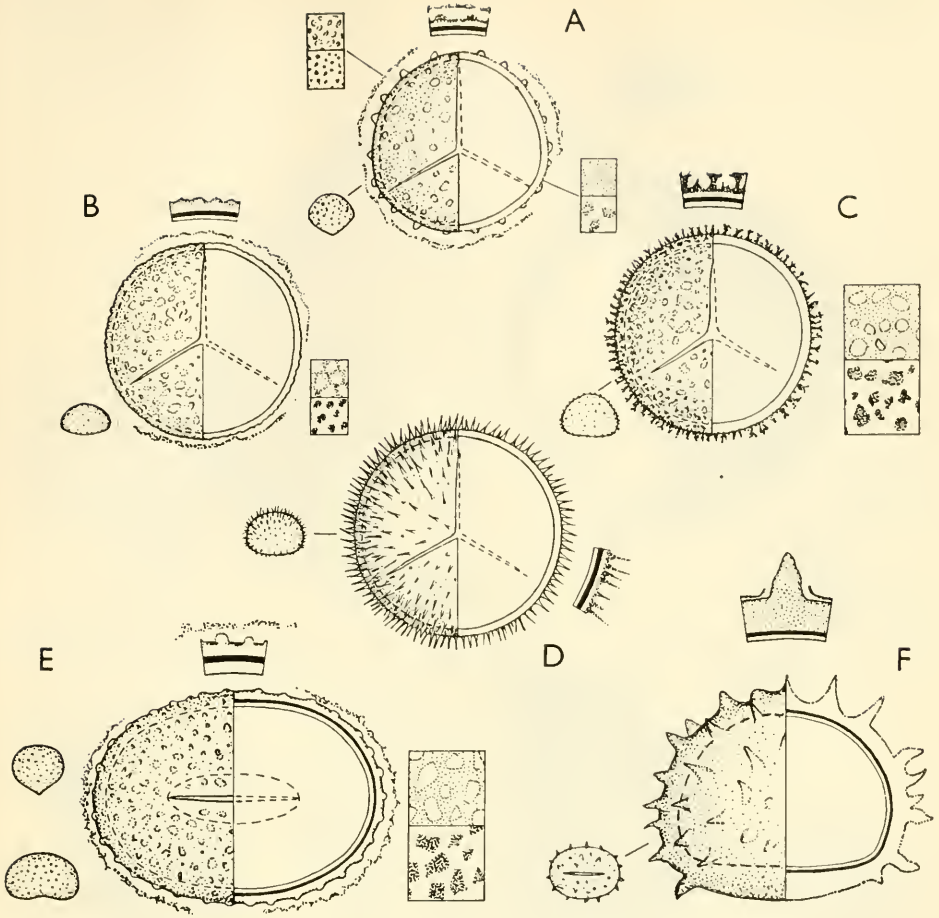

Fig. 144. Marattiales. A, *Angiopteris longifolia*; proximal face (surface and optical section; × 1000). B, *Macroglossum alidae*; proximal face (surface and optical section; × 1000); C, *Archangiopteris henryi*; proximal face (surface and optical section; × 1000). D, *Christensenia aesculifolia*; proximal face (surface and optical section; × 1000); to the left two spores in lateral, transverse and lateral, longitudinal view (× 250). E, *Marattia fraxinea*; proximal face (surface and optical cross-section; × 1000); to the left two spores in transverse lateral and in longitudinal lateral view (× 250). F, *Danaea elliptica*; lateral, longitudinal view (× 1000), proximal face (× 250) and sclerine stratification (× 2000). (From Erdtman in Svensk bot. Tidskr. 1954.)

MARSILEA:—

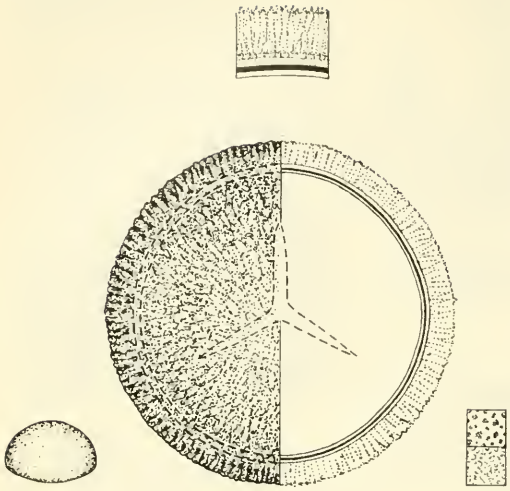

Fig. 145. *Marsilea aegyptiaca*, microspore. From left to right: lateral view (× 250); proximal face (surface and optical section; × 1000); sclerine stratification (× 2000) and LO-patterns.

MATTEUCIA:—

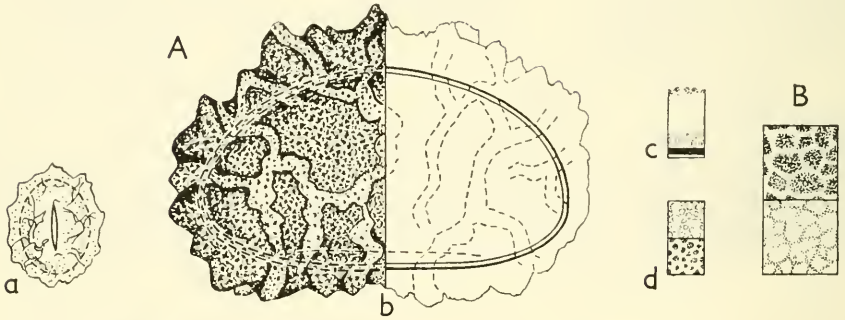

Fig. 146. A, *Matteucia struthiopteris*; a, proximal face (× 250); b, lateral, longitudinal view (surface and optical section; × 1000); c, sclerine stratification (× 2000); d, LO-patterns. B, *M. orientalis*, LO-patterns.

MICROLEPIA:—

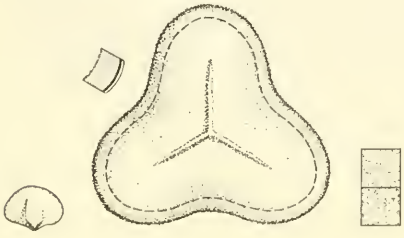

Fig. 147. *Microlepia hirta*. From left to right: lateral view (× 250); sclerine stratification (× 2000); proximal face (× 1000); LO-patterns.

MOHRIA: see Fig. 143 J, p. 78.

NEGRIPTERIS:—

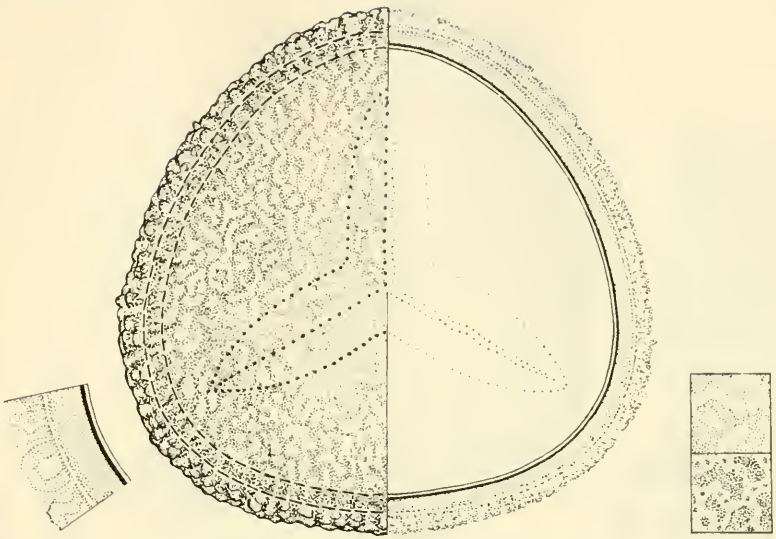

Fig. 148. *Negripteris incana*. From left to right: sclerine stratification (×2000); distal face (surface and optical section; × 1000); LO-patterns.

NEPHROLEPIS:—

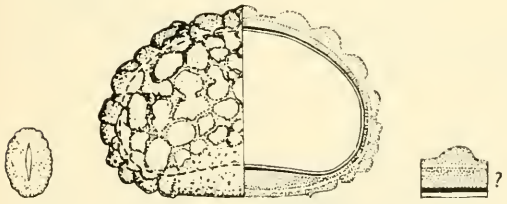

Fig. 149. *Nephrolepis cordifolia*. From left to right: proximal face (×250); lateral, longitudinal view (× 1000); sclerine stratification; (× 2000).

OLEANDRA:—

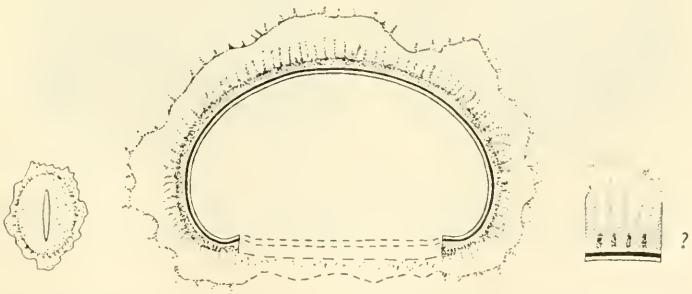

Fig. 150. *Oleandra neriiformis*. From left to right: proximal face (× 250); lateral view (median optical section; × 1000); sclerine stratification (× 2000).

ONOCLEA:—

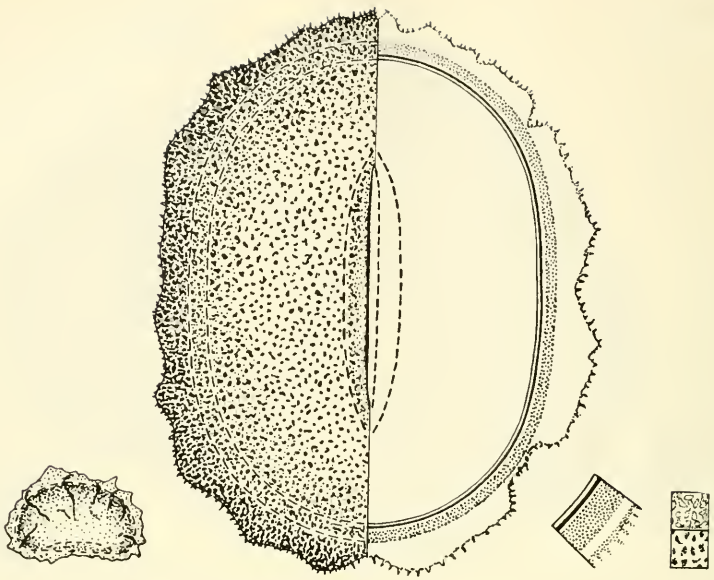

Fig. 151. *Onoclea sensibilis*. From left to right: lateral, longitudinal view (× 250); proximal face (surface and optical section; × 1000); sclerine stratification; × 2000); LO-patterns.

ONYCHIUM:—

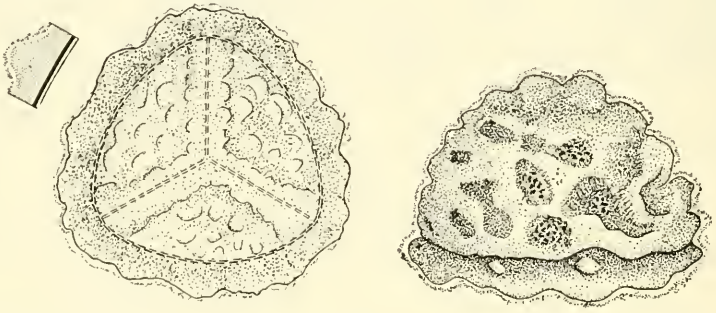

Fig. 152. *Onychium japonicum*. From left to right: sclerine stratification (× 2000); proximal face (× 1000); lateral view (× 1000).

OPHIOGLOSSUM:—

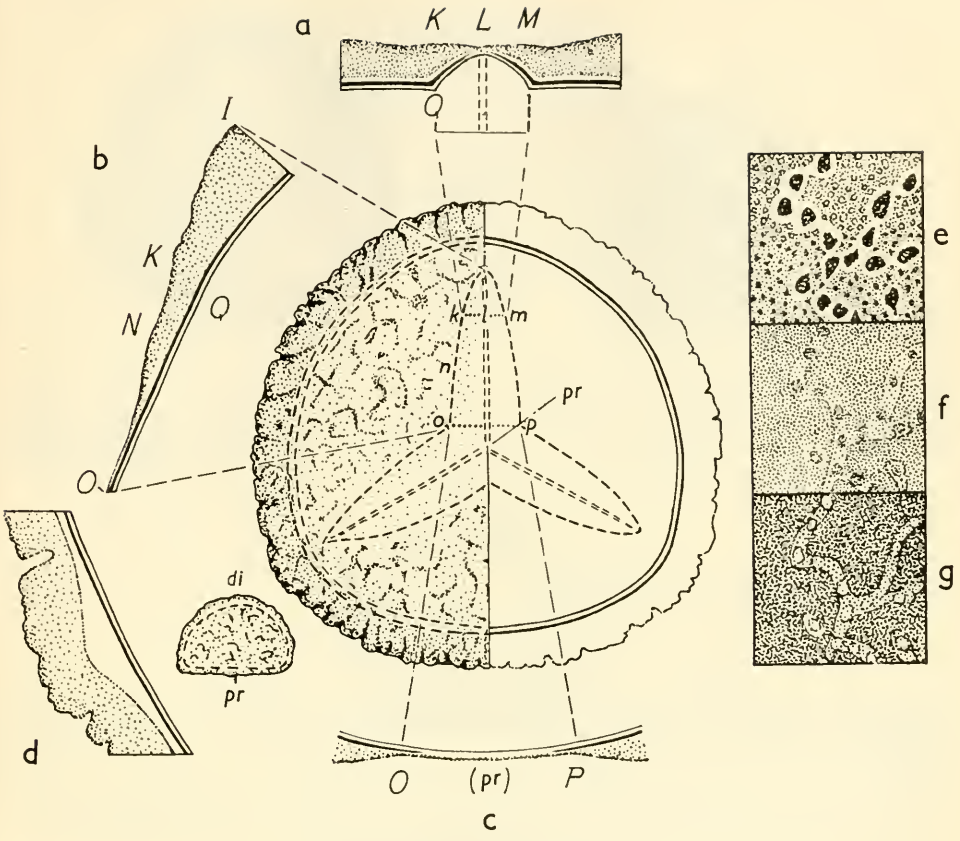

Fig. 153. *Ophioglossum coriaceum*. Main figure: proximal face (× 1000), surface and optical section; a–d, sections through the exine (× 2000; a, b, and c are sections along the lines *klm*, *ikno*, and *op* in the main figure (*klm* corresponds to the letters KLM in fig. a etc.) whereas d exhibits a part of the exine with the sexine locally severed from the nexine (in *Botrychium simplex* transitions have been seen from spores with the sexine adhering to the nexine, as in the main figure above, to such where the sexine is almost completely separated from the nexine—due to the chemical treatment—imparting a ± pansaccate appearance to the spore); e–g, LO-patterns at high, medium, and low focus. Between d and the main figure is as spore seen from the side (× 250; di, distal, pr, proximal pole).—From Erdtman in Svensk bot. Tidskr. 1954.

ORMOLOMA (Fig. 154 A), ORTHIOPTERIS (Fig. 154 B):—

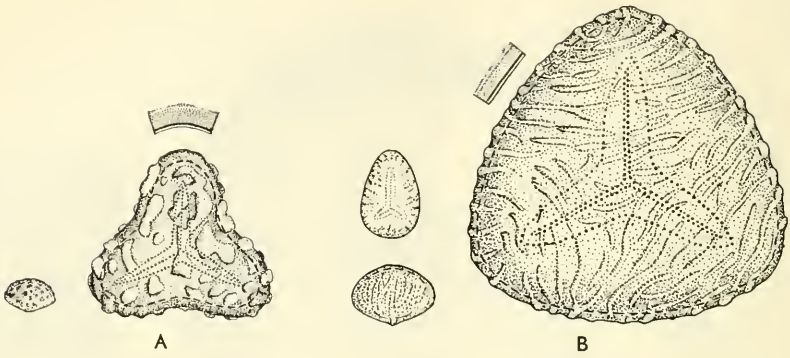

Fig. 154. A, *Ormoloma imrayana*; lateral view (× 250), distal face (×1000), and sclerine stratification (× 2000). B, *Orthiopteris inaequalis*; proximal face (× 1000), exine stratification (× 2000), and—to the left—spore in lateral view (× 250) and proximal face of an aberrant spore (× 250).

ORTHIOPTERIS: see Fig. 154 B.

OSMUNDA (Fig. 155 A–E), LEPTOPTERIS (Fig. 155 G), TODEA (Fig. 155 F):—

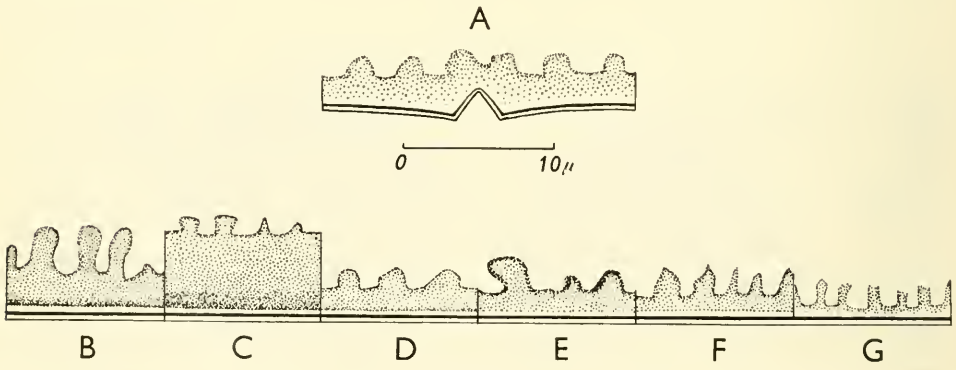

Fig. 155. Osmundaceae, exine stratification (× 2000). A, *Osmunda cinnamomea*, part of exine in proximal face (with laesura). B–G, part of exine in distal face; B, *Osmunda regalis* (subgen. Euosmunda); C, *O. banksiifolia* (subgen. Pleasium); D, *O. cinnamomea* (subgen. Osmundastrum); E, *O. claytoniana* (subgen. Osmundastrum); F, *Todea barbara*; G, *Leptopteris superba*.

PELLAEA:—

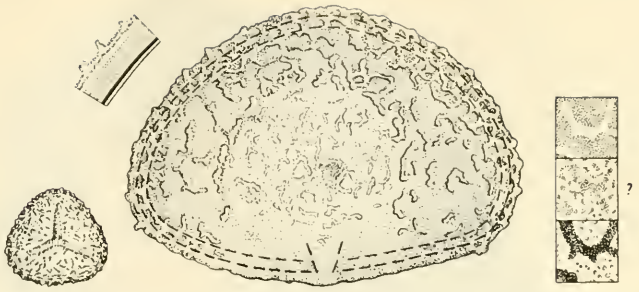

Fig. 156. *Pellaea viridis*. From left to right: proximal face (× 250); sclerine stratification (× 2000); lateral view (× 1000); LO-patterns.

PERANEMA:—

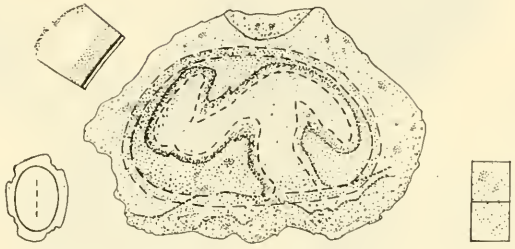

Fig. 157. *Peranema cyatheoides*. From left to right: proximal face (× 250); sclerine stratification (× 2000); spore in lateral, longitudinal view (× 1000); LO-patterns (OL-pattern due to small perforations in the perine).

PHANEROPHLEBIA:—

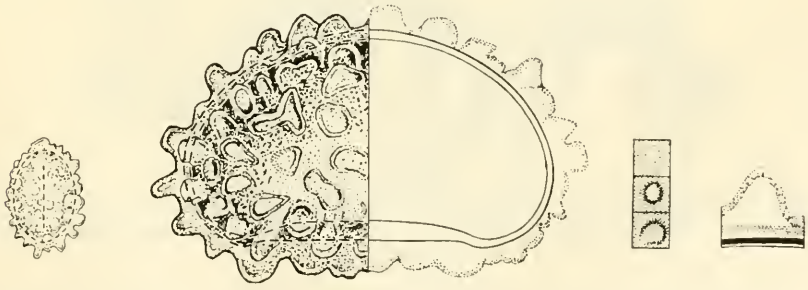

Fig. 158. *Phanerophlebia caryotidea*. From left to right: proximal face (× 250); spore in lateral, longitudinal view (surface and optical section; × 1000); LO-patterns; sclerine stratification (× 2000).

PHANEROSORUS:—

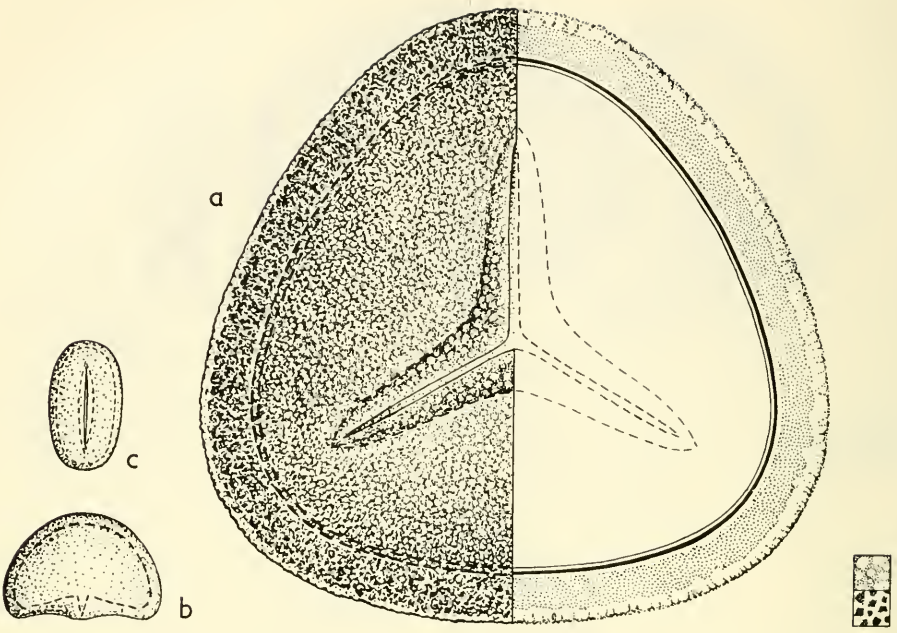

Fig. 159. *Phanerosorus major*; a, proximal face, surface and optical sections (× 1000); b, spore in lateral view (× 250); c, monolete spore, proximal face (× 250). The LO-pattern in the lower right-hand corner is due to the thin perinous cover.

PHLEBODIUM:—

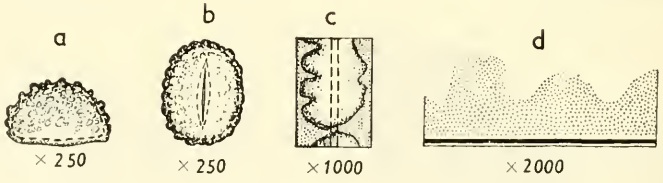

Fig. 160. *Phlebodium aureum*; a, spore in lateral, longitudinal view; b, proximal face; c, part of proximal face with laesura (broken lines); d, exine stratification.

PHYLLOGLOSSUM:—

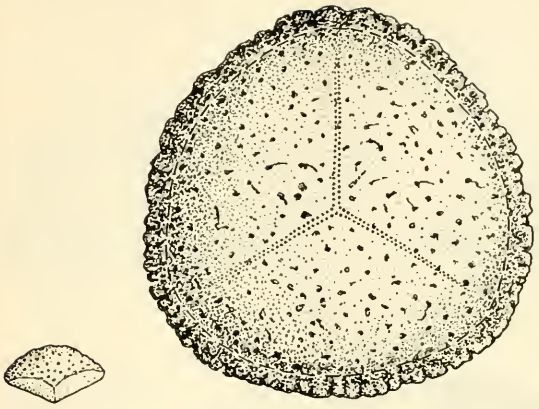

Fig. 161. *Phylloglossum drummondii*; lateral view (× 250) and distal face (× 1000).

PILULARIA:—

Megaspore: *Pilularia globulifera* (Fig. 162 d).
Microspores: *Pilularia globulifera* (Fig. 162 a–c).

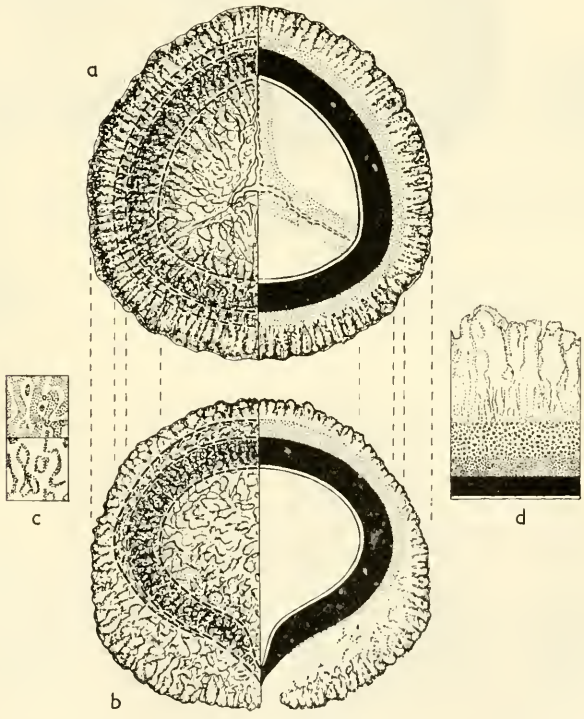

Fig. 162. *Pilularia globulifera*. a–c, microspore. a, proximal face (surface and optical cross-section; × 1000); b, lateral view (surface and optical cross-section; × 1000); c, LO-patterns; d, megaspore, sclerine stratification (× 2000; cf. also Grana palynologica, 1: 2, 1956, Pl. I, Fig. 13, facing p. 126).

PLAGIOGYRIA:—

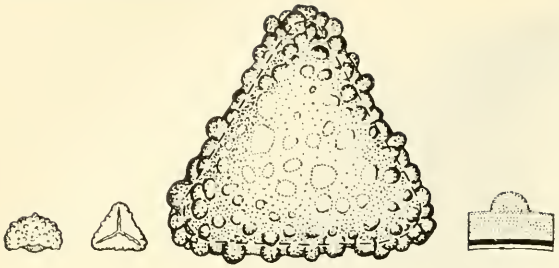

Fig. 163. *Plagiogyria henryi.* From left to right: lateral view (×250); proximal face (×250); distal face (× 250); sclerine stratification (× 2000).

PLATYCERIUM:—

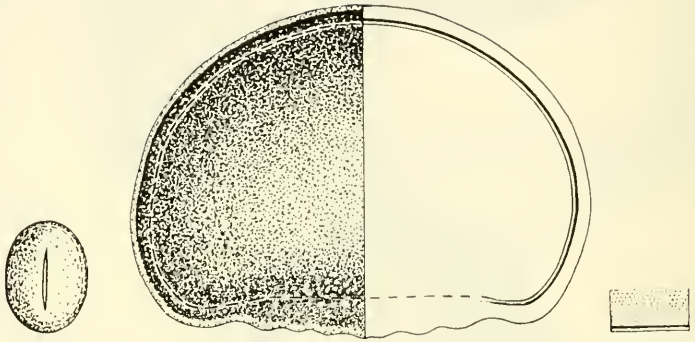

Fig. 164. *Platycerium madagascariense.* From left to right: proximal face (× 250); lateral view (surface and optical cross-section; × 1000); sclerine stratification (× 2000).

PLATYZOMA: see Fig. 114 D, p. 63.

POLYBOTRYA:—

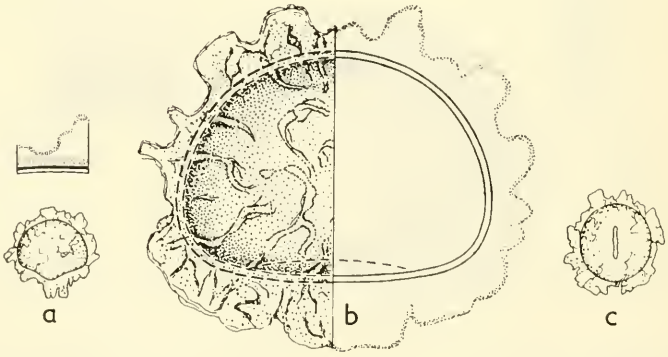

Fig. 165. *Polybotrya appendiculata;* a, lateral, transverse view (× 250); b, lateral, longitudinal view (surface and optical section, × 1000); c, proximal face (× 250); upper left-hand detail: sclerine stratification (× 2000).

PSILOTUM:—

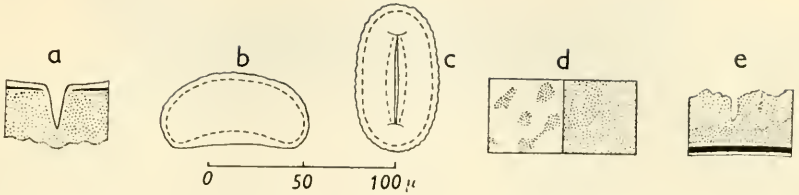

Fig. 166. *Psilotum nudum*; a, laesura (optical cross-section; × 2000); b, lateral, longitudinal view (× 250); c, proximal face (× 250); d, LO-patterns; e, sclerine stratification (× 2000).

PTERIDIUM:—

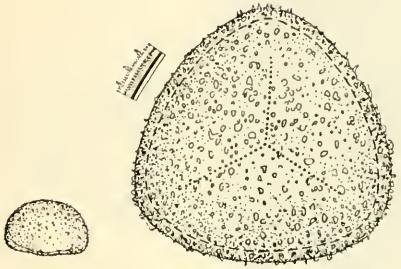

Fig. 167. *Pteridium aquilinum*. From left to right: lateral view (× 250); sclerine stratification (× 2000); distal face (× 1000).

PYRROSIA:—

Fig. 168. *Pyrrosia abbreviata*, sclerine stratification. (× 2000).

SACCOLOMA (Fig. 169 A), CYSTODIUM (Fig. 169 B):—

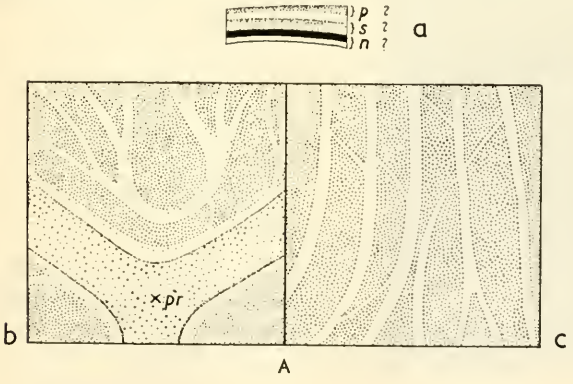

Fig. 169 A. *Saccoloma elegans*; a, sclerine stratification (p, perine?; s, sexine ?; n, nexine ?; × 2000); b, part of proximal face (pr, proximal pole); c, part of distal face (b and c × 4250).

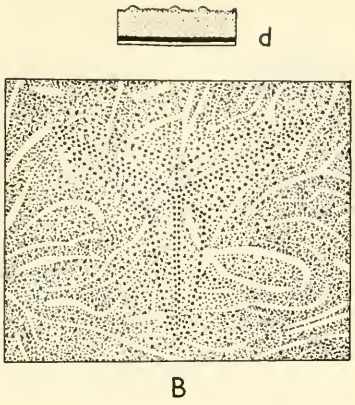

Fig. 169 B. *Cystodium sorbifolium*, part of distal face (× 1000); d, sclerine stratification; the small rounded excrescences of the thin outermost (perinous ?) stratum are cross-sections of the narrow white ridges exhibited in the main figure (× 2000).

SALVINIA:—

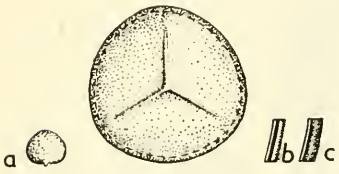

Fig. 170. *Salvinia cucullata*, microspore; a, lateral view (× 250); b, exine stratification at the transition between the two faces (× 2000); c, exine stratification, proximal face (× 2000); main figure: proximal face (× 1000).

SCHIZAEA: see Fig. 143 E, F, p. 78.

SELAGINELLA:—

Megaspores: *S. firmula* (Fig. 171), *S. rupestris* (Fig. 172), *S. selaginoides* (Pl. III, facing p. 94; Fig. 173).

Microspores: *S. apus* (Fig. 174), *S. atroviridis* (Fig. 175), *S. biformis* (Fig. 176), *S. eggersii* (Fig. 177), *S. flagellata* (Fig. 178), *S. kraussiana* (Fig. 179), *S. radiata* (Fig. 180), *S. selaginoides* (Fig. 181), *S. uncinata* (Fig. 182).

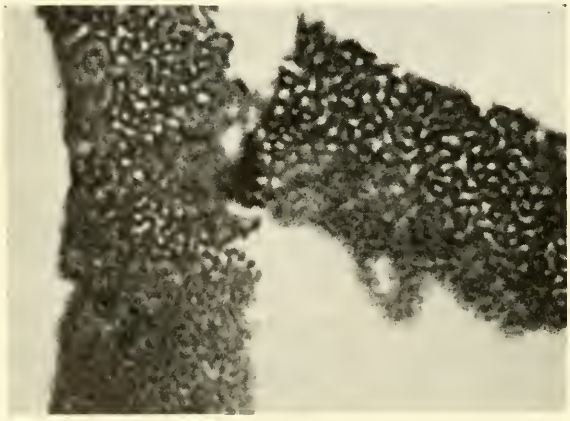

Fig. 171. *Selaginella firmula*. Fragment of section through megaspore membrane. × 2000.

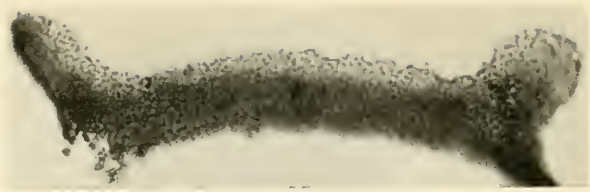

Fig. 172. *Selaginella rupestris.* Fragment of section through megaspore membrane. × 1000.

Fig. 173. *Selaginella selaginoides.* Fragment of section through megaspore membrane (× 2000). An electron micrograph showing the fine structure of part of the membrane is shown in Pl. III (facing p. 94), lower figure.

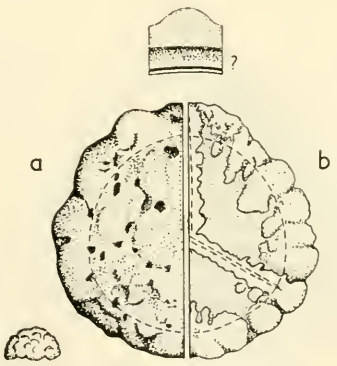

Fig. 174. *Selaginella apus,* microspore. a, distal face; b, proximal face (a, b × 1000). Lower left-hand detail: lateral view (× 250); upper detail: sclerine stratification (× 2000).

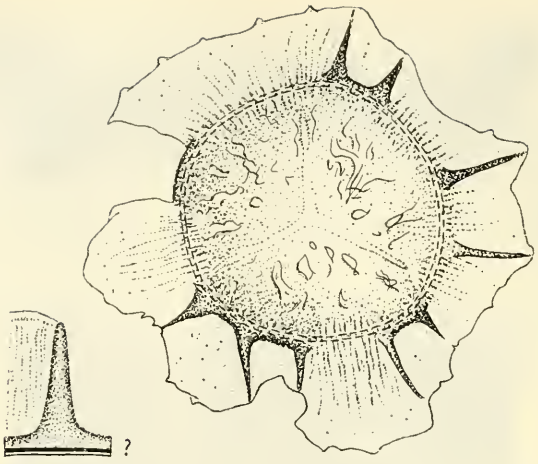

Fig. 175. *Selaginella atroviridis,* microspore; sclerine stratification (× 2000) and distal face (× 1000).

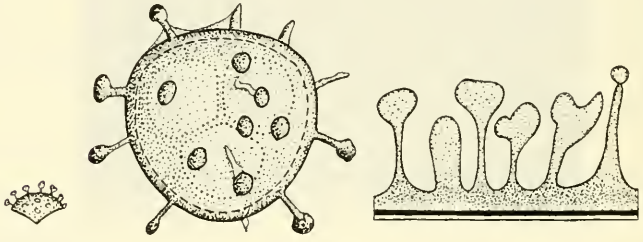

Fig. 176. *Selaginella biformis,* microspore. From left to right: lateral view (× 250); distal face (× 1000); exine stratification (× 2500).

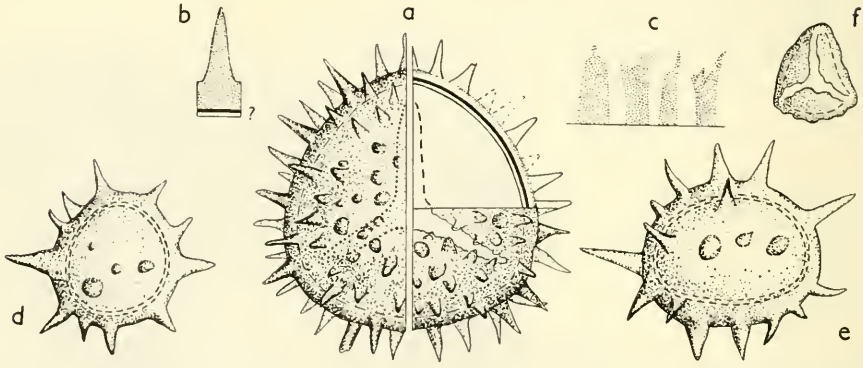

Fig. 177. *Selaginella eggersii,* microspore. a, distal (left) and proximal face (right; surface and section); b, sclerine stratification; c, different types of processes; d–f, aberrant microspores. — a, d–f × 1000; b, c × 2000.

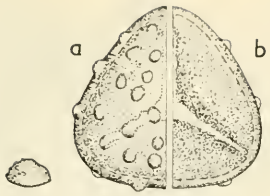

Fig. 178. *Selaginella flagellata*, microspore; lateral view (× 250) and distal (a) and proximal (b) face (× 1000).

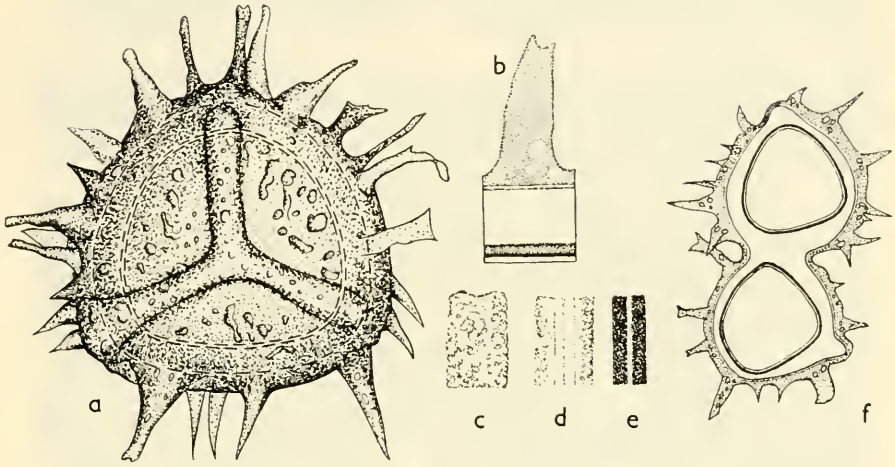

Fig. 179. *Selaginella kraussiana*, microspore; a, proximal face (× 1000); b, sclerine stratification (× 2000); c–e, successive patterns in LO-analysis of the laesura; f, two microspores with common cover (× 1000).

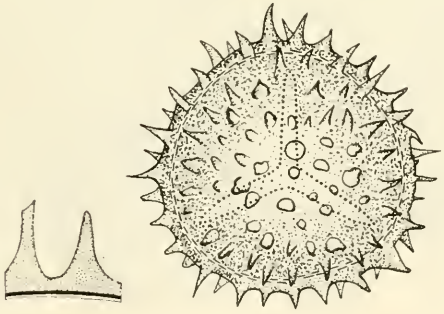

Fig. 180. *Selaginella radiata*, microspore; sclerine stratification (× 2000) and distal face (× 1000).

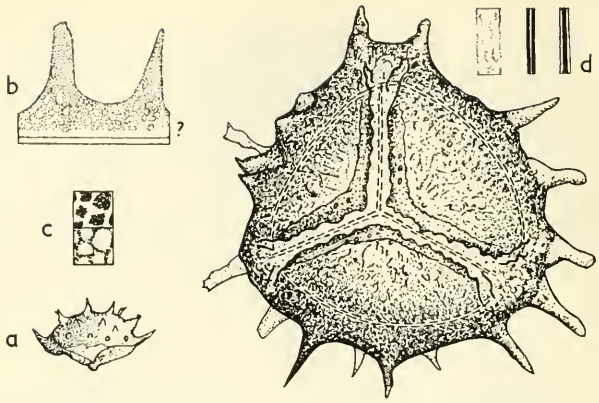

Fig. 181. *Selaginella selaginoides*, microspore. Main figure: proximal face (× 1000). a, lateral view (× 250); b, sclerine stratification (× 2000); c, LO-patterns; d, part of laesura at different adjustments from high (left) to low (right).

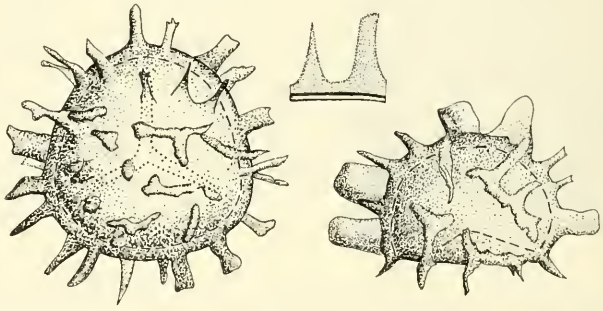

Fig. 182. *Selaginella uncinata*, microspores in polar (left; distal face) and lateral view (right; both × 1000). In the centre: sclerine stratification (×2000).

SELENODESMIUM: see Fig. 188 A, p. 96.

STENOCHLAENA:—

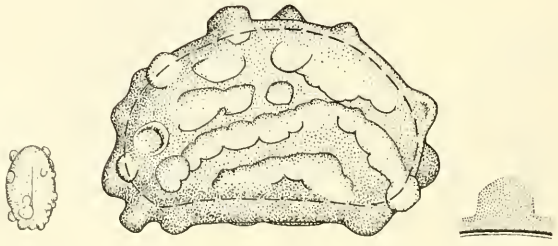

Fig. 183. *Stenochlaena tenuifolia*. From left to right: proximal face (× 250); lateral view (surface and section; × 1000); sclerine stratification (× 2000).

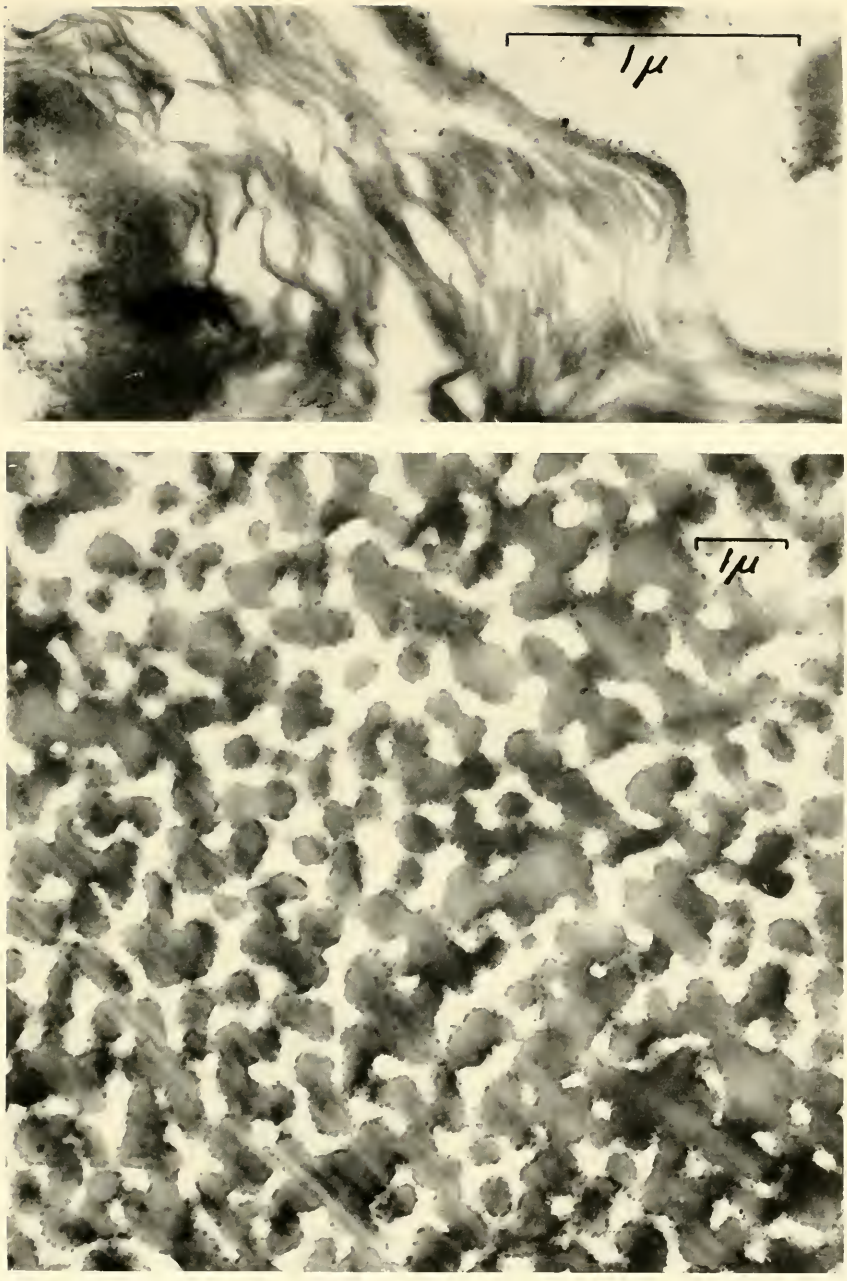

Lycopodium clavatum and *Selaginella selaginoides*. Upper figure: section through the exine in *Lycopodium clavatum*. An outer laminated and an inner granulated layer can be seen. EMG B. M. Afzelius (× 40,000). Lower figure: section through part of the exine of a megaspore of *Selaginella selaginoides*. EMG B. M. Afzelius (× 12,500). (From Svensk bot. Tidskr., vol. 48, 1954.)

STICHERUS: see Fig. 114 B, p. 63.

STROMATOPTERIS: see Fig. 114 A, p. 63.

TAENITIS:—

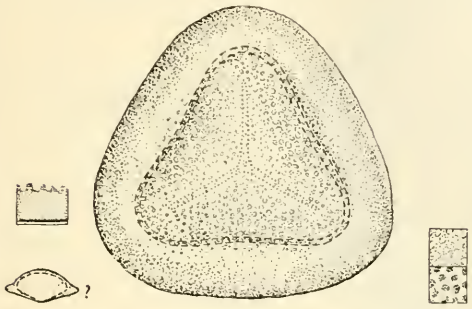

Fig. 184. *Taenitis blechnoides*. From left to right: sclerine stratification (× 2000) and lateral view (× 250); distal face (× 1000); LO-patterns.

TAPEINIDIUM:—

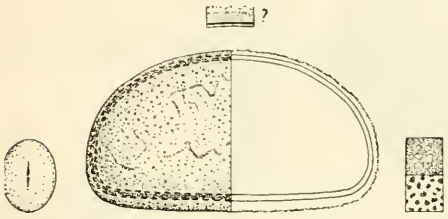

Fig. 185. *Tapeinidium pinnatum*; proximal face (× 250); lateral view (surface and optical cross-section; × 1000); LO-patterns.

THYRSOPTERIS:—

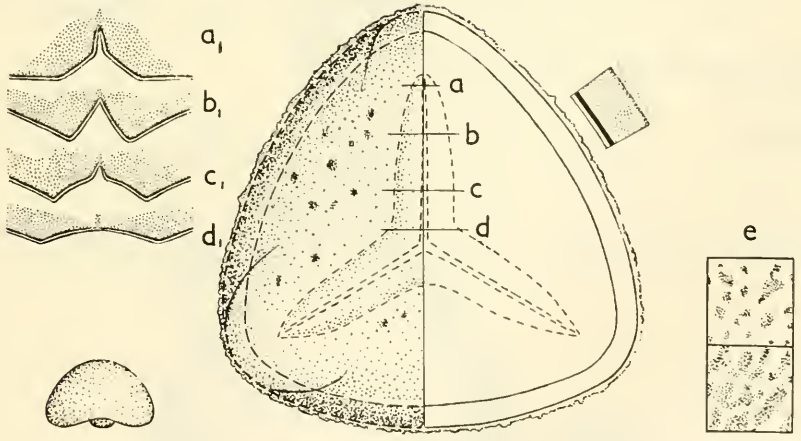

Fig. 186. *Thyrsopteris elegans*; proximal face (surface and optical cross-section; × 1000). Optical cross-sections through the laesura at a–d are shown in a_1–d_1. e, LO-patterns. Lower left-hand detail: lateral view (× 250); upper right-hand detail: sclerine stratification (× 2000).

TMESIPTERIS:—

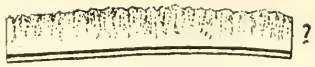

Fig. 187. *Tmesipteris forsteri*, sclerine stratification (× 2000).

TODEA: see Fig. 155 F, p. 84.

TRICHOMANES (Fig. 188 A, B, D), HYMENOPHYLLUM (Fig. 188 C):—

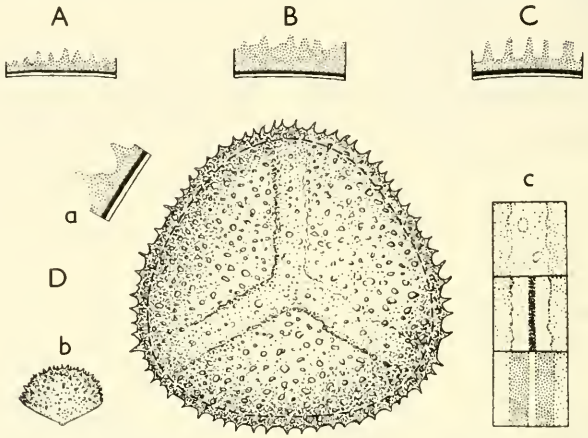

Fig. 188. Hymenophyllaceae. A–C, *Trichomanes* and *Hymenophyllum*, exine stratification (× 2000). A, *T.* (*Selenodesmium*) *rigidum*. B, *T.* (*Macroglena*) *meifolium*. C, *Hymenophyllum* (*Hymenoglossum*) *cruentum*. D, *Trichomanes* (*Vandenboschia*) *radicans*, proximal face (× 1000); a, exine stratification (× 2000); b, lateral view (× 250); c, LO-analysis of laesura.

VANDENBOSCHIA: see Fig. 188 D.

VITTARIA:—

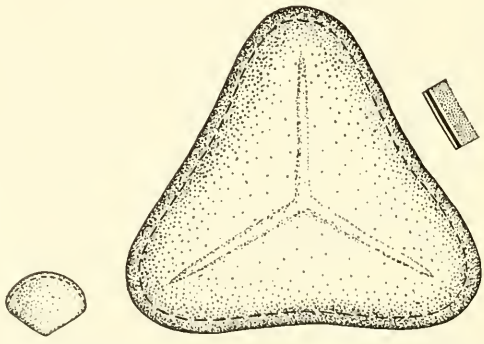

Fig. 189. *Vittaria vittarioides*. From left to right: lateral view (× 250); proximal face (× 1000); sclerine stratification (× 2000).

WOODSIA:—

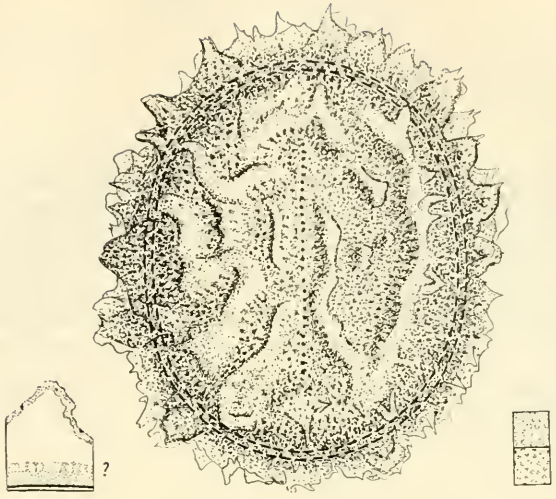

Fig. 190. *Woodsia alpina*. From left to right: sclerine stratification (× 2000); distal face (× 1000); LO-patterns.

XIPHOPTERIS:—

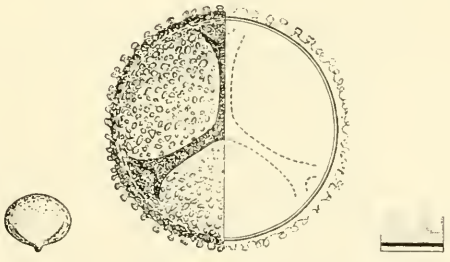

Fig. 191. *Xiphopteris saffordii*. From left to right: lateral view (× 250); proximal face (surface and optical cross-section; × 1000); exine stratification (× 2000).

"... opening several of these dry red Cases, I found them to be quite hollow, without any thing at all in them; whereas when I cut them asunder with a sharp Pen-knife when green, I found in the middle of this great Case, another smaller round Case, between which two, the *interstices* were fill'd with multitudes of stringie *fibres*, which seem'd to suspend the lesser Case in the middle of the other, which (as farr as I was able to discern) seem'd full of exceeding small white seeds ..."

From a description of moss capsules in R. Hooke's Micrographia 1667 (pp. 131, 132).

BRYOPHYTA

Pl. IV (facing p. 108), V (facing p. 109); Figs. 192–253.

HEPATICAE

Aneuraceae: Fig. 240 (p. 118).
Anthocerotaceae: Figs. 194 (p. 100), 208 (p. 106), 225 (p. 112).
Blasiaceae: Fig. 197 (p. 101).
Cleveaceae: Fig. 204 (p. 104).
Codoniaceae: Fig. 213 (p. 108).
Conocephalaceae: Fig. 205 (p. 104).
Corsiniaceae: Fig. 206 (p. 105).
Cyathodiaceae: Fig. 207 (p. 105).
Exormothecaceae: Fig. 211 (p. 108).
Frullaniaceae: Fig. 214 (p. 109).
Grimaldiaceae: Fig. 232 (p. 115).
Marchantiaceae: Fig. 209 (p. 106).
Monocleaceae: Fig. 226 (p. 113).
Oxymitraceae: Fig. 230 (p. 114).
Pelliaceae: Fig. 231 (p. 115).
Plagiochilaceae: Fig. 233 (p. 116).
Radulaceae: Fig. 238 (p. 118).
Ricciaceae: Fig. 241 (p. 119).
Riellaceae: Fig. 242 (p. 120).
Scapaniaceae: Fig. 243 (p. 121).
Sphaerocarpaceae: Fig. 216 (p. 109).
Symphyogynaceae: Fig. 250 (p. 123).
Targioniaceae: Fig. 251 (p. 123).

MUSCI

Andreaeaceae: Fig. 192 (p. 100).
Archidiaceae: Fig. 195 (p. 101).
Bryaceae: Fig. 199 A–C, E (p. 102).
Buxbaumiaceae: Fig. 200 A, B (p. 102).
Calomniaceae: Fig. 201 (p. 103).
Calymperaceae: Fig. 202 (p. 103).
Catascopiaceae: Fig. 224 D (p. 112).
Dicranaceae: Fig. 203 B (p. 103).
Diphysciaceae: Fig. 200 C (p. 102).
Ditrichaceae: Fig. 203 A (p. 103).
Encalyptaceae: Fig. 210 (p. 107).
Ephemeraceae: Fig. 227 (p. 113).
Fissidentaceae: Fig. 212 (p. 107).
Funariaceae: Pl. IV, V.
Georgiaceae: Fig. 215 (p. 109).
Gigaspermaceae: Fig. 217 (p. 110).
Grimmiaceae: Fig. 239 (p. 118).
Hedwigiaceae: Fig. 218 (p. 110).
Helicophyllaceae: Fig. 219 (p. 110).
Hookeriaceae: Fig. 220 (p. 111).
Hylocomiaceae: Fig. 221 (p. 111).
Lembophyllaceae: Fig. 228 A (p. 113).
Leptostomaceae: Fig. 222 (p. 111).
Leskeaceae: Fig. 223 (p. 111).
Leucobryaceae: Fig. 203 C (p. 103).
Meeseaceae: Fig. 224 A–C (p. 112).
Mniaceae: Fig. 199 D (p. 102).
Neckeraceae: Fig. 228 B (p. 113).
Oedipodiaceae: Fig. 229 (p. 114).
Orthotrichaceae: Fig. 253 (p. 124).
Pleurophascaceae: Fig. 234 (p. 116).
Polytrichaceae: Fig. 235 (p. 116).
Pottiaceae: Figs. 193 (p. 100), 236 (p. 117).
Rhizogoniaceae: Fig. 237 (p. 117).
Schistostegaceae: Fig. 244 (p. 121).
Sphagnaceae: Fig. 246 (p. 121).
Spiridentaceae: Fig. 247 (p. 122).
Splachnaceae: Fig. 248 (p. 122).
Symphyodontaceae: Fig. 249 (p. 122).
Timmiaceae: Fig. 252 (p. 124).

ACROSCHISMA:—

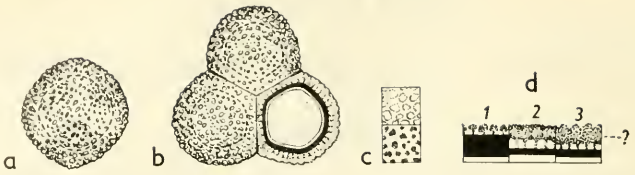

Fig. 192. *Acroschisma wilsonii*; a, distal face (× 1000); b, tetrad (× 1000); c, LO-patterns (distal face); d, exine stratification (1, in chlorinated spores); × 2000.

ANOECTANGIUM:—

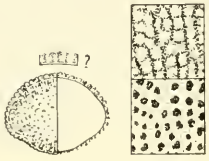

Fig. 193. *Anoectangium aestivum*; spore in lateral view, surface and optical section (distal pole upwards; × 1000); LO-patterns (distal face).

ANTHOCEROS:—

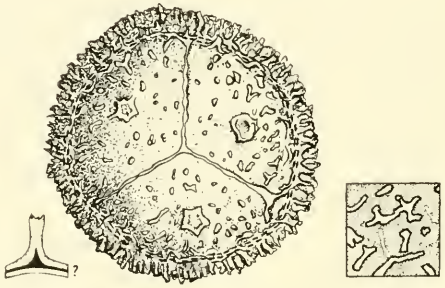

Fig. 194. *Anthoceros tuberculatus*; from left to right: sclerine stratification (× 2000); proximal face (× 825); LO-pattern.

ARCHIDIUM:—

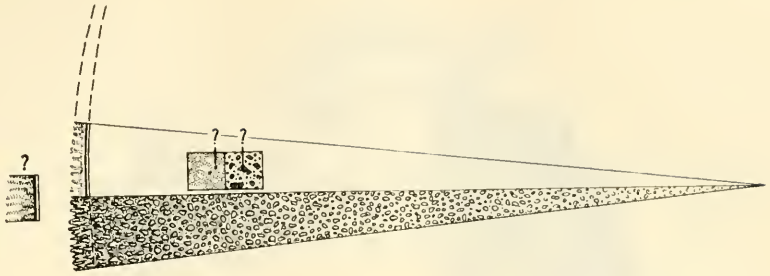

Fig. 195. *Archidium alternifolium*; part of spore surface (× 1000).

ATHALAMIA:—

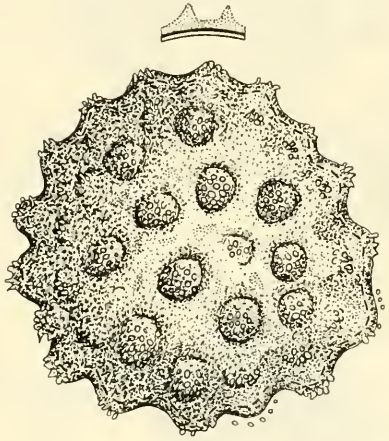

Fig. 196. *Athalamia nana*; spore (× 1000) and sclerine stratification (×2000).

BLASIA:—

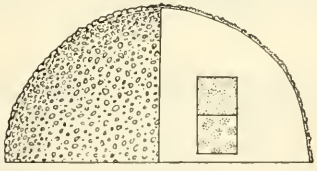

Fig. 197. *Blasia pusilla*; part of spore, surface and optical section (× 1000).

BLINDIA: see Fig. 203 B, p. 103.

BRACHIOLEJEUNIA:—

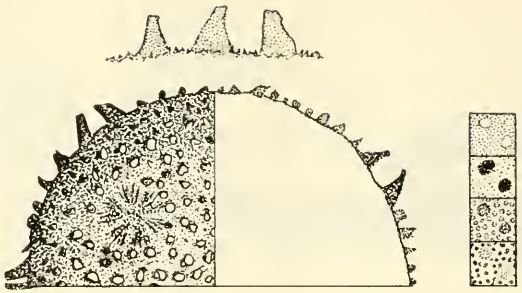

Fig. 198. *Brachiolejeunia sandwicensis*; part of spore, surface and optical section (× 1000); sclerine stratification (× 2000) and LO-patterns.

BRYUM (Fig. 199 A, B), CINCLIDIUM (Fig. 199 E), MIELICHHOFERIA (Fig. 199 E), POHLIA (Fig. 199 C):—

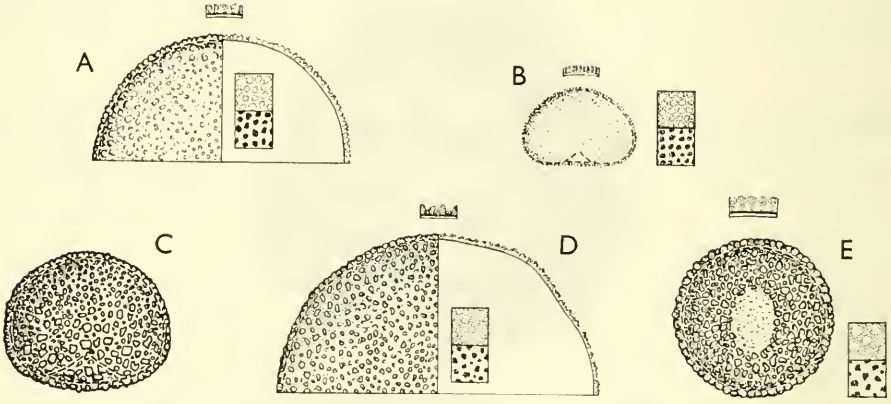

Fig. 199. Bryaceae (A, B, C, E), Mniaceae (D). — A, *Bryum mammillatum*; part of spore, surface and optical section (× 1000). B, *B. caespiticium*; spore in lateral view (× 1000). C, *Pohlia elongata*; spore in lateral view (× 1000). D, *Cinclidium subrotundum*; part of spore, surface and optical section (× 1000). E, *Mielichhoferia elongata*; cf. proximal face (× 1000).

BUXBAUMIA (Fig. 200 A, B), DIPHYSCIUM (Fig. 200 C):—

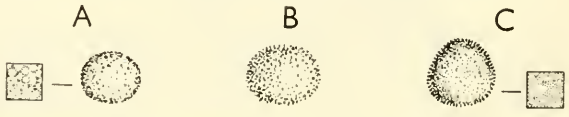

Fig. 200. Buxbaumiales. A, *Buxbaumia aphylla*. B, *B. viridis*. C, *Diphyscium foliosum*. (A–C × 1000).

CALOMNIUM:—

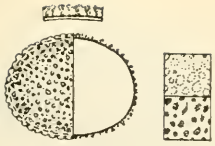

Fig. 201. *Calomnium laetum*; surface and optical section (× 1000), exine stratification (× 2000) and LO-patterns.

CALYMPERES:—

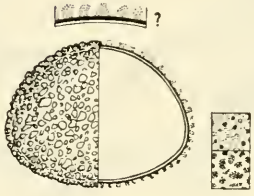

Fig. 202. *Calymperes afzelii*; surface and optical section (× 1000), exine stratification (× 2000) and LO-patterns.

CATASCOPIUM: see Fig. 224 D, p. 112.

CERATODON (Fig. 203 A), BLINDIA (Fig. 203 B), LEUCOBRYUM (Fig. 203 C):—

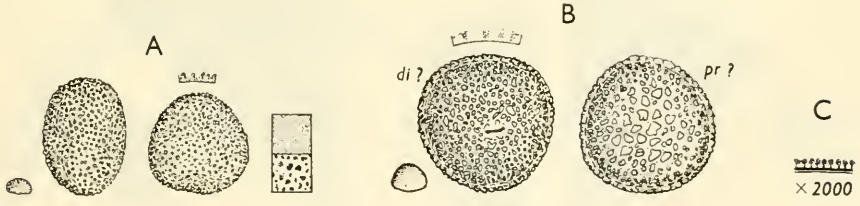

Fig. 203. Dicranales. — A, *Ceratodon purpureus*; from left to right: spore in lateral view (× 250); two spores (cf. proximal face; × 1000); LO-patterns. B, *Blindia acuta*; from left to right: spore in lateral view (× 250); cf. distal face (× 1000); cf. proximal face (× 1000). C, *Leucobryum glaucum*; exine stratification (× 2000).

CINCLIDIUM: see Fig. 199 D, p. 102.

CLEVEA:—

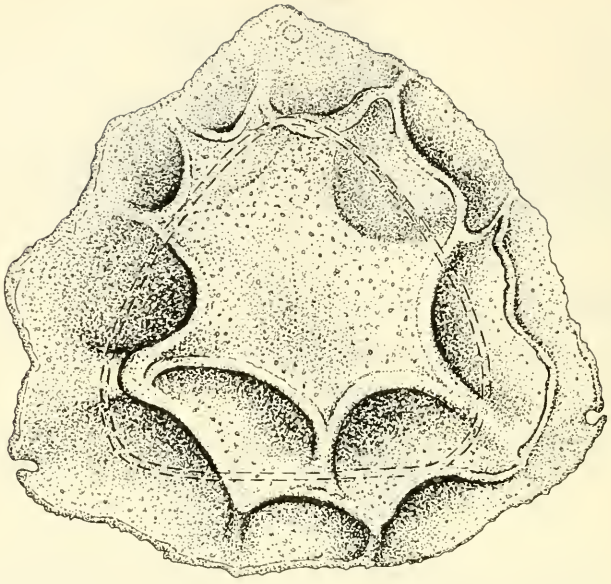

Fig. 204. *Clevea robusta*; distal face (× 1000).

CONOCEPHALUM:—

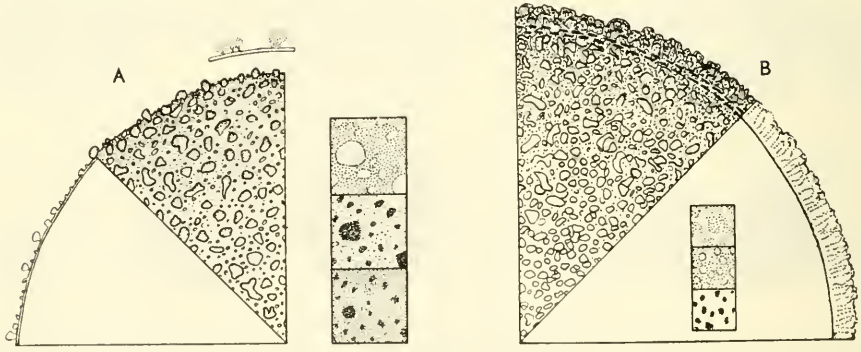

Fig. 205. A, *Conocephalum* (*Fegatella*) *conicum*; part of spore (× 1000), optical section and surface; LO-patterns. B, *C. supradecomposilum*; part of spore (× 1000), surface and optical section (with LO-patterns).

CORSINIA:—

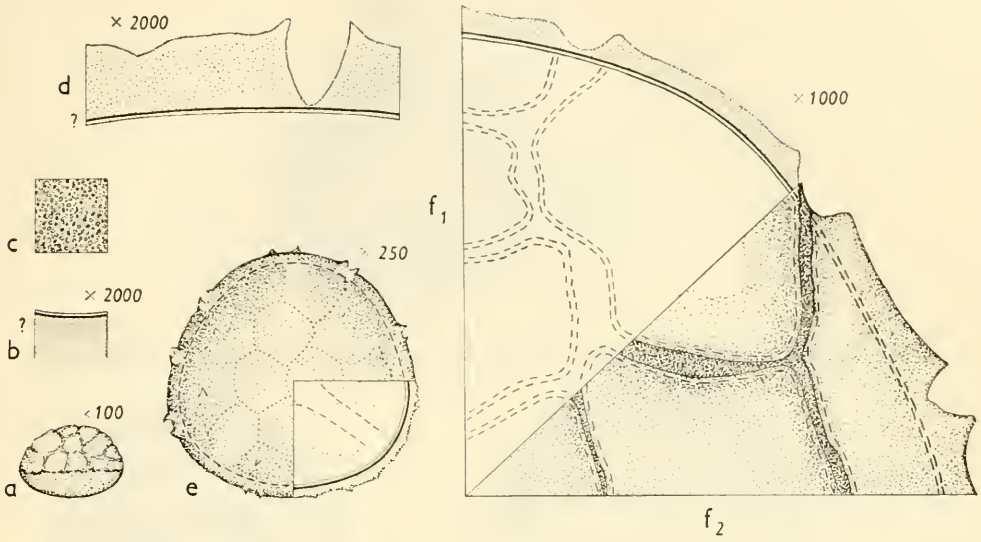

Fig. 206. *Corsinia marchantioides*. a, lateral view; b, sclerine stratification in the less convex face; c, LO-pattern; d, sclerine stratification in the more convex face; e, polar view (less convex face); f_1, f_2: part of spore in polar view (f_1, optical section, f_2, surface).

CYATHODIUM:—

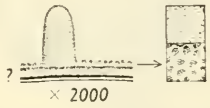

Fig. 207. *Cyathodium africanum*; sclerine stratification and LO-patterns.

DENDROCEROS:—

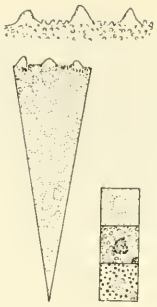

Fig. 208. *Dendroceros crispatus*; part of spore surface (× 1000).

DIPHYSCIUM: see Fig. 200 C, p. 102.

DUMORTIERA:—

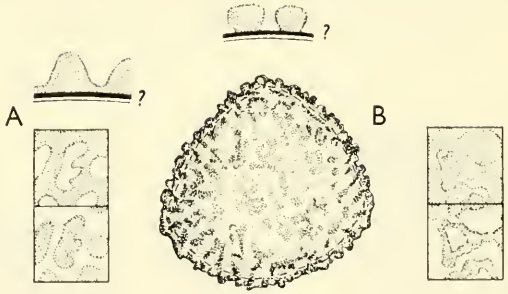

Fig. 209. *Dumortiera hirsuta*; exine stratification (× 2000) and LO-patterns. B, *D. velutina*; spore in polar view (× 1000), exine stratification (× 2000), and LO-patterns.

ENCALYPTA:—

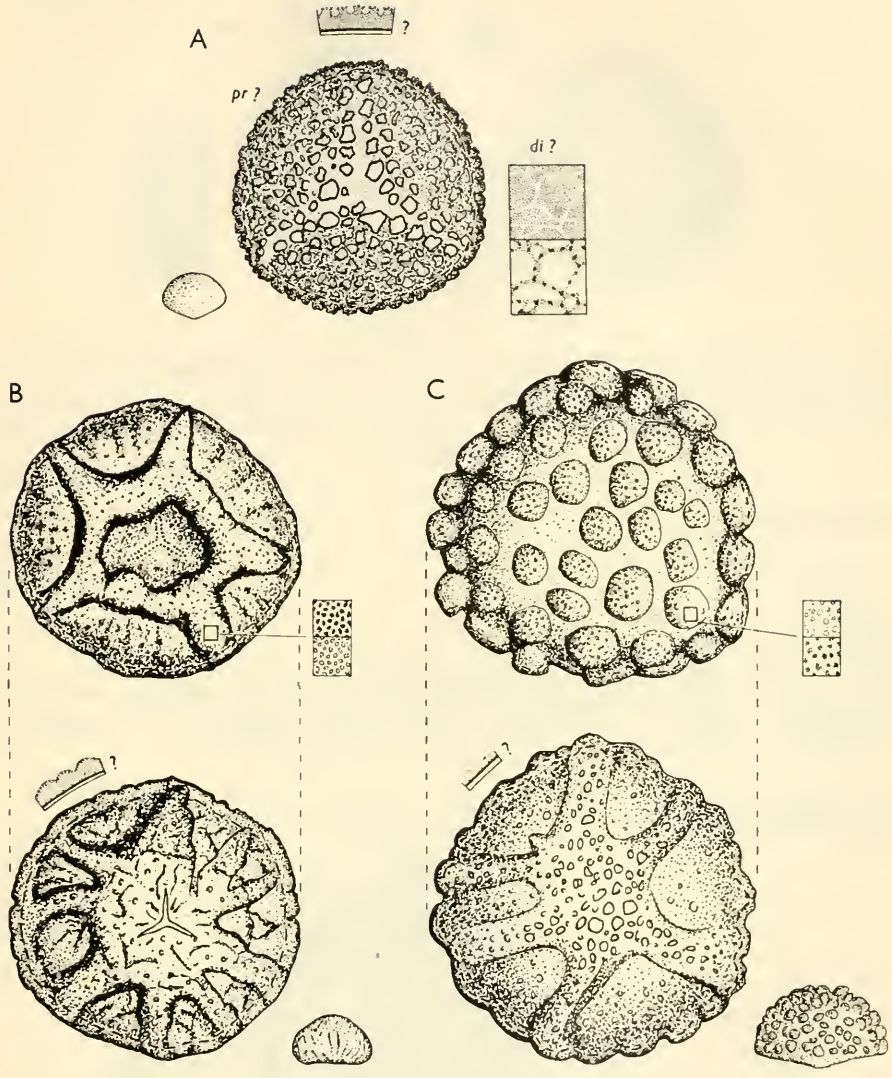

Fig. 210. A, *Encalypta alpina*. From left to right: spore in lateral view (×250); cf. proximal face (× 1000); LO-patterns in the distal (?) face. B, *E. ciliata*; distal face (upper figure) and proximal face (lower figure; both × 1000); the lower right-hand detail shows a spore in lateral view (× 250). C, *E. rhabdocarpa*; distal face (upper figure) and proximal face (lower figure; both × 1000); the lower right-hand detail shows a spore in lateral view (× 250).

EXORMOTHECA:—

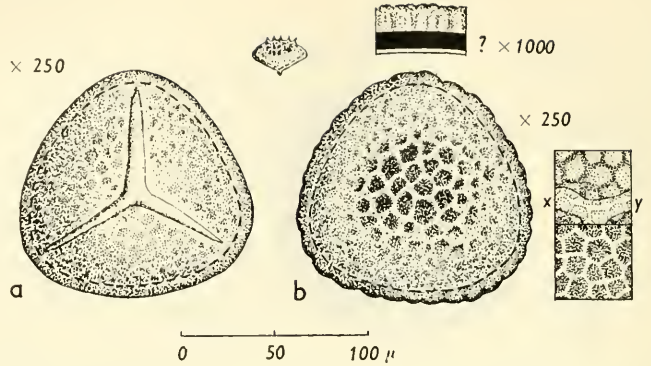

Fig. 211. *Exormotheca fimbriata*; a, proximal, b, distal face (× 250). The LO-patterns to the extreme right exhibit—at x-y—a part of one of the muroid ridges shown in b, and also the "insulous" condition in the bottom of the lumina.

FISSIDENS:—

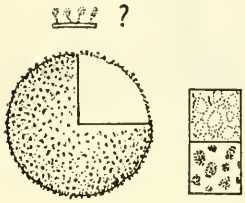

Fig. 212. *Fissidens adiantoides*; surface and optical section (× 1000), exine stratification (× 2000), and LO-patterns.

FOSSOMBRONIA:—

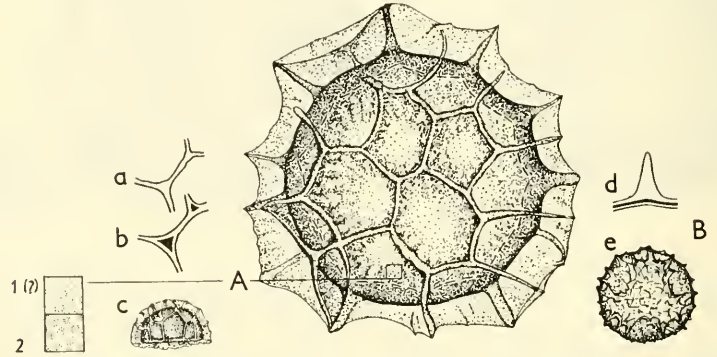

Fig. 213. A, *Fossombronia angulosa*; spore (× 1000); a, part of "muri" at high and, in b, at slightly lower adjustment of the microscope; c, spore, lateral view (× 250); the LO-patterns to the extreme left show the patterns at the bottom of the lumina. B, *F. dumortieri*; d, exine stratification (with "murus", × 2000); e, spore (proximal face ?), × 250.

FRULLANIA:—

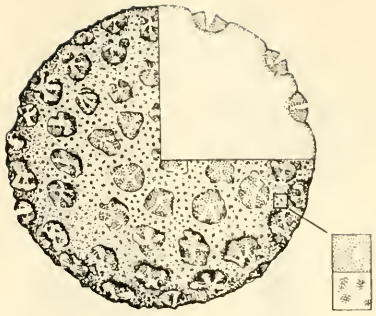

Fig. 214. *Frullania involvens*; surface and optical section (× 1000).

FUNARIA: see Pl. IV, V (facing pp. 130, 131).

GEORGIA:—

Fig. 215. *Georgia pellucida*; from left to right: spore in lateral view (× 250); spore in polar view (× 1000); LO-patterns.

GEOTHALLUS:—

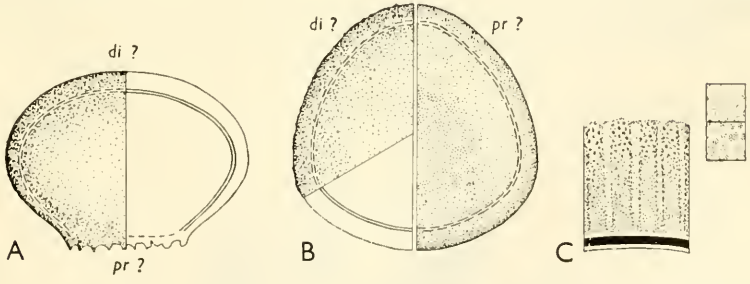

Fig. 216. *Geothallus tuberosus*; A, lateral view (× 250); B, polar view (di = cf. distal face, surface and optical section; pr = cf. proximal face, surface, × 250); C, sclerine stratification (about × 2000).

GIGASPERMUM (Fig. 217 B), LORENTZIELLA (Fig. 217 A):—

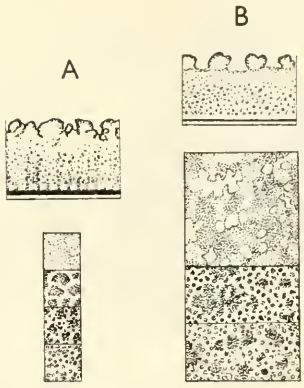

Fig. 217. Gigaspermaceae. — A, *Lorentziella paraguensis*; sclerine stratification (× 2000) and LO-patterns. B, *Gigaspermum repens*; sclerine stratification (× 2000) and LO-patterns.

HEDWIGIA (Fig. 218 A), HEDWIGIDIUM (Fig. 218 B):—

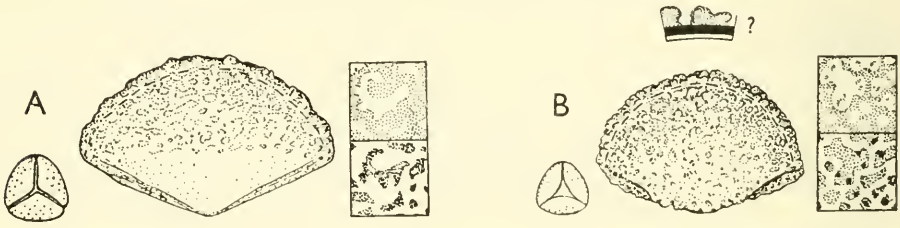

Fig. 218. Hedwigiaceae. — A, *Hedwigia ciliata*; from left to right: proximal face (× 250); spore in lateral view (× 1000); LO-patterns. B, *Hedwigidium integrifolium*; from left to right: proximal face (× 250); spore in lateral view (× 1000); LO-patterns. (From Erdtman in Svensk bot. Tidskr. 1954.)

HEDWIGIDIUM: see Fig. 218 B.

HELICOPHYLLUM:—

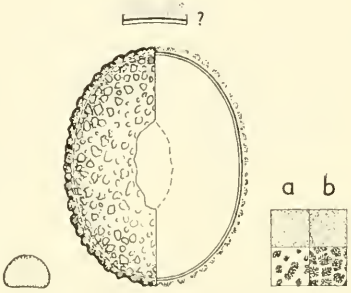

Fig. 219. *Helicophyllum torquatum*; a, LO-patterns, proximal face; b, LO-patterns, distal face; the central figure shows the proximal face of a spore, surface (left) and optical section (right; × 1000).

HOOKERIA:—

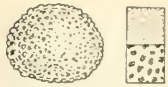

Fig. 220. *Hookeria albicans*; spore (× 1000) and LO-patterns.

HYLOCOMIUM:—

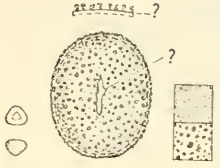

Fig. 221. *Hylocomium splendens*; the main figure shows the supposed proximal spore face (× 1000).

ISOTHECIUM: see Fig. 228 A, p. 113.

LEPTOSTOMUM:

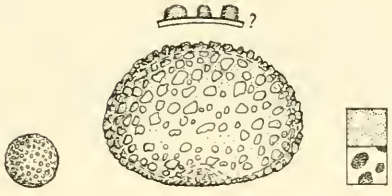

Fig. 222. *Leptostomum macrocarpum*; from left to right: spore in cf. transverse lateral view (× 250); spore in longitudinal lateral view (× 1000); LO-patterns. Upper detail figure: exine stratification (× 2000).

LESKEA:—

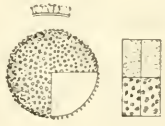

Fig. 223. *Leskea polycarpa*; spore, surface and optical section (× 1000). The left part of the right-hand detail figure shows the LO-patterns of the cf. distal face, the right part those of the cf. proximal face.

LEUCOBRYUM: see Fig. 203 C, p. 103.

LORENTZIELLA: see Fig. 217 A, p. 110.

MEESEA (Fig. 224 A, B), CATASCOPIUM (Fig. 224 D), PALUDELLA (Fig. 224 C):—

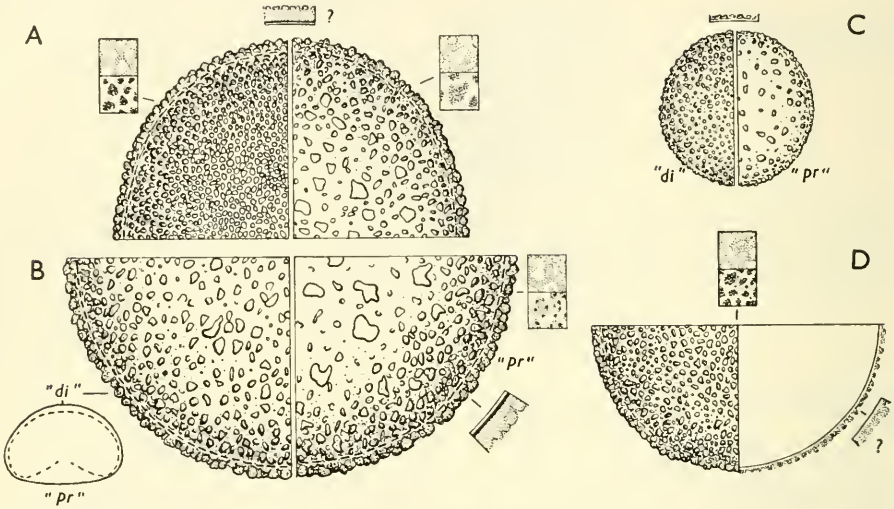

Fig. 224. Meeseaceae (A–C), Catascopiaceae (D). — A, *Meesea longiseta*, cf. distal face (left) and cf. proximal face (right; × 1000). B, *M. uliginosa*, cf. distal face (left) and cf. proximal face (right; × 1000). C, *Paludella squarrosa*, cf. distal face (left) and cf. proximal face (right; × 1000). D, *Catascopium nigritum*, part of spore (× 1000), surface (left) and optical section (right).

MEGACEROS:—

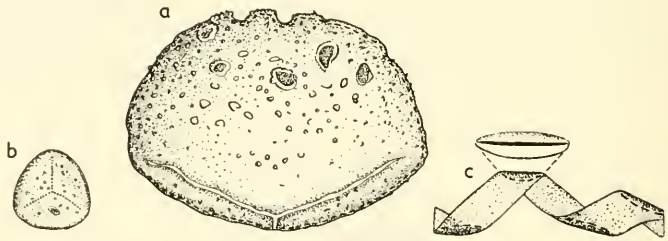

Fig. 225. *Megaceros aosanus*; a, spore in lateral, slightly oblique view (×1000); b, distal face (× 250); c, elater (× 1000; the detail figure shows the wall stratification, × 2000).

MIELICHHOFERIA: see Fig. 199 E, p. 102.

MONOCLEA:—

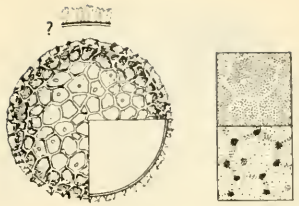

Fig. 226. *Monoclea forsteri*; spore (× 1000), exine stratification (× 2000), and LO-patterns.

NANOMITRIUM:—

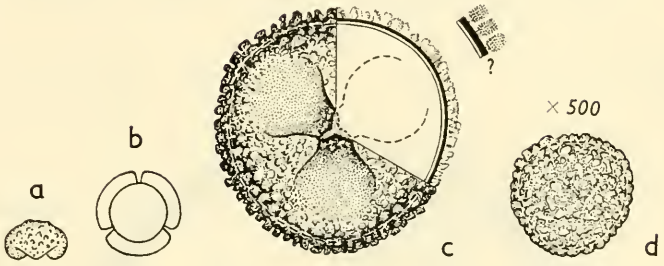

Fig. 227. *Nanomitrium tenerum*; a, lateral view (× 250); b, outline of tetrad (× 250); c, proximal face, surface and optical section (× 1000); d, distal face (× 500).

NECKERA (Fig. 228 B), ISOTHECIUM (Fig. 228 A):—

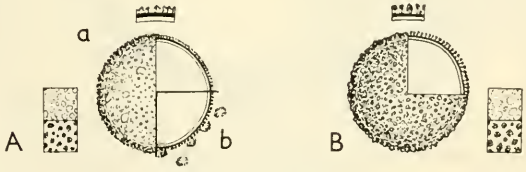

Fig. 228. Neckerinales. — A, *Isothecium myosuroides*; LO-patterns and spore (× 1000); a, surface; b, optical section (upper quadrant without, lower quadrant with, easily detachable "granules"). B, *Neckera complanata*; spore (× 1000), surface and optical section; exine stratification (× 2000), and LO-patterns.

OEDIPODIUM:—

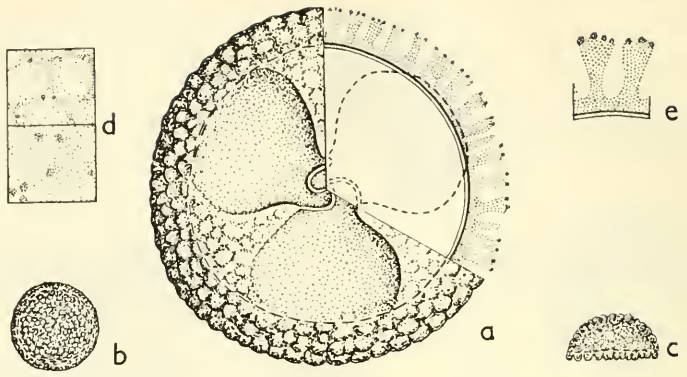

Fig. 229. *Oedipodium griffithianum*; a, proximal face, surface and optical section (× 1000); b, distal face (× 250); c, lateral view (× 250); d, LO-patterns; e, sclerine stratification (about × 2000).

OXYMITRA:—

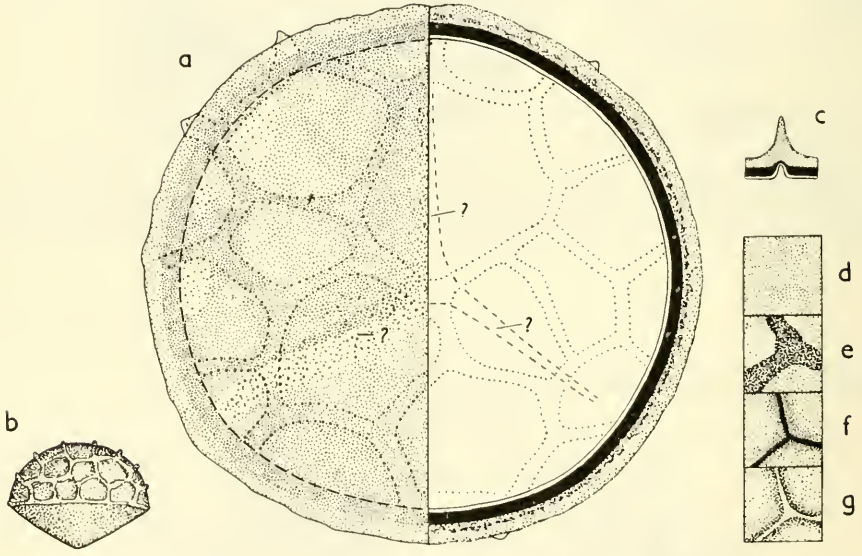

Fig. 230. *Oxymitra paleacea*; a, proximal (?) face, surface (left) and section (right; × 1000); b, spore in lateral view (× 250); c, optical section through a "murus" in the reticulum; d–g, LO-analysis of a "muriferous" part of the spore surface.

PALUDELLA: see Fig. 224 C, p. 112.

PELLIA:—

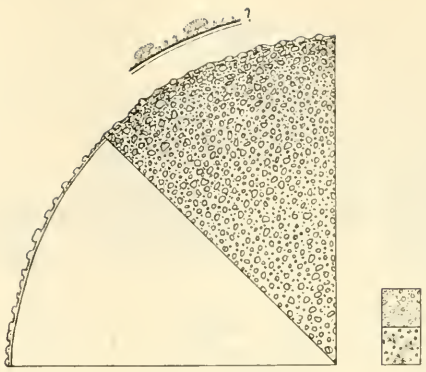

Fig. 231. *Pellia epiphylla*; part of a spore, optical section and surface (×1000); exine stratification (× 2000).

PHASCUM: see Fig. 236 A, p. 117.

PLAGIOCHASMA:—

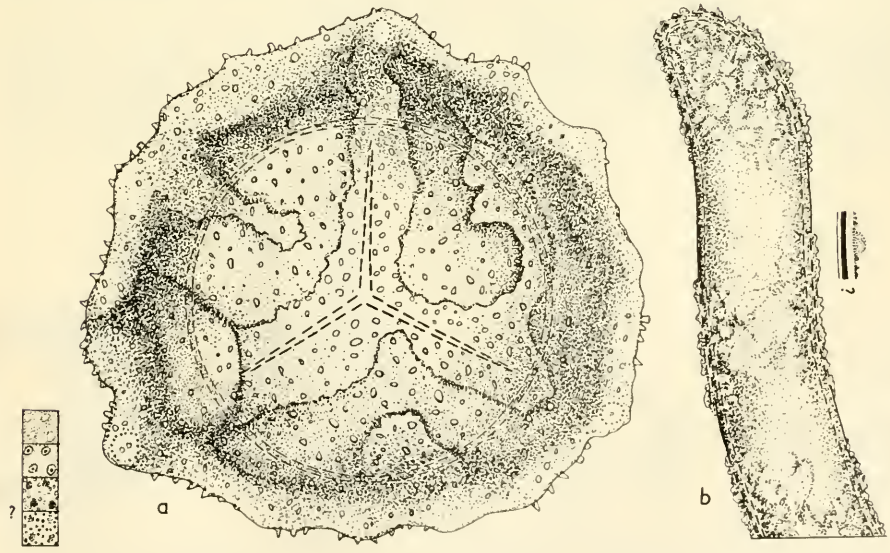

Fig. 232. *Plagiochasma intermedium*; a, proximal face (× 1000) and LO-patterns; b, one half of an elater (× 1000).

PLAGIOCHILA:—

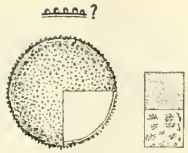

Fig. 233. *Plagiochila asplenioides*; spore (surface and optical section, × 1000); LO-patterns.

PLEUROPHASCUM:—

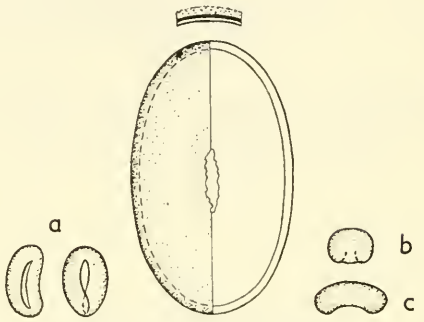

Fig. 234. *Pleurophascum quadrilobum*; main figure: proximal face (surface and optical section; × 1000); a, proximal face (× 250) of slightly irregular spores; b, transverse side view (× 250); c, longitudinal side view (× 250, distal pole upwards).

POHLIA: see Fig. 199 C, p. 102.

POLYTRICHUM:—

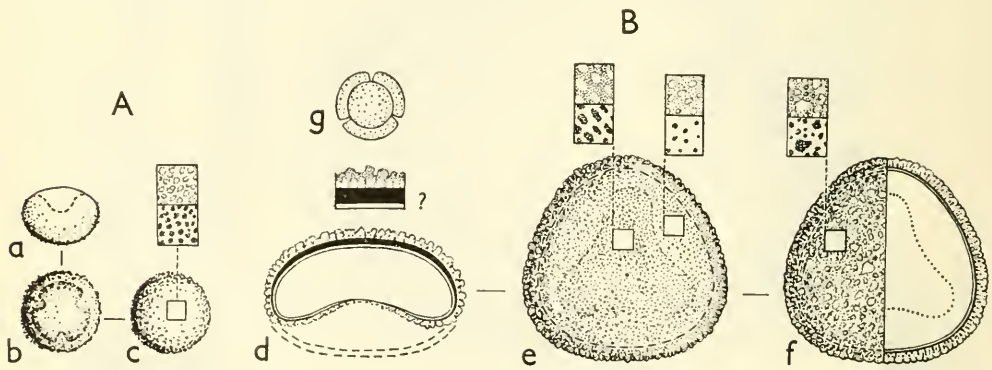

Fig. 235. A, *Polytrichum juniperinum* (× 1000); a, spore in lateral view (proximal pole upwards); b, proximal face; c, distal face and LO-patterns of the square shown in the centre of the face. B, *P. gracile*; d, lateral view; e, proximal (tenuitatiferous) face; f, distal face; g, tetrad (× 250; d–f × 1000).

POTTIA (Fig. 233 B), PHASCUM (Fig. 233 A):—

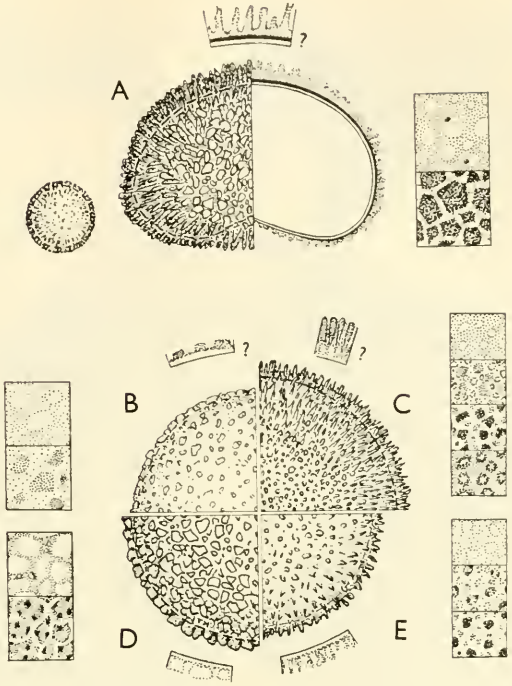

Fig. 236. Pottiaceae (see also Fig. 193, p. 100). — A, *Phascum cuspidatum*, from left to right: spore in polar view (× 250); spore in lateral view, surface (left) and optical section (right; × 1000); LO-patterns. B–E, surface (×1000; only a fourth of a hemisphere shown), sclerine stratification (about × 2000), and LO-patterns in *Pottia crinita* (B), *P. davalliana* (C), *P. truncata* (D), and *P. heimii* (E).

PYRRHOBRYUM:—

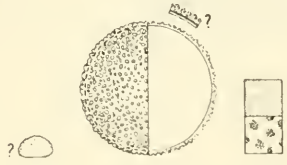

Fig. 237. *Pyrrhobryum spiniforme*. From left to right: spore in lateral view (× 250); spore in polar view (× 1000), surface (left) and optical section; LO-patterns.

RADULA:—

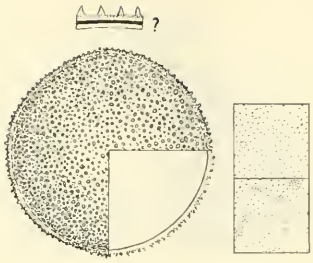

Fig. 238. *Radula lindbergiana*; surface and optical section (lower right-hand quadrant; × 1000); exine stratification (× 2000), and LO-patterns.

RHACOMITRIUM:—

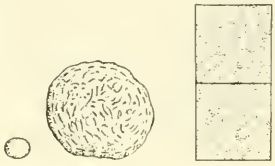

Fig. 239. *Rhacomitrium microcarpon*. From left to right: spore in lateral view (× 250); spore in polar view (× 1000); LO-patterns.

RICCARDIA:—

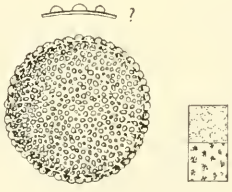

Fig. 240. *Riccardia latifrons*; spore (× 1000); exine stratification (× 2000); LO-patterns.

RICCIA:—

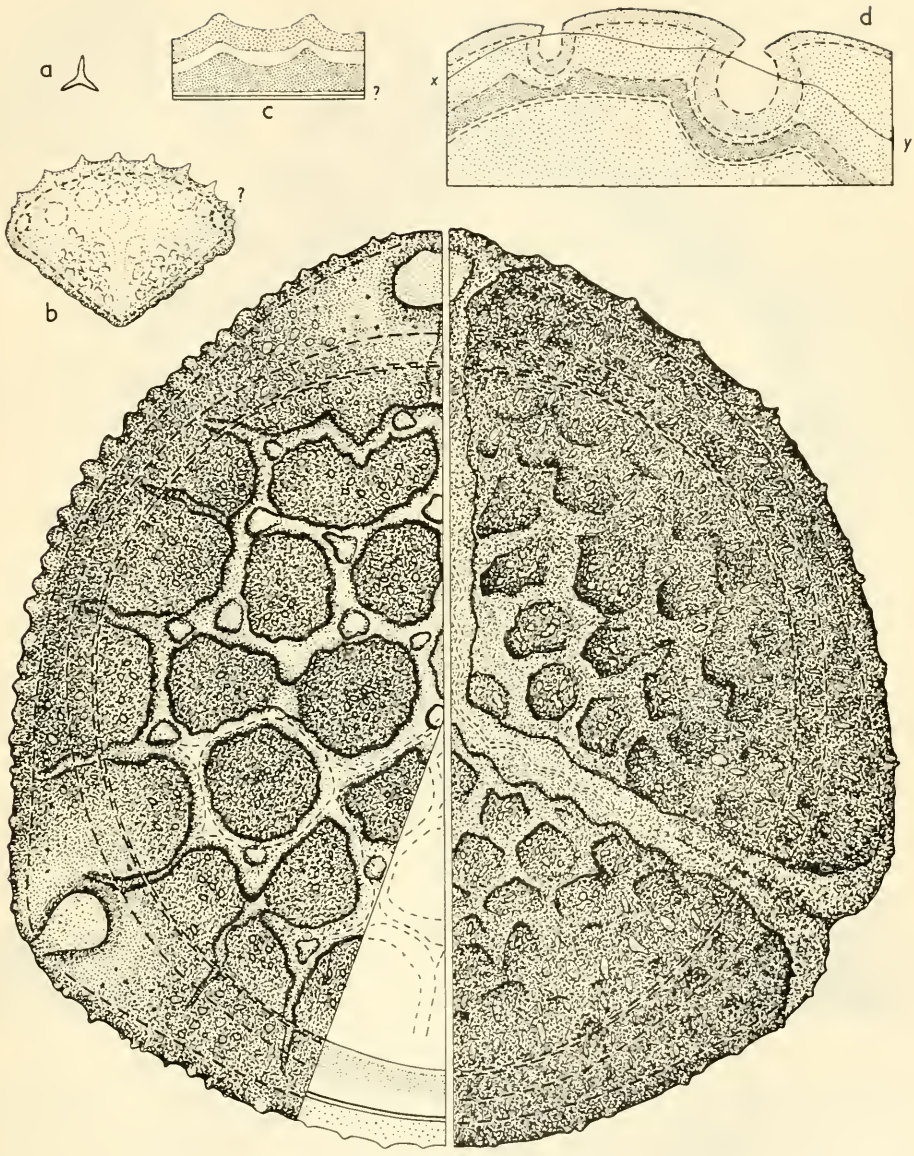

Fig. 241. *Riccia beyrichiana*; main figure: distal face, surface and optical section (left); proximal face, surface (right; × 1000); a, laesura (?); b, spore in lateral view (× 250); c, outline of sclerine stratification (without attempt to classify the layers); d, spore margin (optical section); x–y, approximate limit between distal and proximal face.

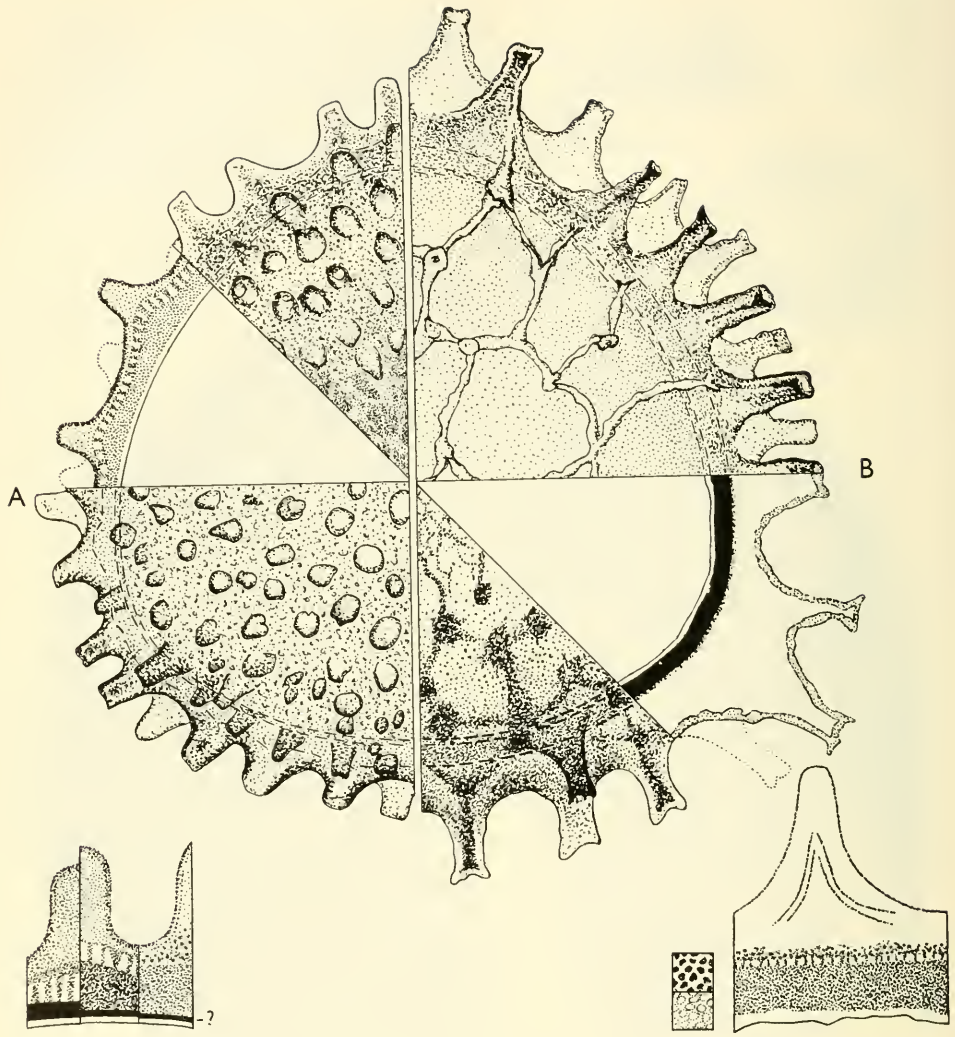

Fig. 242. A, *Riella halophila* (left). B, *R. purpureospora* (right). The sectors in the main figure (A + B) are as follows (enumerated clockwise, beginning at A): sclerine, optical section; part of proximal (?), tenuitatiferous (?) face; part of distal (?) face; sclerine, optical section; part of proximal (?), tenuitatiferous (?) face; part of distal (?) face. In the lower left-hand detail figure tentative interpretations of the sclerine stratification in *R. halophila* are exhibited. The lower right-hand detail shows an outline of the sclerine stratification in *R. purpureospora* (the second layer from below should have been blackened in, not dotted); the OL-pattern is due to reticuloid arrangement of the 'sexinous' (cf. endosexinous) elements in the third layer from below.

SCAPANIA:—

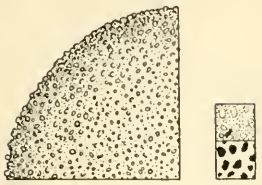

Fig. 243. *Scapania paludicola*; part of spore surface (× 1000); LO-patterns.

SCHISTOSTEGA:—

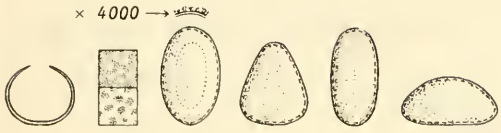

Fig. 244. *Schistostega osmundacea*; LO-patterns and five spores (× 1000; from left to right: optical section, distal face of three spores, and spore in lateral view); the upper detail figure exhibiting the exine stratification is enlarged about 4000 times.

SOUTHBYA:—

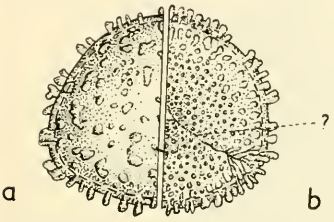

Fig. 245. *Southbya stillicidiorum*; a, cf. distal face; b, cf. proximal face (× 1000).

SPHAGNUM:—

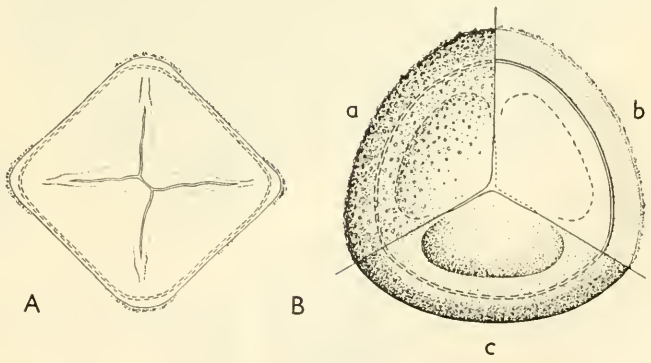

Fig. 246. A, *Sphagnum fimbriatum*; deviating ("tetrachotomolaesurate" or "4-lete") spore (× 1000). B, *S. palustre*; proximal face of normal (3-lete) spore (× 1000); a, with perine (surface); b, with perine (optical section); c, without perine (surface).

SPIRIDENS:—

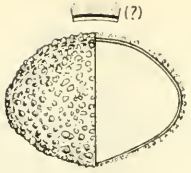

Fig. 247. *Spiridens aristidifolius*; spore in lateral view (× 1000); exine stratification (× 2000).

SPLACHNUM (Fig. 248 C), TAYLORIA (Fig. 248 B), VOITIA (Fig. 248 A).

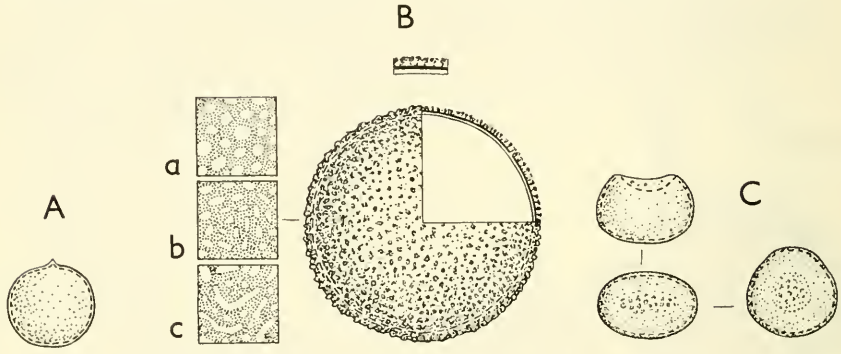

Fig. 248. Splachnaceae. — A, *Voitia nivalis* (× 1000). B, *Tayloria lingulata*; surface and optical section (× 1000), LO-patterns, and exine stratification (× 2000). C, *Splachnum vasculosum*; two bilateral spores (the upper in lateral view, proximal face upwards; the lower in polar view, showing the cf. proximal tenuitas) and one ± radiosymmetric spore (× 1000).

STROEMIA: see Fig. 253 A, p. 124.

SYMPHYODON:—

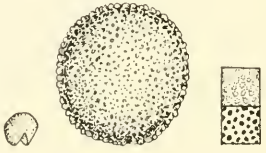

Fig. 249. *Symphyodon echinatus*; spore in lateral (?) view (× 250); spore in polar (?) view (× 1000); LO-patterns.

SYMPHYOGYNA:—

Fig. 250. *Symphyogyna podophylla*; four spores (three × 250, one × 1000); LO-patterns.

TARGIONIA:—

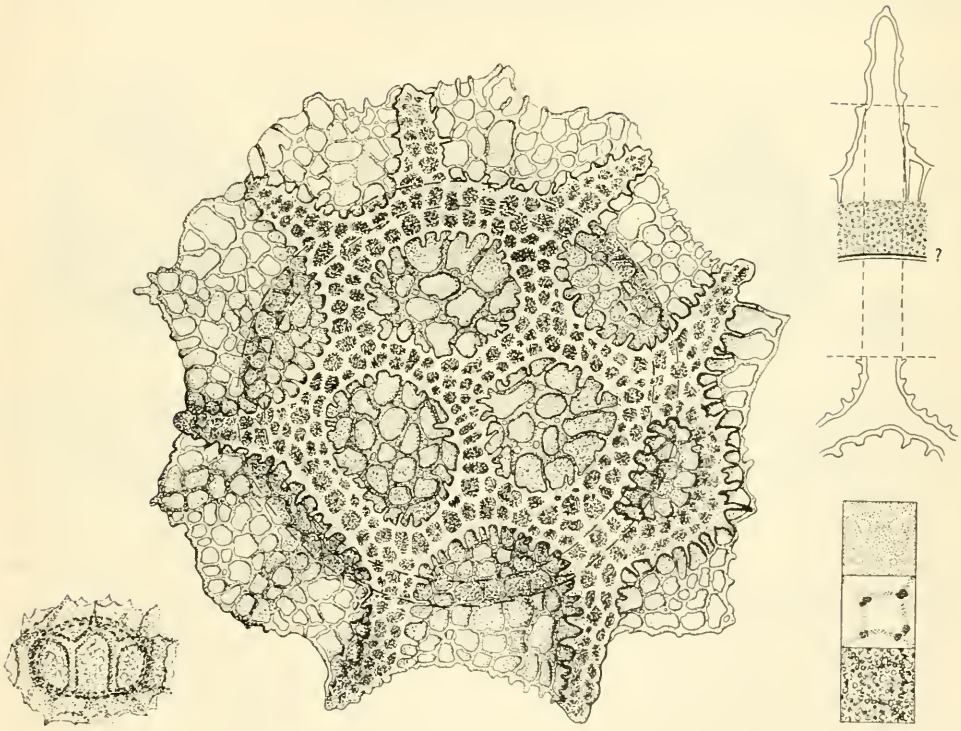

Fig. 251. *Targionia hypophylla*; from left to right: spore in lateral view (× 250); spore in polar view (× 1000); sclerine stratification and LO-patterns.

TAYLORIA: see Fig. 248 B, p. 122.

TIMMIA:—

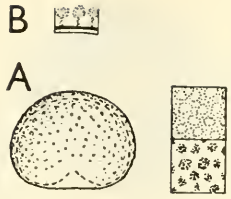

Fig. 252. A, *Timmia austriaca*; spore in lateral view (× 1000); LO-patterns. B, *T. anomala*; exine stratification (× 2000).

ULOTA (Fig. 253 B), STROEMIA (Fig. 253 A):—

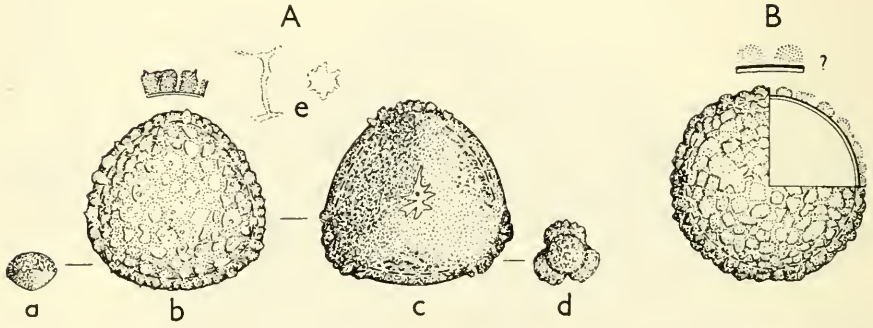

Fig. 253. A, *Stroemia gymnostoma*; a, spore in lateral view (× 250); b, distal face (× 1000); c, proximal face (× 1000); d, tetrad (× 250); e, outline of apertures. B, *Ulota bruchii*; surface and optical section (× 1000).

VOITIA: see Fig. 248 A, p. 122.

SUPPLEMENT

ON NEW METHODS IN PHYSICAL CELL RESEARCH AND THEIR APPLICATION IN STUDIES OF POLLEN GRAINS AND SPORES

BY

B. M. AFZELIUS

The rapid development in physical cell research has recently provided much news of interest to pollen and spore morphology. Deeper understanding of the cell, the morphology and composition of its organellae and their finest constituents down to macromolecular dimensions can be gained through the ever-widening application of refined techniques such as phase contrast and polarization microscopy, ultra-violet light, interference, and electron microscopy. Certain indirect methods are also of interest (e.g. X-ray diffraction) and there are microscopical and other methods for obtaining quantitative cytochemical data. Micrographs of macromolecules can thus be made (cf. Wyckoff 1949, p. 189) and it is even possible (cf. e.g. Frey-Wyssling 1954) to determine the macromolecular or particle weight by microscopical methods. From a study of electron micrographs (Steinmann in Finean, Sjöstrand, and Steinmann 1953) of the small spherical particles constituting the lamellae of chloroplast grana Frey-Wyssling was able to calculate their size as being equal to one to four Svedberg units, containing eight to twelve chlorophyll molecules (the molecular weight of one Swedberg unit = 17,600). Moreover, micrographs showing the exact localization of enzymes in the cell are now available (Sheldon, Zetterqvist, and Brandes 1955). By means of microscopical interferometric methods it is, furthermore, possible to determine mass as small as 0.01 pg/μ^2 (Davies, Engström, and Lindström 1953; 1 pg = 10^{-12} g). Microspectroscopical methods allow of determination of mass as small as 0.001 pg (Caspersson 1950).

To be able to make use of the new developments in the field of microscopy it is often necessary to introduce new methods for preparing the material to be studied. Thus the invention of the electron microscope (Knoll and

Ruska 1932) called for intense research for new methods of preparation. As far as biology is concerned satisfactory results were not achieved until ultra-thin sections could be made by routine methods—almost 20 years after the invention of the electron microscope. Several new ways of preparation might be convenient in ordinary light microscopy but ultra-thin sectioning will, no doubt, eventually be the most useful one.

In response to a request of visitors to the Palynological Laboratory, Stockholm–Bromma, some of the problems met with when using the ultra-thin section technique will be discussed in the following.

Methods of preparation

For studies of ultra-thin sections of non-acetolyzed pollen grains and spores it is, i.a., advisable to consider the question of fixation carefully. For light microscopical work fixation by means of formalin, or freezing and drying is often sufficient. Fixation with osmic acid is, however, to be preferred; in fact, in electron microscopical studies it is, so far, the only reliable fixative. Osmic acid also acts as an electron stain. In acetolyzed exines the staining effect of the osmic acid is negligible and probably of no use. Experiments ought to be made to discover, if possible, other heavy metals or ions suitable as electron stains. In investigations of mammalian tissues a buffered solution of osmium tetroxide is usually used (acetate-veronal buffer at pH 7.2; cf. Rhodin 1954). The same fixative has been used by Turian (1956) and Afzelius (1955). In the opinion of P. Sitte (personal communication, November 1956), buffering of the solution is not particularly important when fixing plant cells which have not formed a large vacuole, since the buffer might penetrate the cell more rapidly than the osmic acid and thus cause a poisoning of the cell before fixation. Sitte, moreover, emphasized the importance of using an isotonic solution of 1 per cent osmium tetroxide by adding sugar or urethan. The slow penetration of osmic acid presents a problem familiar to all who have tried this type of fixation. In pollen grains the fixative probably penetrates into the grains more readily through the aperture membranes than through the wall proper. (N.B. In order to obtain good fixations to meet the high demands of electron microscopy it might be advisable to cut large pollen grains or spores before fixing). Wettstein has obtained very good results by using osmium vapour (cf. Pl. IV, V).

The necessity of using suitable embedding media in the study of thin sections by means of phase contrast has recently been stressed. Ordinary histological techniques have, as a rule, been adjusted to the use of much thicker sections, for which glycerol jelly is often a good embedding medium. Thin sections (about 500–5000 Å thick) should preferably be studied in

water, ultra-thin sections (thickness < 500 Å) in air (water and air are better than glycerol jelly on account of their lower refractive index). The following formula shows the importance of a wide difference between the refractive index of the object and that of the embedding medium when the geometrical thickness of the section is decreased:

$OPD = e(n_1 - n_2)$; *OPD*, optical path difference (see p. 131); n_1, refractive index of the object; n_2, that of the enclosing medium; e, geometrical thickness of the object.

If air is used as an enclosing medium it is, of course, possible to apply cover slips and immersion oil in the ordinary way. For theoretical reasons, however, full use cannot be made of the numerical aperture of the microscope. Good results have, nevertheless, been obtained by this method. When specifying the thickness of the sections, e.g. ultra-thin sections embedded in air, the figures originally obtained from electron micrographs of shadowed sections (Sjöstrand, personal communication) have been used. The present author has measured the thickness of ultra-thin sections by means of interference microscopy. These measurements, in general, tend to give slightly higher values than those calculated from shadowed sections.

It may perhaps not be superfluous to point to another circumstance that might cause confusion. If thin exine sections are studied by means of an ordinary light microscope a number of diffraction lines can usually be seen, due to superposed light waves in the thin exine. The number of the waves can be altered by changing the wave length of the light used (Ingelstam, personal communication). The diffraction lines must not be mistaken for lamellae or demarcation lines between different layers of the exine as has apparently been done by Pflug in describing optical sections of entire grains [cf. Pflug 1953, p. 66: "Exospore and Exinen sind aus konzentrischen Schalen (Lamellae) zusammengesetzt; das ist in unzähligen Fällen beobachtet. Fraglich ist nur deren Zahl. Sie ist einmal subjektiv bedingt durch die Schärfe der Optik"].

Ultra-thin sections should always be properly stained in order to obtain as much information on wall stratification, cell contents etc. as possible. The fact that the immature wall of certain fungus spores is easily penetrated by stains (Nannfeldt, personal communication) seems to open up a possibility for obtaining further details on sporoderm formation. Further research work in sporoderm morphogenesis is indeed necessary.

In this context another problem may be mentioned: electron micrographs of acetolyzed exines often show that the exine, the endonexine excepted, is altogether homogeneous-amorphous (cf. e.g. EMG by Afzelius in Erdtman, 1956a, Fig. 1, p. 132). No demarcation lines can be observed at a resolution of 40–50 Å. Oshurkova (1956) in a review of a paper on the fine

structure of the pollen wall in *Clivia miniata* (Afzelius 1955) criticizes the use of several terms to indicate different parts of this continuous layer. If attention is paid to fine structure only this criticism seems to be justified in the case of *Clivia*, and many other pollen types. There are, however, exceptions. The basal part of sexinous rods in pollen grains of *Cobaea penduliflora* (Erdtman 1952), *Cucurbita* (Mühlethaler 1955), *Linum*, and some other genera (Erdtman 1956b) is fixed well into the nexine. Studies of ultra-thin sections, suitably stained, would probably shed more light on these and similar problems, and make possible further contributions to the elucidation of the morphogenesis of the sporoderms.

Electron microscopy

There are practically no pollen grains or spores small enough to make possible a study of unsectioned grains or spores in the electron microscope. However, some efforts along these lines have in fact been made (cf. e.g. Burton 1946). Ueno (1949, and personal communication 1956), isolated "viscin threads" of *Oenothera odorata* and *Gaura lindheimeri* etc., and studied them, without further preparation, by means of electron microscopy. These threads, or part of them, probably consist of the same material as the exine, since they are not dissolved if heated in an acetolysis mixture (cf. Erdtman 1952, Fig. 170B:b, p. 292, and Fig. 171A, p. 293).

Fragmentation of material, by means of ultra-sonics or other methods, was often carried out before the introduction of ultra-thin sectioning techniques (cf. the spine of a malvaceous pollen grain, Fig. 151A, p. 262, in Erdtman 1952). It is a rapid method of preparation, but rather rough and unsatisfactory. Many fragments will be too thick and thus instantly charred by the electron beam; they defile the microscope and the method cannot be used in high resolution microscopy. Although now outmoded in electron microscopy, this technique can still be of some use in ordinary microscopical investigations. The interpretation of the micrographs is easier if the material consists of one or a few structural units only, as when dealing with acetolyzed exines.

Replica methods are often useful in the study of the surface details of pollen grains and spores. Sitte (1953) has modified the wax impression method by Mahl (1942), whereas Bradley (1954, 1957), and Mühlethaler (1955) have used, with much success, a carbon replica method devised by Bradley. Bradley has thus provided new information concerning the colpi in the pollen grains of *Lamium album*; he has also found that the spores of *Russula verrucosa* are covered with a thin amyloid film.

Fragmentation and replica-making can be combined with shadowing by means of metal-evaporation, although this treatment is too rough in studies of cytoplasm etc. (silver, or aluminium, is often used in light microscopy, palladium in electron microscopy). The thickness of the metal film must be calculated with care, as must also the angle at which the metal atoms are to strike the material (cf. micrographs in Wyckoff 1949, p. 110, 121, and 227–232). In high resolution electron microscopy the method has now almost lost its importance since sufficient contrast is preferably obtained by using suitable electron stains.

A particularly penetrating evidence concerning the structure of the wall will, no doubt, ultimately be derived from studies of ultra-thin sections. Various types of fine structure in the resistant part of pollen and spore walls have recently been described by various authors. At a resolution of about 30 Å (cf. EMG, Figure 142, page 77) acetolyzed sporoderm seems to consist of small granules, 50–60 Å in diameter. They are either arranged in lamellae, with the granules in a single layer, or grouped into an amorphous type of structure. The lamellate fine structure can be transformed into the latter type of structure by means of oxydation, as has been proved in *Lycopodium clavatum* (Afzelius 1956). Hitherto, attention has mainly been centred on the fine structure of the exine. Electron microscopy may, however, also help to reveal the fine details in non-acetolyzed sporoderms and the interior of pollen grains and spores, as shown by some electron micrographs by D. von Wettstein reproduced in Pl. IV and V. The following constitutes von Wettstein's description and interpretation of his EMG:s:

The spore wall of *Funaria hygrometrica* is divided into three layers, intine, inner exine, and outer exine, each of which is structurally homogeneous and cannot be subdivided. The intine consists of a three-dimensional framework of fibrillae (probably cellulose). In properly fixed material the cytoplasm of the spore is in close contact with the intine and obviously not separated from it by a membrane (Pl. IV, Fig. c). The outermost layer of the cytoplasm seems to consist of a framework of fibrillae related in size, but not in chemical composition, to that of the intine. If, in the course of fixation, the cytoplasm is separated from the intine, some sort of membrane appears in the micrographs. The inner layer of the exine in *Funaria* displays a higher electron density than the intine. A kind of fibrillar structure seems to be present although obscured by a substance between the fibrillae. The intine/exine limit is marked by a fine and dense zone about 50–100 Å in thickness (Pl. IV, Fig. c). In Pl. IV, Fig. b, the exine seems to be separated from the intine by a special, comparatively thick, layer. Obviously, a corresponding layer is lacking in Figs. a and c in the same plate. These, however, exhibit radial, strictly perpendicular sections through the wall, whereas Fig. b exhibits an oblique section, as can be inferred from the

greater thickness of the exine as well as of the intine. Thus the effect of a special layer between exine and intine is produced by the high focal depth of the electron microscope. In reality, this layer is nothing else than an overlapping of the intine and exine, due to oblique cutting.

The outer part of the exine consists of a thin layer provided with large processes. It shows a high electron density and no inner structure could be resolved so far. The processes are finely papillate and exhibit a considerable variation as to size and shape. Tangential sections through the outer part of the exine (Figs. d–e) reveal the presence of a thin superficial layer (about 150–300 Å thick) covering the processes as well as the rest of the exine surface. This layer has an extremely high electron density. The inner (infrasporodermal) part of the spore consists of cytoplasm, organellae, and reserve substances. Two kinds of organellae, viz. the mitochondria and the plastids, are easy to identify: the former contain a folded structure, which is also encountered in other plants and in animals; the plastids are considerably larger and provided with some traces of lamellae and globular particles. They lack the typical structure found in fully grown and assimilating chloroplasts. In Pl. IV, Fig. a, three chloroplasts and part of a fourth can be seen. The membranes surrounding the plastids display an interesting structure.

In the last-mentioned figure there are many other small bodies with a slightly irregular surface, possibly reserve substances. They appear to consist of two components, a central grain with small electron scattering power (white in the picture), and a surrounding layer of electronoptically dense and homogeneous material. There is reason to believe that these particles constitute a polysaccharide enclosed in a fatty substance. As can be concluded from this description, a tangential section gives a more or less uneven "black" area in the pictures. Organellae and inclusions of other kinds are depicted in Figs. f–i, amongst which are a great number of droplets with a strong electron scattering power. The other three organellae in these figures differ in size and structure. They have a special type of surface membrane which is composed of a thin layer supported by dense droplets, giving, in cross-section, the impression of a pearl necklace. The chemical constitution and function of these organellae are unknown.

In Paris, in 1954, Frey-Wyssling, when summing up the facts known about the submicroscopic structure of the plant cell, intimated that the fine structure of the ground plasm was influenced by the fixative used but was still largely unknown. He further intimated that the presence of microsomes and mitochondria had been proved, but that a lamellate structure similar to that demonstrated in the large mitochondria of the kidney had not yet been found. Neither was it possible to ascertain if the nucleus was provided with a true nuclear membrane or not. The last two questions now

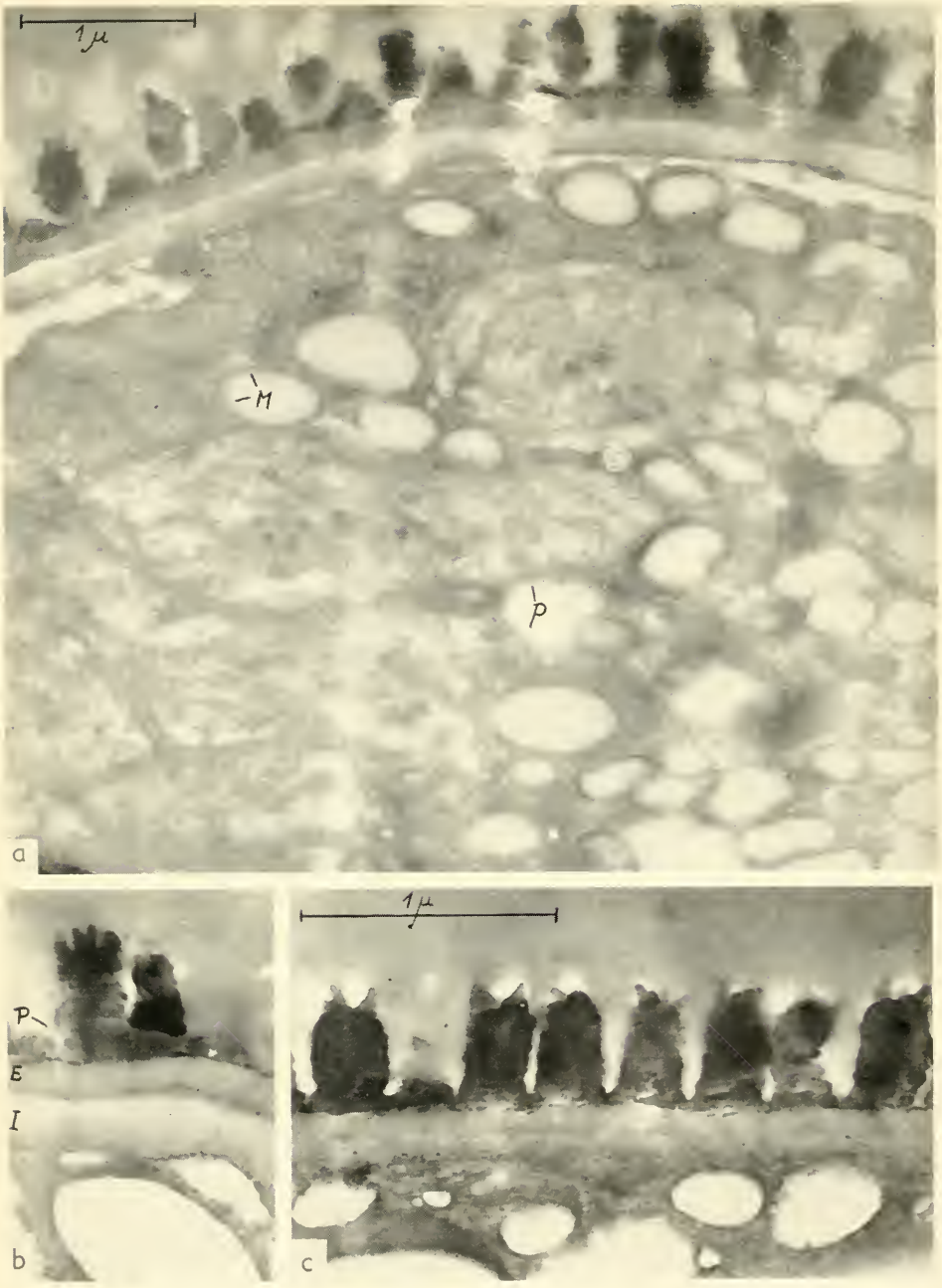

Pl. IV. *Funaria hygrometrica*. EMG D. von Wettstein. a, section through part of a spore; M, mitochondria; P, plastid. × 23,000. — b, oblique section of sporoderm (intine and two-layered exine) ×34,000. — c, radial (perpendicular) section through sporoderm; cytoplasm, intine, and exine closely connected. × 34,000.

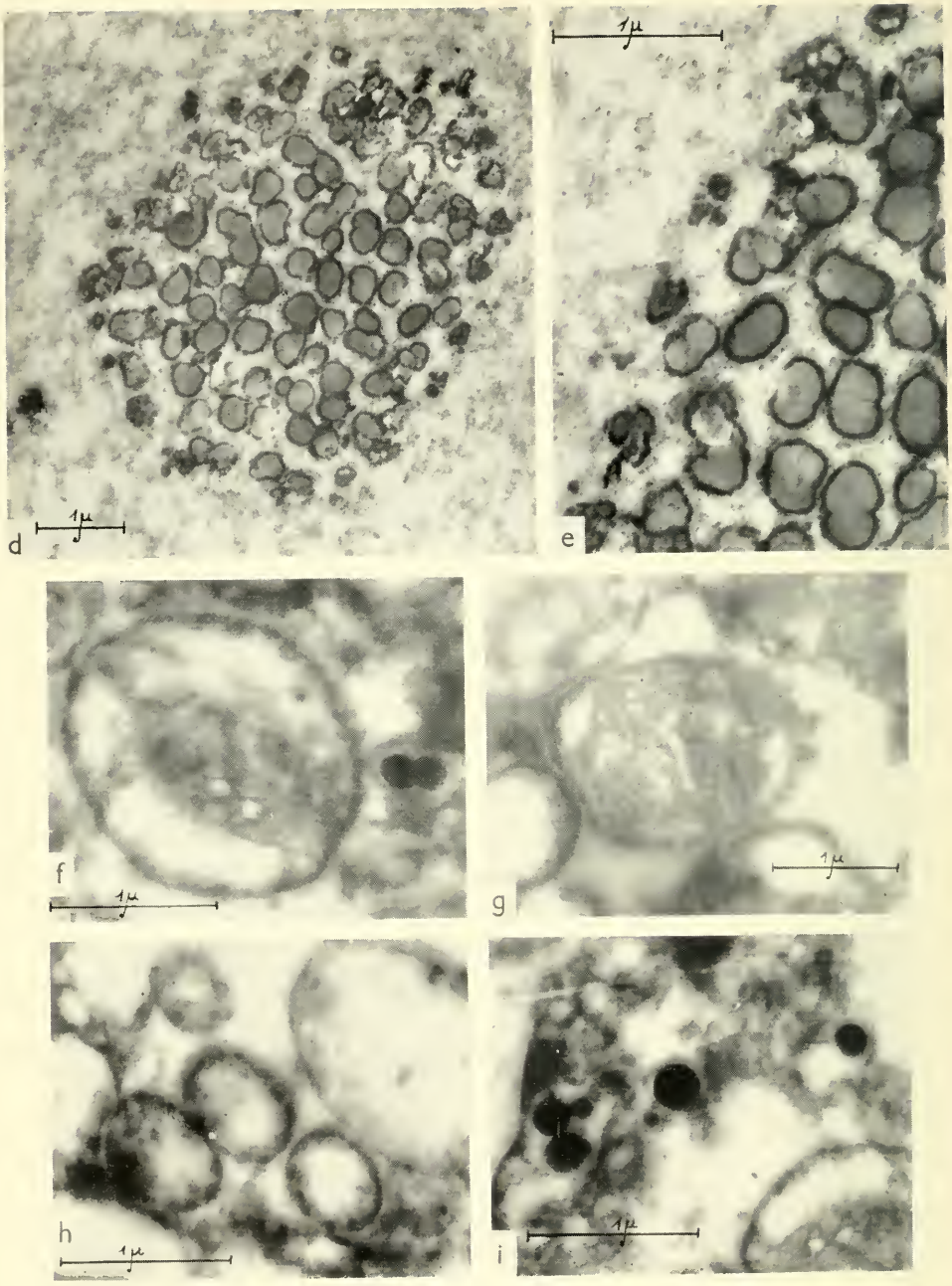

Pl. V. *Funaria hygrometrica*. EMG D. von Wettstein. d, outer part of exine (tangential section). × 12,000. — e, same as d; note the fine structure of the interior, main part of the processes. × 23,000. — f–i, particles in the cytoplasm. f, h, i × 23,000; g × 17,000.

seem to be answered in the affirmative by Turian and Kellenberger (1956), whose recent studies, together with those of von Wettstein, are certainly the most penetrating analysis of plant cell ultra-structure known to the present author.

Polarization microscopy, X-ray diffraction, UV-microscopy and their possible application

Polarization microscopy seems to be of little use in the study of acetolyzed exines; a form birefringence has not been revealed and it has equally not been possible to trace the fine lamination of the exine in *Lycopodium* in this way. Probably the lamellate layer is too thin to provide an effect in the polarization microscope. Freytag (manuscript Sept. 1956) has shown that an outer non-sporopolleninous layer can be demonstrated in some pollen grains by means of polarized light [cf. also electron microscopical studies of a similar layer by Afzelius (1955) and Bradley (1956)]. Likewise, X-ray diffraction does not provide any information about the exine and, therefore, seems to be of no use for obtaining information on the fine lamination in *Lycopodium clavatum*. This is possibly due to the fact that the laminated layers are not parallel but curved and undulating (Engström, personal communication 1955). Engström has investigated dry, non-acetolyzed pollen grains of *Alnus glutinosa* and spores of *Lycopodium clavatum* by means of low angle diffraction without obtaining positive results. On the other hand, Labouriau and Cardoso, when investigating *Lycopodium* exines by means of wide angle diffraction patterns, encountered a crystalline structure, a fact which seems difficult to explain (Acad. Bras. Ciênc. 1948).

UV-optics have chiefly been used in microspectroscopical investigations. Wilkins (1953) describes the absorption difference between the two types of nuclei in the pollen grains in a UV-micrograph obtained by means of reflection microscopy.

Interference microscopy

The light passing through small objects in a microscope will be delayed in comparison to that passing through the surrounding medium, if the object, as is generally the case, has higher refractive index than the surrounding medium. The interference microscope aims at measurements of the "optical path difference" (OPD, i.e., the difference in optical path through the object and an equal thickness of the surrounding medium,

e.g. water). When the OPD is known, the dry mass (m), as shown by Davies, Wilkins, Chayen and La Cour (1954), can be calculated from the following formula:

$$m = \frac{\Phi_w \cdot A}{\chi}$$

Φ_w = OPD in water; A = area cm²; χ for a dry object can be calculated from the formula $\chi = \frac{n_0 - n_w}{\varrho_0}$ where ϱ_0 is the density of the object, n_0 is the refractive index of the object, and n_w that of water.

In cell substances χ usually varies between 0.14 and 0.19. A χ value of 0.18 will give dry weight determinations with an error not exceeding 10 %. If the cell consists of a substance of one kind only, the error will be greater; in a mixture it will be less. In cells with plenty of storage products, e.g. many kinds of pollen grains and spores, it may not be advisable to use the average value of χ.

The thickness of the preparation or cell (t), is calculated from the formula

$$\Phi_w = (n_0 - n_w)\, t$$

All interferometric methods provide about the same accuracy. The OPD measurements of homogeneous, phase-even objects can be made with a precision of ± 20 Å ($\pm 2 \times 10^{-7}$ cm). In measurements of heterogeneous objects the same precision cannot be attained. Due to diffraction effects measurements of areas smaller than about 5 μ^2 are not advisable. It is thus possible to make determinations of dry weight of 0.05 pg (0.01 pg/μ^2).

In order to get the best resolution the Dyson interference microscope and that by Baker have a condenser with a large numerical aperture. The light traverses the object obliquely and the measurement values therefore tend to be slightly too high (Ingelstam and Johansson 1957). In another interference microscope described by Johansson and Afzelius (1956) and Johansson (1957), parallel light, perpendicularly passing the object, is used. Thereby a greater precision in OPD measurements is achieved.

Measurements of the mass difference at various stages of pollen grain development, as well as at various stages of enzymatic digestion of pollen grains have been made by Davies *et al.* (1954). Measurements of the OPD of the exine, intine, cytoplasm, and nucleus of pollen grains have also been made (Johansson and Afzelius 1956).

Besides the interferometric methods, quantitative cytochemical data may be obtained in other ways. Engström (1951) and Engström and Lindström (1947, 1950) have measured the mass of cells by means of soft X-rays. The method has also been tried on pollen material by Dahl and Engström (1954). Davies, Engström, and Lindström (1953) comment upon the X-ray

absorption method and make comparisons with interferometric ones. Using the X-ray technique measurements of 0.1 pg/μ^2 can be made. The Dyson interference microscope provides measurements one order of magnitude greater (Davies *et al.* 1953), that is 0.01 pg/μ^2. Furthermore, it is possible to apply the interference microscope in investigations of living material.

G. Bahr (1957) has succeeded in using the electron microscope for quantitative cytochemical measurements. As an example it may be mentioned that his calculation of the weight of a single microsome gives an approximate value of 8 to 16 $\times 10^{-19}$ g.

General methodological problems

There is no longer a tendency to separate form and function but to try to coordinate understanding of both in order to obtain an integrated picture of the living cell. It is, however, not an easy task to evaluate data obtained by different direct and indirect methods and to combine them to form a conception of the cell. It must also be borne in mind that different results are occasionally obtained even when applying the same technique to identical material. Likewise certain EMG:s may be interpreted in different ways by different workers etc. To my mind no purpose is served in trying to reconcile results and interpretations which do not fit; at the present state of knowledge and technique it is better to accept and acknowledge the divergences. But such problems, especially those arising from differences in interpretations, lead beyond the more particular problems of our field into those of a more methodological/epistemological character.

REFERENCES

Afzelius, B. M. 1955. On the fine structure of the pollen wall in *Clivia miniata*. *Bot. Not.* 108.

—— 1956. Electron microscope investigations into exine stratification. *Grana palynologica* I: 2.

Bahr, G. F. 1957. Changes in liver cell elements during stimulated protein synthesis. Stockholm. (Thesis.)

Bradley, D. E. 1954. Evaporated carbon films for use in electron microscopy. *Brit. J. Appl. Phys.* 5: 65.

—— 1957. Some botanical applications of the carbon replica technique. Proceed. 1st European regional conference on electron microscopy, Stockholm.

Burton, E. F. 1946. The electron microscope. New York.

Caspersson, T. O. 1950. Cell growth and cell function. A cytochemical study. New York.

Dahl, O. and Engström, A. 1954. X-ray analysis of mass of pollen grains. Huitième Congrès international de Botanique. Rapports et Communications, Section 6.

Davies, H. G., Engström, A., and Lindström, B. 1953. A comparison between the X-ray absorption and optical interference methods for the mass determination of biological structures. *Nature*, Lond. 172, p. 1041.

Davies, H. G., Wilkins, M. H. F., Chayen, J., and La Cour, L. F. 1954. The use of the interference microscope to determine dry mass in living cells and as a quantitative cytochemical method. *Quart. J. Micr. Sci.* 95: 3.

Dyson, J. 1950. An interferometer microscope. *Proc. Roy. Soc. Lond.* A, 204, p. 1077.

Engström, A. 1946. Quantitative micro- and histochemical elementary analysis by roentgen absorption spectrography. *Acta radiol.*, Suppl. 63.

Engström, A. and Lindström, B. 1947. Histochemical analysis by X-rays of long wavelengths. *Experientia* 3: 5.

—— 1950. A method for the determination of the mass of extremely small biological objects. *Biochim. biophys. Acta* 4–6.

Erdtman, G. 1952. Pollen morphology and plant taxonomy. I. Angiosperms. Uppsala.

—— 1956 (a). Current trends in palynological research work. *Grana palynologica* 1: 2.

—— 1956 (b). "LO-analysis" and "Welcker's rule", a centenary. *Svensk bot. Tidskr.* 50: 1.

Finean, J. B., Sjöstrand, F. S., and Steinmann, E. 1953. Submicroscopic organization of some layered lipoprotein structures. *Exp. Cell Res.* 5: 2.

Freytag, K. 1957. Doppelbrechende Stäbchen im Ölüberzug der Pollenkörner. *Svensk bot. Tidskr.* (In press.)

Frey-Wyssling, A. 1954. Report on the submicroscopic structure of plant cells. Huitième Congres international de Botanique. *Rapports et Communications*, Section 9.

Ingelstam, E. 1957. Some questions about merits of interference microscopes. *Exp. Cell Res.*, Suppl. IV, p. 150–157.

Ingelstam, E. and Johansson, L. P. 1957. Paper on aperture correction in *J. Sci. Instr.* (In press.)

Johansson, L. P. 1957. An interferometer microscope for rapid measurements of optical thickness in technical and biological objects. *Exp. Cell Res.*, Suppl. IV, p. 158–164.

Johansson, L. and Afzelius, B. M. 1956. Measurements of optical path difference by means of coloured birefringent interference and a new compensation method. *Nature*, Lond., 178, p. 137.

Knoll, M. and Ruska, A. 1932. The electron microscope. *Z. Physik* 78.

Mahl, H. 1942. Die übermikroskopische Oberflächendarstellung mit dem Abdruckverfahren. *Naturwiss.* 30: 14, 15.

Mühlethaler, K. 1955. Die Struktur einiger Pollenmembranen. *Planta* 46.

Oshurkova, M. V. 1956. [Swedish studies of sporoderms by means of electron microscopy.] *Bot. J. USSR Acad. Sci.* 41. (In Russian.)

Pflug, H. 1953. Zur Entstehung und Entwicklung des angiospermiden Pollens in der Erdgeschichte. *Palaeontographica* 95.

Rhodin, J. 1954. Correlation of ultrastructural organization and function in normal and experimentally changed proximal convoluted tubule cells of the mouse kidney. An electron microscopic study including an experimental analysis of the conditions for fixation of the renal tissue for high resolution electron microscopy. Stockholm. (Thesis.)

Sheldon, H., Zetterqvist, H. and Brandes, D. 1955. Histochemical reactions for electron microscopy: acid phosphates. *Exp. Cell Res.* 9: 3.

Sitte, P. 1953. Untersuchungen zur submikroskopischen Morphologie der Pollen- und Sporenmembranen. *Mikroskopie* 8: 9/10.

Sjöstrand, F. S. 1953. A new microtome for ultra-thin sectioning for high resolution microscopy. *Experientia* 9: 3.

Turian, G. and Kellenberger, E. 1956. Ultrastructure du corps paranucléaire, des mitochondries et de la membrane nucléaire des gamètes d'*Allomyces macrogynus*. *Exp. Cell Res.* 11.

Ueno, J. 1949. [On the structure of viscin threads as revealed by the electron microscope.] *Kagaku* 19: 7. (In Japanese.)

Wettstein, D. von, 1957. Chlorophyll-Letale und der submikroskopische Formwechsel der Plastiden. *Exp. Cell Res.* 12: 3.

Wilkins, M. H. F. 1953. The performance of spherical-mirror reflecting objectives when used for ultra-violet photomicrography. *J. Roy. Microscop. Soc.* 73: 2.

Wyckoff, R. W. 1949. Electron microscopy. Technique and applications. New York and London.

ON THE CUTTING OF ULTRA-THIN SECTIONS

BY

J. RADWAN PRAGLOWSKI

Preliminary treatment of pollen or spore material and filling of gelatine capsules with methacrylate

Before embedding in methacrylate, the pollen or spore material to be sectioned is successively washed in a centrifuge tube with distilled water (three times), 95 per cent alcohol (twice), and absolute alcohol (three times). The material should remain in the last-mentioned fluid for 24 hours. The alcohol is then decanted and some methacrylate (methyl methacrylate one part, butyl methacrylate seven parts) is poured into the tube. (N. B. Liquid methacrylate contains a stabilizer which impedes polymerization and must be washed away with a two per cent NaOH solution before the methacrylate is poured into the tube.) The methacrylate is renewed three times at intervals of two hours and should be shaken, often and thoroughly, in order to prevent the pollen grains from sedimenting. After the last re-filling the fluid is shaken once again and transferred by means of a small suction pipe to gelatine capsules (No. 3 from Parke, Davis & Co., London; see Fig. 254). It is important to add a proper amount of pollen grains ot the methacrylate. If too many grains are added the polymerization of the methacrylate (vide postea) may be rendered more difficult.

Polymerization in UV light

The liquid methacrylate is polymerized, i.e., transferred into a solid state by exposition to UV radiation; this method is to be preferred to polymerization induced by heat with the aid of a catalyzer, since the catalyzer may oxidize the sporopollenine. The filled gelatine capsules are covered with lids and fastened in pairs to a length of tape. About ten capsules to every tape are fastened in this way and exposed to the light produced by a 120 watt UV lamp. The distance between the lamp and the tape should be about

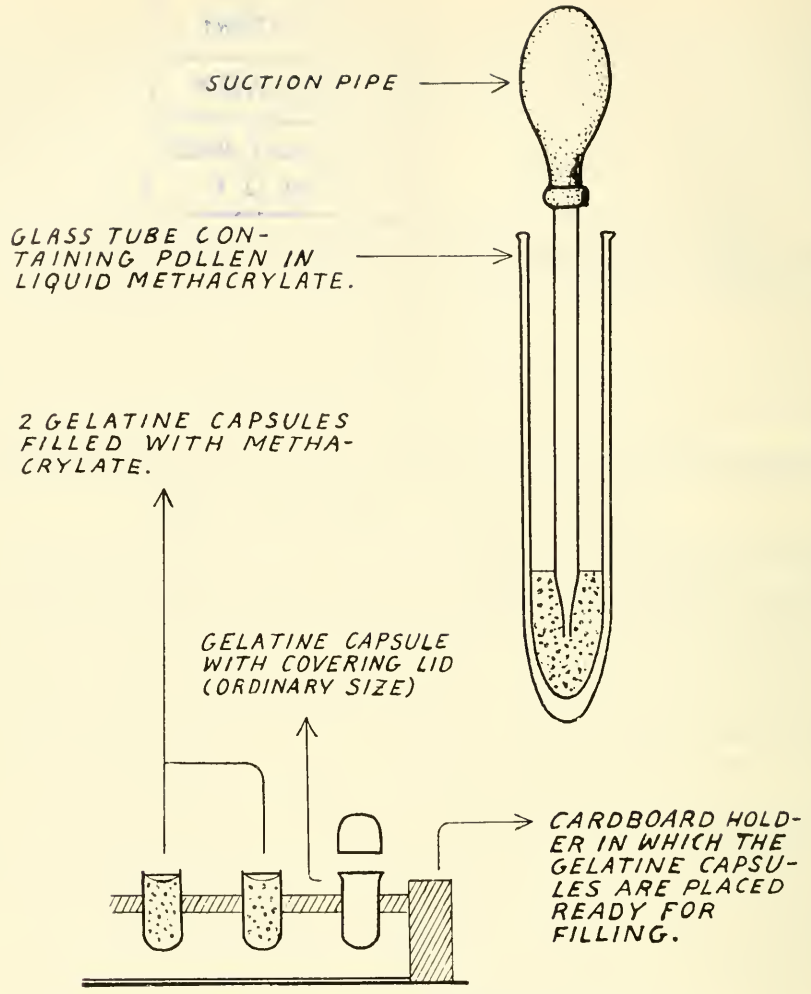

Fig. 254. Outfit for filling the gelatine capsules.

15 cm. At the Palynological Laboratory, Bromma, the gelatine capsules are usually exposed to UV radiation during five nights, approximating 15 hours per night. During the first night, before the hardening of the plastic, the heat from the UV lamp should be checked by a ventilator in order to avoid the formation of air-bubbles in the sediment at the bottom of the capsules before the methacrylate solidifies (Fig. 255). After about 80 hours of exposition to the UV lamp the plastic is, as a rule, sufficiently hard for cutting.

Cutting is rendered difficult if there are air-bubbles in the methacrylate. The bubbles may be due to various causes, for instance, as already men-

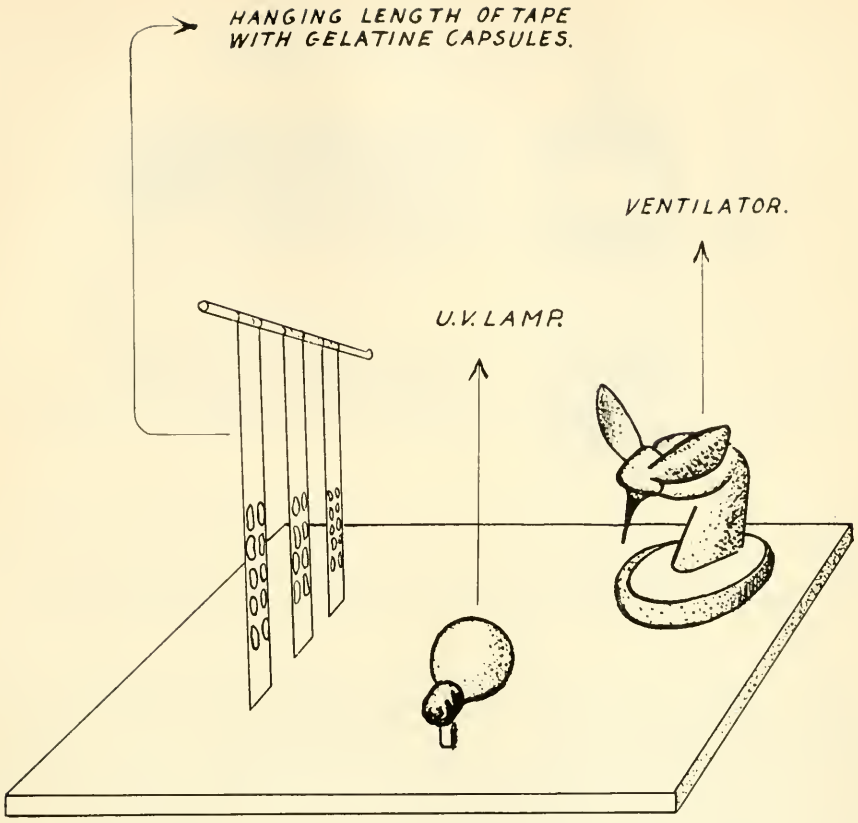

Fig. 255. Polymerization of the methacrylate with UV light.

tioned, to over-heating during the initial stages of polymerization, or to an over-concentration of pollen grains, or insufficient washings of the pollen material with methacrylate. A capsule with air-bubbles can, nevertheless, be used for cutting if the pyramid (see below) is made either at the side of the bubble or just above it.

The cutting of the pyramid

After soaking in water the gelatine capsules can be easily removed from the plastic units which, when dry, are ready for cutting. A unit is fixed in a steel object-holder (made by LKB-Produkter, Stockholm 12) in such a way that three to four millimetres of the pollen-bearing part protrude from its mouth (Fig. 256). After trimming the top of the plastic unit with a razor blade (Fig. 257), a thin foursided process, the pyramid, containing the pollen grains or spores for sectioning is carved from the apex.

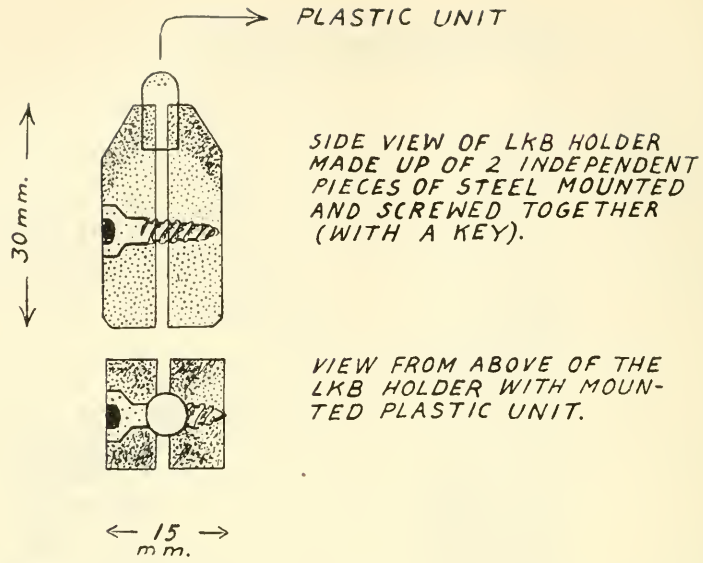

Fig. 256. LKB object-holder with plastic unit mounted (1:1).

When estimating the size of the pyramid, the following three factors should be taken into account: 1. the desired thickness of the sections (the thicker the sections the larger, and especially the higher, the pyramid must be); 2. the size of the pollen grains (the size of the pyramid should be increased or decreased in proportion to the size of the pollen grains; if large pollen grains or spores—diameter about 80 μ or more— are to be cut sometimes as few as 1–3 pollen grains will be sufficient, cf. Fig. 258); 3. the concentration of the pollen grains (cf. Fig. 259; if the concentration

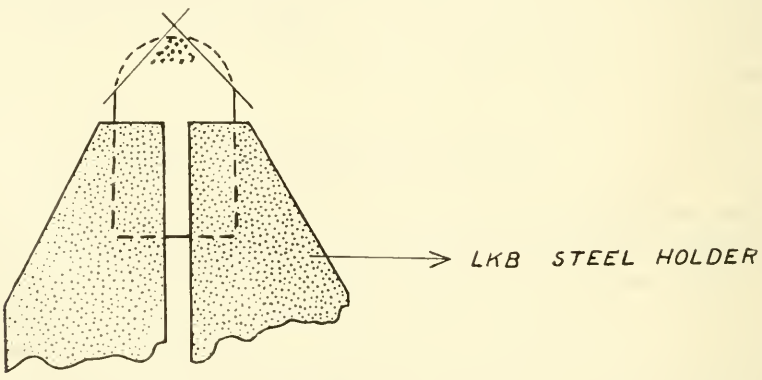

Fig. 257. Preliminary cutting of the plastic unit.

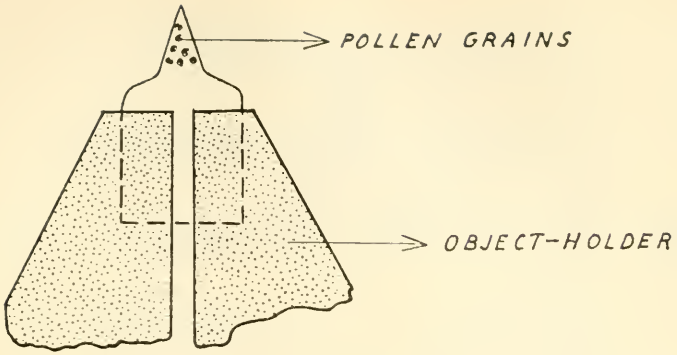

Fig. 258. Plastic unit with ready-made pyramid. (N.B. The pyramid is enlarged about 10 times, the rest of the figure about 3 times.)

is low, the dimensions of the pyramid, with a view to increasing the number of pollen grains to be sectioned, must be larger). The total height of the pyramid should not exceed half a millimetre if sections of a thickness of about 0.25–0.50 μ are to be made). These recommendations have been followed when working with the modified Spencer microtome model 821 and are not always valid for ultra-thin sectioning.

The best results are obtained by working with samples rich in pollen grains and absolutely clean. Organic debris renders cutting more difficult, shreds the sectioned pollen fragments, or covers them, and decreases the value of the sections on the whole. Inorganic material (e.g. silicon or other mineral particles) will damage the microtome knife.

Fig. 260 illustrates the order, directions etc., to be followed when moulding the pyramid, but it goes without saying that there can be many modi-

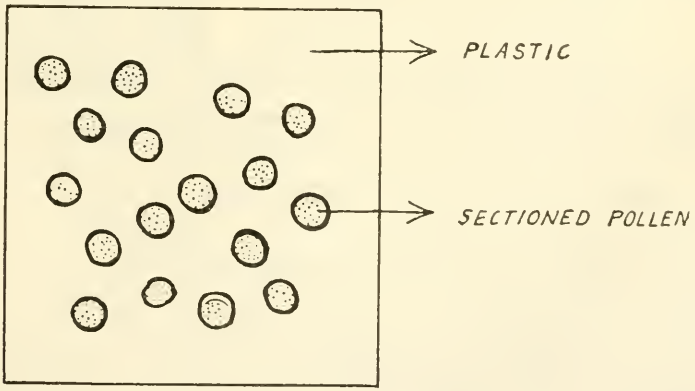

Fig. 259. Section from the basal part of the pyramid. × 100.

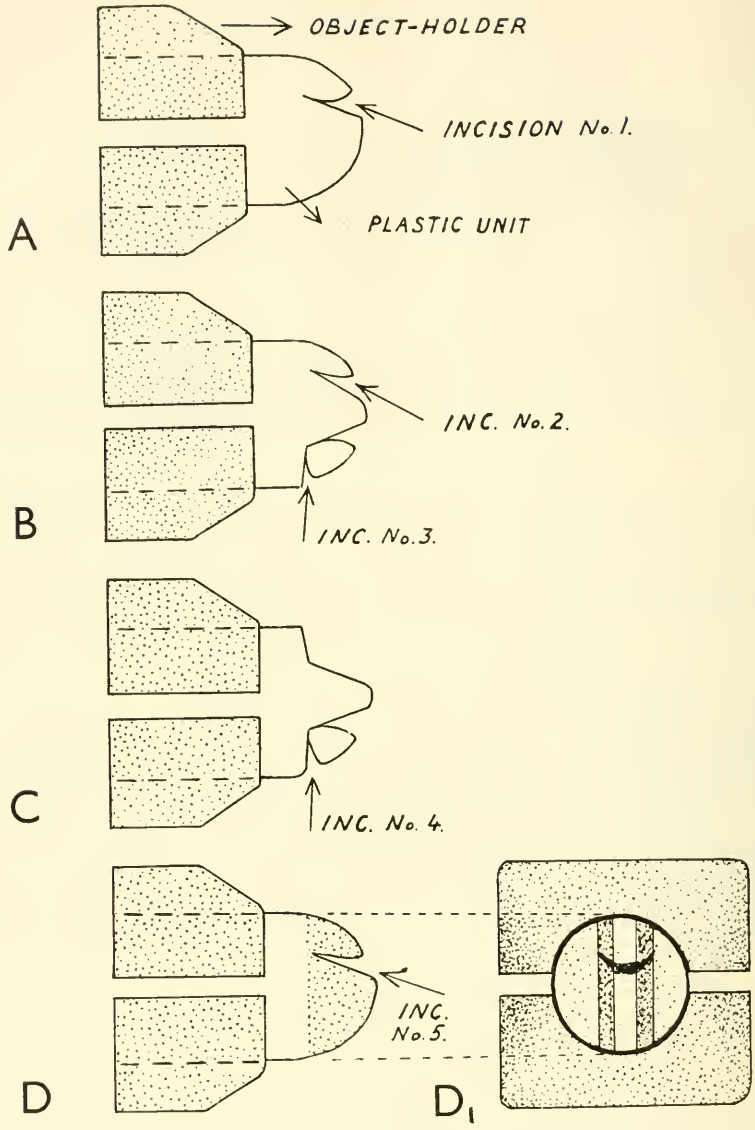

Fig. 260. Moulding of the pyramid. (N.B. Plastic unit 4:1, object-holder about 2:1.) — A. Incision No. 1. — B. The object-holder is turned 180° and incisions Nos. 2 and 3 are made. A part of the apex of the plastic unit will fall away with incision No. 3, after which the object-holder is turned again 180°. — C. Incision No. 4 cuts off the other part of the apex of the plastic unit. Two sides of the pyramid are now ready. The object-holder is then turned 90°. — D. Incision No. 5. D_1 shows the object-holder with the plastic unit in top perspective after incision No. 5. — E. The object-

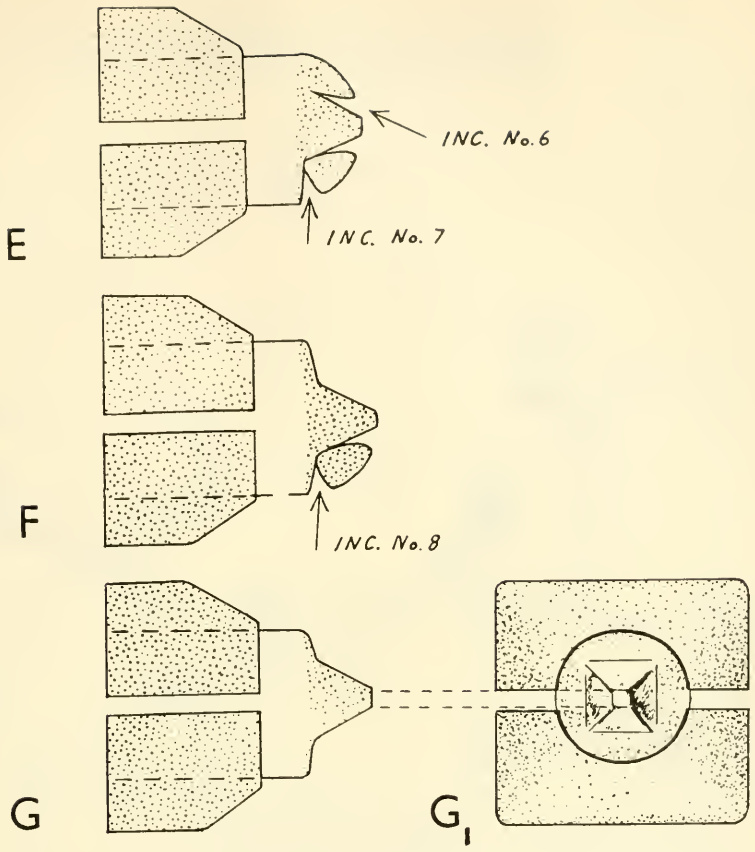

holder is then turned 180° and incisions Nos. 6 and 7 are made, after which it is again turned 180°. — F. Incision No. 8 cuts away the last part of the plastic unit, and the coarse cutting of the pyramid is now complete. — G. Side view. G_1 Front view of the object-holder with ready-cut pyramid,

fications according to individual ways of working. Usually, the moulding cannot be considered to be complete in eight cuts, and further fine trimming along the lines illustrated in Fig. 260 is always necessary. The height of a properly moulded pyramid is always greater than the base.

The grinding of the microtome knife

American "Eversharp" razor blades are used for cutting. After removing the fat with ether the blade is mounted in a special holder (LKB-Produkter, Stockholm). The grinding is performed on a sheet of planed glass. A suitable amount of grinding powder (type B. 5125, Linde Air Products Co.) and

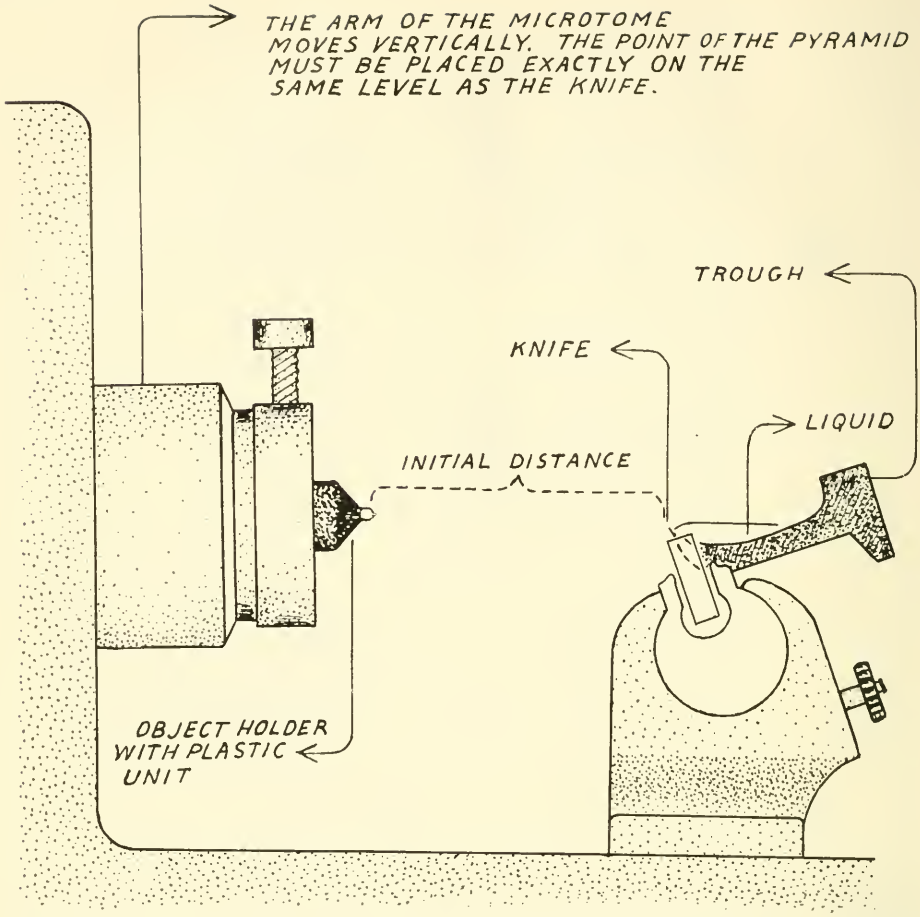

Fig. 261. Adjusting of the Spencer microtome model 821 for sectioning.

teepol (teepol one part and distilled water four parts) should be available. The powder is thoroughly mixed with the teepol to a homogeneous, easy-flowing mixture. Ordinarily, grinding takes about 15 minutes. The pressure on the knife should be at a minimum during the last five to eight minutes of grinding. After rinsing in running water and drying with a few drops of absolute alcohol, the knife is ready to use. It should be used immediately after grinding in order to avoid rust, contamination by dust etc.

The sectioning

The knife is cleansed with acetone and mounted in a curved position in a special trough (made by LKB-Produkter, Stockholm). Care must be

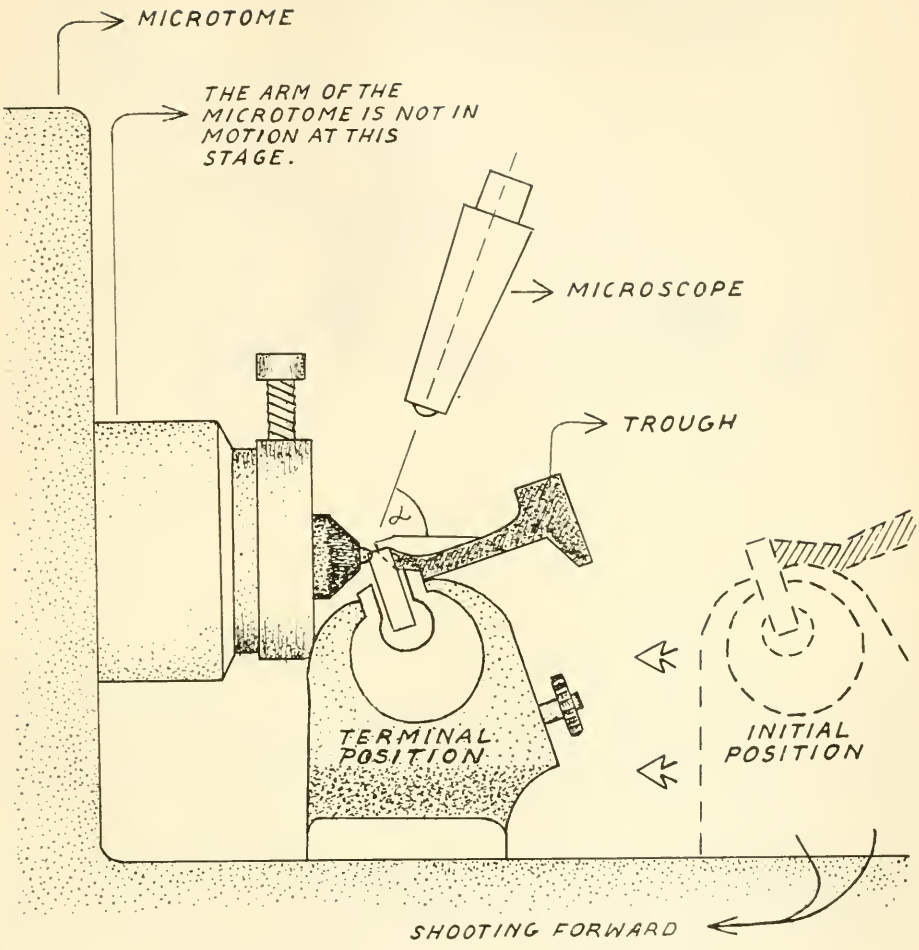

Fig. 262. Adjusting of the microtome for sectioning (continued).

taken to ensure that its edge is parallel with the end of the trough. The latter, together with the knife, is then fixed in the microtome. At the same time, the object-holder is tightly screwed into the mobile part of the microtome. The screw controlling the thickness of the sections is adjusted in accordance with the desired thickness. Concomitantly, a final adjustment of the pyramid in relation to the knife should be made. The general conditions of stability must also be observed, particularly a steady under-carriage. This process, as well as that of cutting, is followed through a binocular microscope ($\times 20$).

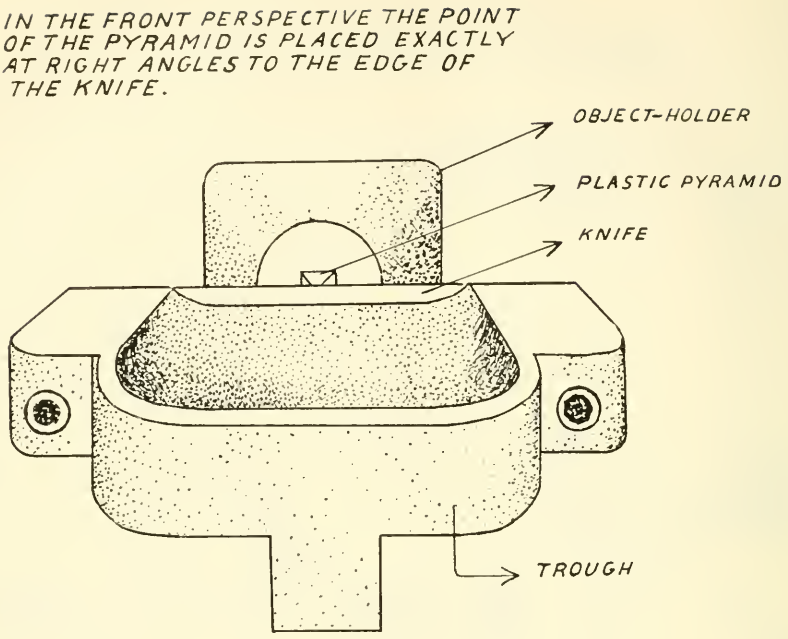

Fig. 263. Pyramid and trough, front view.

By hand, and with the motor off, the pyramid is brought to the level of the knife. In order to prevent damage to the pyramid through the vertical movement of the microtome, the trough with the knife should be placed at a safe distance. The knife is then slowly brought forward to the apex of the pyramid.

Fig. 261 outlines the mobile part of the microtome, the knife-trough part (side view), and the vertical adjustment of the lever of the microtome with the mounted plastic unit. Fig. 262 shows the knife-trough block and the microscope.

The final adjusting for sectioning is followed under the microscope. In the visual field will be seen the facet of the knife, the liquid (20 per cent alcohol in water) with which the trough has been filled, and the plastic unit with a part of its holder. One of the base lines of the pyramid must be parallel to the facet of the knife which should be brought as near as possible to the apex of the pyramid without coming into contact with it. The knife-trough block is then fixed, and the level of the liquid checked (the surface should be slightly convex).

The motor is then started. Some introductory movements of the microtome carry the apex of the pyramid towards the knife. The microtome feeds at every second stroke. Normally, the sections assemble in the

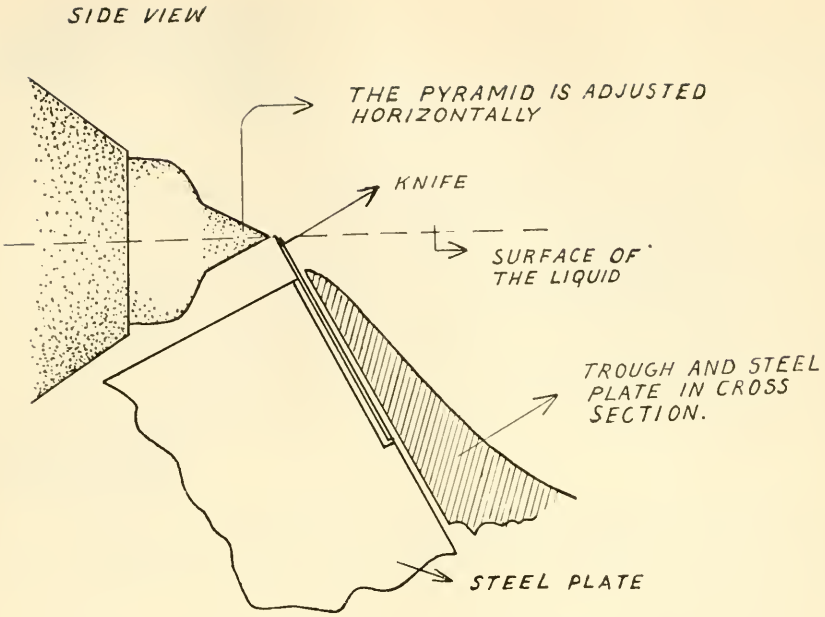

Fig. 264. Pyramid and part of trough, side view.

trough, grouping themselves into wreaths, strips, or small flocks. If there is too much liquid they will disseminate and, furthermore, water will possibly adhere to the pyramid. Inspection of the sections through the microscope will be rendered difficult or impossible by disturbing light refraction, resulting from an exaggerated convexity of the surface of the liquid etc. Occasionally, the sections will roll themselves up on the surface of the liquid, but they will regain their original shape if allowed to float in the trough for a few minutes before fishing up. — The above methods of embedding, cutting of pyramids, grinding and sectioning have been recommended by, i.a., F. S. Sjöstrand, Karolinska Institutet, Stockholm.

The fishing-up of the sections

The sections are fished up from the trough with a thin, fine-pointed, soft brush, and transferred to a slide which has been thoroughly cleansed (albumin glycerine is not used). A drop of alcohol (20 per cent) is placed on the centre of the slide. The brush is then inserted into the liquid and slowly pushed towards that part of the knife where the sections are assembled. When the tip comes under the sections the brush is carefully lifted up over the surface of the water, turned upside down, and allowed to touch the surface of the liquid on the slide. At this stage a preliminary

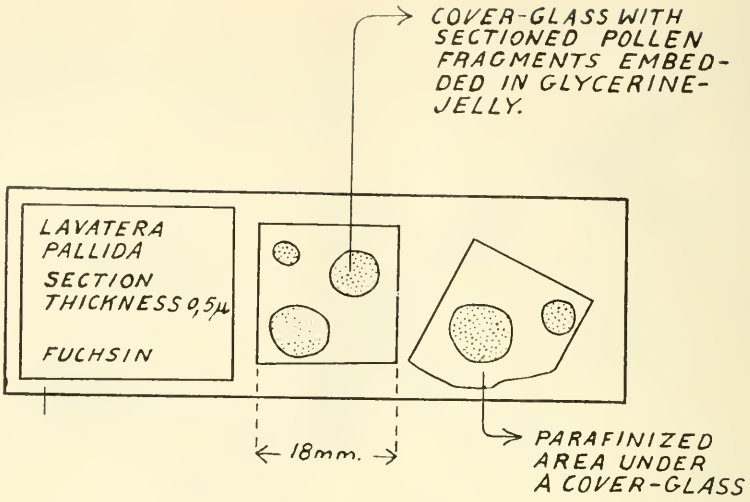

Fig. 265. Microscope slide with sectioned pollen walls.

check under the microscope can be made in order to get an idea of the quality of the sections.

Further treatment depends on the number of sections transferred to the slide. If there are only a few it is better to allow the liquid on the slide to dry in the air. If the slide contains a great number of sections it is better to wash it with one or two drops of absolute alcohol. Although this procedure will probably wash away a number of the sections it is, nevertheless, worth while because the alcohol will separate the sections from each other and, at the same time, remove any dust etc. on the slide. When dry, the slide is rinsed once more with absolute alcohol. After the alcohol has evaporated the plastic is dissolved in acetone.

The dissolving of the plastic, staining and mounting

The acetone usually dissolves the plastic in a few hours (generally, the slide is left over-night in the acetone). After inspection under the microscope at low magnification (about ×60) good section-bearing areas are marked with a diamond. The slide is then again carefully rinsed with absolute alcohol and with slowly running water. If the sections are not to be stained, the slide is ready for mounting.

Staining with fuchsin, safranine, or methylene blue is useful, and in fact often necessary, particularly if the thickness of the sections is only

0.5 μ or less. The stains are dissolved in cuvettes filled with water (approximately a knife's point to a cuvette). Staining is effected in about 1–5 hours. Bismarck brown, malachite green, and other stains have been tried, but with less satisfactory results. Staining greatly facilitates the localizing of the sections as unstained sections thinner then 0.3 μ are often difficult to locate under an ordinary microscope.

After staining, the slide is rinsed with water and allowed to dry. Meanwhile, minute glycerine jelly cubes (about 1 mm^3) are cut, and a number of cover-slips carefully cleaned. The cubes are placed on those parts of the slide which have previously been marked with the diamond. The size of the cubes should vary in relation to the size of the section-bearing areas. A cover-slip is then placed on top of each jelly cube, and the jelly slowly melted. Care should be taken to prevent the jelly from spreading to the edge of the cover-slip.

The slide is then sealed with paraffin-wax. To this end a small piece of paraffin (melting point about 70 centigrades) is placed at the edge of the cover-slip. The slide is then slowly heated in order to melt the paraffin which is sucked in under the cover-slip forming a protecting zone around the section-bearing glycerine jelly (Fig. 265). When the paraffin has cooled and hardened, the slide is cleaned with a knife and cotton wool soaked in benzol.

For further information see "Sjöstrand Ultra-Microtome. Instructions for use". (Distributed by LKB-Produkter, Stockholm 12.)

INDEX

The references to illustrations are distinguished by heavy figures. Generic names are in italics. The names of species are not included.